Prey-predator "Host-parasite" Models with Adaptive Dispersal:

Application to Social Animals

by

Komi Segno Messan

A Dissertation Presented in Partial Fulfillment
of the Requirements for the Degree
Doctor of Philosophy

Approved November 2017 by the
Graduate Supervisory Committee:

Yun Kang, Co-chair
Carlos Castillo-Chavez, Co-chair
Gloria D. Degrandi-Hoffman
Marco A. Janssen

ARIZONA STATE UNIVERSITY

December 2017

ABSTRACT

Foraging strategies in social animals are often shaped by change in an organism's natural surrounding. Foraging behavior can hence be highly plastic, time, and condition dependent. The motivation of my research is to explore the effects of dispersal behavior in predators or parasites on population dynamics in heterogeneous environments by developing varied models in different contexts through closely working with ecologists. My models include Ordinary Differential Equation (ODE)-type meta population models and Delay Differential Equation (DDE) models with validation through data. I applied dynamical theory and bifurcation theory with carefully designed numerical simulations to have a better understanding on the profitability and cost of an adaptive dispersal in organisms. My work on the prey-predator models provide important insights on how different dispersal strategies may have different impacts on the spatial patterns and also shows that the change of dispersal strategy in organisms may have stabilizing or destabilizing effects leading to extinction or coexistence of species. I also develop models for honeybee population dynamics and its interaction with the parasitic Varroa mite. At first, I investigate the effect of dispersal on honeybee colonies under infestation by the Varroa mites. I then provide another single patch model by considering a stage structure time delay system from brood to adult honeybee. Through a close collaboration with a biologist, a honeybee and mite population data was first used to validate my model and I estimated certain unknown parameters by utilizing least square Monte Carlo method. My analytical, bifurcations, sensitivity analysis, and numerical studies first reveal the dynamical outcomes of migration. In addition, the results point us in the direction of the most sensitive life history parameters affecting the population size of a colony. These results provide novel insights on the effects of foraging and Varroa mites on colony survival.

I dedicate my PhD thesis to my parents Adika and Josee Messan for always encouraging me and relentlessly giving everything they have so I can reach my full potential.

ACKNOWLEDGMENTS

Firstly, I would like to express my sincere gratitude to my advisor Dr. Yun Kang for her dedication and her encouragements at the time when I did not believe in myself. Her guidance helped me in all the time of research and writing of this thesis. I could not have imagined having a better advisor and mentor for my Ph.D study. I am also deeply grateful for my co-advisor Dr. Carlos Castillo-Chavez for his continuous support of my Ph.D study and related research. His mentorship throughout my PhD study have been crucial in my growth as a researcher.

Besides my advisors, I would like to thank the rest of my thesis committee: Dr. Gloria DeGrandi-Hoffman for all her enthusiasm, hospitality, immense support, and always being ready to guide me when I needed her. Dr. Marco Janssen for his insightful comments, encouragement, and many useful skills learned in his class.

My sincere thanks also goes to Dr. Dominic P. Clemence, my undergraduate mathematics professor at North Carolina A&T State University, who first opened my eyes to the world of biomathematics which has lead to this PhD thesis. I also want to thank all the elementary to high school teachers that have taught me the value of hard work. Without their precious support, it would not be possible to arrive where I am today.

I thank my fellow officemate and friend, Daniel Burkow, for the stimulating discussions and for always being ready to provide suggestions. I am extremely grateful to the wonderful communities at Arizona State University and the the amazing friends that I have made, Kehinde Salau, Oyita Udiani, Dustin Padilla, Made Eka, Fereshteh Nazari, Jordan Bates, Anarina Murillo, Kamal Barley, Juan Renova, Victor Moreno, Baltazar Espinoza, to name a few. Also, I am grateful to the following staff at the SAL MCMSC of Arizona State University (ASU), Sherry Woodley, Margaret Murphy-Tillis, Dawn Bies who provided a wonderful environment to conduct my research. The path was not easy but you guys made it fun and for that I am indebted to you all.

This accomplishment was made possible only through the following fundings: the U.S. Department of Education (GAANN grant program), ASU Dissertation writing Fellowship, ASU Graduate Completion Fellowship, James S. McDonnell Foundation 21st Century Science Initiative in Studying Complex Systems Scholar Award, Natural Science Foundation of Jiangsu Province, Tianyuan Fund for Mathematics of NSFC, NSF-DMS, and NSF-IOS/DMS. Last but not the least, I would like to thank my family: my wife Marisabel Rodriguez Messan for her tremendous emotional support and sleepless nights working together; my parents and to my brothers and sister for supporting me spiritually throughout writing this thesis and my life in general.

TABLE OF CONTENTS

CHAPTER Page

CHAPTER Page

LIST OF TABLES

LIST OF FIGURES

Figure Page

Figure Page

Figure Page

Chapter 1

INTRODUCTION

1.1 Overview

A pressing challenge nowadays is to mitigate the deleterious ramification caused by an ever-growing economy on terrestrial biodiversity (e.g fast growing population, pollution, industrialization, etc.). These adverse repercussions have heightened conditions leading to increase fragmentation of habitat patches causing discontinuities in an individual's preferrered environement (Meyer and Turner, 1992) . The survival probability of species in isolated subpopulations hence depend on their ability to disperse. Bowler and Benton (2005) defines dispersal as: *"any movement between habitat patches, and habitat patches as areas of suitable habitat separated in space from other such areas, irrespective of the distance between them"*. Throughout this dissertation, the use of dispersal will rely on the later defintion.

Dispersal in patchy prey predator communities has been shown to have a tremendous effect at the population level of various species. For example Lengyel and Epstein (1991) along with many others have shown the destabilization, stabilization, and chaos-induced effect of dispersal in a prey predator's ecosystem (Pascual, 1993; Jansen, 1995; Briggs and Hoopes, 2004; Cressman and Křivan, 2013; Chewning, 1975). Jansen (1995) investigated how and when spatial interaction can regulate populations of predator and prey using the Rosenzweig-MacArthur model with the two species migrating between the patches . Jansen observed that the paradox of enrichment fails to be established in the spatial model. However, the theory is sometimes perceived in non-spatial models. The Rosenzweig-MacArthur model has also been used to show the diffusion induced instability or chaos in

two patch predator and prey systems (Lengyel and Epstein, 1991; Pascual, 1993; Cressman and Křivan, 2013). Dispersal can locally affect stability even in the absence of environmental variability as illustrated by Hastings (1977). There are hence many theoretical works regarding the role of dispersal and foraging behavior in prey-predator interaction. Many of these works are however heavily centered around foraging activities that are driven by random search behavior. While the random search hypothesis may be true for certain species, many insects in the ecosystem exhibit different mode of dispersal as foraging behavior (Hastings, 1983; Harrison, 1980; Ghosh and Bhattacharyya, 2011).

Foraging strategies in social insects and animals are often shaped by change in an organism's natural surrounding. The dispersal behavior is hence often highly plastic, time, and condition dependent thus it is an adaptive process. Debenedictis (2014) defines adaptation as *"an alteration in the structure or function of an organism or any of its parts that result from natural selection"*. This dissertation is hence concerned with understanding what are the impacts of plastic dispersal strategy (i.e. adaptive dispersal) in social animals living in a patchy environment. The motivation of the work presented in this dissertation is divided in two categories. First I analyze and visualize the role of dispersal in a general framework of prey-predator ecosystem where only predators are mobile and the dispersal mechanism is driven by multiple foraging strategies (i.e. predators have multiple dispersal strategy while preys are immobile). The second portion of this research focuses on an application to honeybee population dynamics and its interaction with the parasitic Varroa mite where an adaptive dispersal occurs in both species and this work is validated by empirical data.

1.2 Research Questions

The central question of this dissertation is: What is the role of an adaptive dispersal in host-parasite interactions?

The following sub-questions are formulated in order to answer the precedent question:

1. what are the spatial patterns generated in the environment where predator dispersal is driven by multiple dispersal strategy?

2. Under what conditions can adaptive dispersal favor coexistence of a social insect subject to an infestation by predators?

3. What are the most important life history parameters affecting the population size of social insects with an adaptive foraging pattern where the social insects are subject to parasitic's infestation?

1.3 Random and Non-random Foraging Behavior in Social Animals

Biotic interactions play an important role on landscape mosaic and the functionality of the ecosystem as a whole (Levin, 1974; Wisz et al., 2013; Bascompte, 2009). As result, spatial self-organization may emerge from local interactions and dispersal ability is considered to be one of the key factors promoting the self-organized spatial pattern (Aarssen and Turkington, 1985; Solé and Bascompte, 2006; Soro et al., 1999). Several hypotheses have been proposed regarding the key driven force of dispersal and many of them highlight the random foraging activities of species (Neuvonen, 1999; Viswanathan et al., 1996; Zimmerman, 1982; Jansen, 1995; Lengyel and Epstein, 1991).

Nevertherless, dispersal of a predator is usually driven by its non-random foraging behavior which is often prompt by prey-contact stimuli, conspecific attraction, or benefit of assessment (Ghosh and Bhattacharyya, 2011; Cressman and Křivan, 2013; Kummel et al., 2013). Among many communities of insects, the profusion of predators in a given area tends to diminish preys in that specific area. It is natural for most preys to migrate to different areas due to increase in danger resulting from predators' abundance, and this could constitute another pretext for dispersal (Ghosh and Bhattacharyya, 2011; Savino and Stein, 1989; Fraser and Cerri, 1982). Random foraging like models are hence not suitable for cer-

tain migratory species that have dispersal dependent on population density. Such work was presented by Kang et al. (2017) in which we proposed a model with the assumption that predators move towards patches with more concentrated prey-predator interactions. The dynamics of our model was then compared to the results obtained in the classic two patch model in order to elucidate how different dispersal strategies may have different impacts on the dynamics and spatial patterns. Note that the work presented in Kang et al. (2017) will not be discussed in detailed in this dissertation as my goal is to access the role of adaptive dispersal in social animals.

1.4 Multiple Foraging Strategy in a Single Specie

In nature, the art of fitness maximization in both animals and social insects depend significantly upon an optimal diet in quantity and quality. Foraging strategies are therefore shaped by change in an organism's natural surrounding. As a result, many species encompass multiple foraging strategies that vary with respect to environmental stimuli (see example of ants foraging strategies in Traniello (1989). Through a literature review on an aerial dispersal in spiders, Duffey (1998) concluded that an aerial dispersal in many species is stimulated by overcrowding, lack of food, and physiological need to move to new habitats at a certain stage in the life cycle. Motivated by observations on iguanid lizards, Kiester and Slatkin (1974) proposed a model for resource assessment in which the animal examines the movements, density and activity of conspecific individuals in addition to food resources, and uses these cues to organize its own foraging movements. A field study by Stamps (1988) suggests that Anolis aeneus juveniles are attracted to conspecific territorial residents under natural conditions in the field. Kummel et al. (2013) showed through their field work that the foraging behavior of Coccinellids are not only governed by conspecific attraction but also through passive diffusion and retention on plants with high immobile aphids number (Kummel et al., 2013). In their work, Kummel et al. (2013)

investigated whether self-organization can occur in the absence of lateral connectivity in a field consisting only of Aphids and Coccinellids and they found that small colonies of Aphids tended to grow, large colonies stay the same or change slightly, and mid-sized colonies mostly decline. In addition, Kummel et al. (2013) noted that the predation pressure of small colonies of Aphids is highly correlated with the size of the largest Aphids colonies which is an indication of density-dependent dispersal of Coccinellids. These theoretical and field experiments illustrate the evidence of multiple strategies of movement in insects which is rarely considered when modeling the network of interacting organism. Thus an important ecological question remains: what are the spatial patterns generated in the environment where predator dispersal is driven by multiple dispersal strategy? Chapter 2 will provide an answer to this question using the results that we recently published in the Journal of Discrete and Continuous Dynamical System - B (Messan and Kang (2017)).

1.5 Role of Adaptive Dispersal on Honeybee and Mite Interaction in a Patchy Environment

Honeybees play a vital role in sustaining our planet's ecosystem. Studies have demonstrated that the majority of food consumed by humans rely on bees' pollination for abundant yields and better quality (Klein et al. (2007); McGregor et al. (1976); Watanabe et al. (1994)). Thus honeybees represent an amazing asset as agricultural pollinators in United States and globally. Aside from the value obtained from the food production, bees provide food and nutrients to other organisms in nature (e.g fruit and seed to birds), hence making them very valuable for the conservation of our biodiversity. In oder to efficiently collect nutrient necessary for their colony and supply food to other organisms through their pollination, honeybees must correctly utilize a foraging strategy guarantee a maximum yield for their colony while reducing energy and risk from predation and other natural disasters resulting from weather conditions. Through a field study, Visscher and Seeley (1982)

measured certain temporal and spatial patterns in the foraging activities of a bee colony. It was found that the strategy of a honeybee colony involves surveying the food source patches within a vast area around its nest, pooling the reconnaissance of its many foragers, and using this information to focus its forager force on a few high quality patches within its foraging area. Furthermore, Harpur et al. (2014) found many instances of positive selection acting on honeybees' genes that influence worker traits by analyzing 40 individual genomes. This foraging behavior in honeybees hence fall in the category of an "adaptive dispersal" from the definition of adaptation proposed by Debenedictis (2014).

Nonetheless, there has been a sharp decrease in honeybee population globally with many colonies disappearing. While the exact causes of this colony collapse phenomenon have yet been discovered, some known factors may constitute a possible portal to the disorder (e.g. stressful apiculture practices, honey bee diseases, or parasitism by mites). Infestation by *Varroa destructor (Acari: Varroidae)* has strongly been suggested to be one of the important triggering factors inducing colonies to collapse (DeGrandi-Hoffman et al. (2016); Kang et al. (2015); DeGrandi-Hoffman et al. (2014); Sumpter and Martin (2004)). In chapter 3, I investigate the dynamical outcomes of honeybee dispersal subject to mite infestation within a two patch framework using a simple two patch honeybee-mite interaction model and provide conditions under which dispersal can save colony from collapsing. These results were recently published in the Journal of Mathematical Modelling of Natural Phenomena (Messan et al. (2017)).

In order to clearly capture the dynamics generated by bee's dispersal within a colony, I constructed a single patch honeybee-brood-mite interaction model which was validated by empirical data. I then measure the most sensitive parameter affecting population size within a colony and the potential spatial pattern caused by such parameters. Unveiling the many facets causing the disturbance of a bee's population size could be the first step in the

direction of designing an appropriate control measure and possibly eradicating the colony collapse incident. This work is illustrated in chapter 4 of the dissertation.

1.6 Contribution and Significance

Using dynamical systems approach, this research analyzes and visualizes the role of adaptive dispersal driven by complex nonlinear behaviors. As some of the realistic mechanisms that drive dispersal in social animals have not been studied due to the complication that arise in analyzing such models, I provide novel solutions generated by dispersal through theoretical analysis as well as bifurcation simulations. This work bring together some of the existing work regarding dispersal and how my new proposed models are more biologically relevant for certain species. Moreover, this work combines both real data and dynamical system models to illustrate the significance and relevance of systems of ordinary differential equations, delay differential equation, and stage structure model in population biology.

Finally, my study of honeybee-parasite model (in chapter 3 and 4 of the dissertation) provides a good understanding of the synergistic effects of parasitism on honeybee population dynamics. The current results provide a baseline for further studies that can incorporate seasonal and nutritional effects on bees population dynamics operating in a multi-patch environment.

Chapter 2

A TWO PATCH PREY-PREDATOR MODEL WITH MULTIPLE FORAGING STRATEGIES IN PREDATOR: APPLICATIONS TO SOCIAL ANIMALS

2.1 Abstract

We propose and study a two patch Rosenzweig-MacArthur prey-predator model with immobile prey and predator using two dispersal strategies. The first dispersal strategy is driven by the prey-predator interaction strength, and the second dispersal is prompted by the local population density of predators which is referred as the passive dispersal. The dispersal strategies using by predator are measured by the proportion of the predator population using the passive dispersal strategy which is a parameter ranging from 0 to 1. We focus on how the dispersal strategies and the related dispersal strengths affect population dynamics of prey and predator, hence generate different spatial dynamical patterns in heterogeneous environment. We provide local and global dynamics of the proposed model. Based on our analytical and numerical analysis, interesting findings could be summarized as follow: (1) If there is no prey in one patch, then the large value of dispersal strength and the large predator population using the passive dispersal in the other patch could drive predator extinct at least locally. However, the intermediate predator population using the passive dispersal could lead to multiple interior equilibria and potentially stabilize the dynamics; (2) The large dispersal strength in one patch may stabilize the boundary equilibrium and lead to the extinction of predator in two patches locally when predators use two dispersal strategies; (3) For symmetric patches (i.e., all the life history parameters are the same except the dispersal strengths), the large predator population using the passive dispersal can generate multiple interior attractors; (4) The dispersal strategies can stabilize the

system, or destabilize the system through generating multiple interior equilibria that lead to multiple attractors; and (5) The large predator population using the passive dispersal could lead to no interior equilibrium but both prey and predator can coexist through fluctuating dynamics for almost all initial conditions.

2.2 Introduction

Dispersal of predator plays an important role in regulating, stabilizing, or destabilizing population dynamics of both prey and predator (Cantrell and Cosner, 2004). There are fair amount of field experiements and literature on mathematical models of prey-predator interacting in a patchy environments. For instance, the works of Nguyen-Ngoc et al. (2012); Namba (1980); Auger and Poggiale (1996); Jánosi and Scheuring (1997); Silva et al. (2001); Hansson (1991); Fraser and Cerri (1982); Savino and Stein (1989); Hanski (1999) explored the effects of dispersal on population dynamics of prey-predator models, when dispersal is driven by local population density alone. These theoretical works show that the local population density selected dispersal can increase species persistence provided the movement between patches does not synchronize local population dynamics. In most communities of social animals however, foraging is often a sophisticated recruitment processes that often results in collective decisions to exploit the most profitable resources (Lihoreau et al., 2010). The varied foraging driving forces of dispersal include population density, kin selection relatedness, conspecific attraction, interspecific interactions, food availability, patch size and qualities, etc. There has been a large number of empirical studies supporting the effects of various parameters on dispersal mechanisms and strengths Bowler and Benton (2005). For example, the field work by Kiester and Slatkin (1974) showed evidence of Iguanid lizards that encompass two or more dispersal strategies as foraging movements. Kummel et al. (2013) showed through their field work that the foraging behavior of Coc-

cinellids are governed not only by the conspecific attraction but also through the passive diffusion and retention on plants with high immobile aphids number.

Organisms must hence adapt to change in the environments (e.g. temperature variation, precipitation, season, etc.), size and nature of their colonies (see an example of effect of young brood on honeybee foraging in Tsuruda and Page Jr (2009), or anti-predator cues in order to meet their fitness goal. Field experiments has hence demonstrated in many insects that foraging is not driven by a unique process but multiple processes (Kummel et al., 2013; Kiester and Slatkin, 1974). However, there is a limited theoretical work on studying how combinations of different dispersal strategies affect population dynamics of prey-predator models in the patchy environment due to the complications that arise in analyzing such models.

In this chapter, we introduce a new version of a Rosenzweig-MacArthur two patch prey-predator model in which prey is immobile and predator use two different dispersal strategies as foraging movement between the patches. The first dispersal strategy is driven by the prey-predator interaction strength (also called "predation strength") and the second dispersal is prompted by the local population density of predators which is referred as "the passive dispersal". The dispersal strategies used by predators are measured by the proportion of the predator population using the passive dispersal which is a parameter ranging from 0 to 1. Our objective is to assess the dynamics generated by different dispersal strength on the population of prey and predators.

2.3 Model Derivations and the Related Dynamics

Let $u_i(t),\ v_i(t)$ be the population of prey and predator in Patch i at time t, respectively. In the absence of dispersal, we assume that the population dynamics of prey and predator

follow the well-known Rosenzweig-MacArthur prey-predator model as follows:

$$\begin{aligned} \frac{du_i}{dt} &= r_i u_i \left(1 - \frac{u_i}{k_i}\right) - \frac{b_i u_i v_i}{1 + b_i h_i u_i} \\ \frac{dv_i}{dt} &= \frac{c_i b_i u_i v_i}{1 + b_i h_i u_i} - \delta_i v_i \end{aligned} \tag{2.1}$$

where r_i is the intrinsic growth of prey at Patch i; k_i is the prey carrying capacity at Patch i; b_i is the predator attacking rate at Patch i; h_i is the predator handling time at Patch i; c_i is the energy conversion rate at Patch i; and δ_i is the mortality of predator at Patch i. After similar rescaling approach used in Liu (2010) by letting

$$x_i \to b_i h_i u_i,\ y_i \to b_i h_i v_i / c_i,\ t \to t/r_1,\ d_i \to \delta_i / r_1,\ a_i \to \frac{c_i}{r_1 h_i} \text{ and } K_i \to \frac{k_i}{b_i h_i},$$

the model (2.1) is presented as the following scaled model:

$$\begin{aligned} \frac{dx_i}{dt} &= \frac{r_i}{r_1} x_i \left(1 - \frac{x_i}{K_i}\right) - \frac{a_i x_i y_i}{1 + x_i} \\ \frac{dy_i}{dt} &= \frac{a_i x_i y_i}{1 + x_i} - d_i y_i \end{aligned} \tag{2.2}$$

where $\frac{r_i}{r_1}$ is the relative intrinsic growth of prey at Patch i; K_i is the relative prey carrying capacity at Patch i; a_i is the relative predator attacking rate at Patch i; and d_i is the relative mortality of predator at Patch i.

Now we introduce a two patch prey-predator model based on the scaled model (2.2). We assume that prey is immobile and predator uses two dispersal strategies moving between patches. Let ρ_i be the dispersal rate of predator at Patch i, then the dispersal of predator between two patches is driven by the following two mechanisms.

1. The first mechanism relies on the strength of the prey-predation interaction in its patch (also called "the predation strength"). This mechanism is a combination of conspecific attraction and patch quality measured by the prey population density Kummel et al. (2013). Predator are hence attracted toward patches with high prey-predator

interaction strength. Thus, the net dispersal of predators using "the predation strength dispersal" at Patch i is given by

$$\rho_i \left(\underbrace{\frac{a_i x_i y_i}{1+x_i}}_{\text{attraction strength to Patch i}} y_j - \underbrace{\frac{a_j x_j y_j}{1+x_j}}_{\text{attraction strength to Patch j}} y_i \right).$$

This assumption is also supported by the study of Grünbaum and Veit (2003) in which the authors noted that the feeding success of *Black-browed Albatrosses* depends on prey availability and predator density.

2. The second dispersal mechanism is termed as "the passive dispersal" in which the dispersal is driven by the local population density of predator. The effects of this dispersal strategy have been well studied by many researchers Jansen (1995); Matthysen (2005); Nguyen-Ngoc et al. (2012); Poggiale (1998); Namba (1980); Jánosi and Scheuring (1997); Silva et al. (2001); Hastings (1983). For example overcrowding of predators in a patch may decrease the resource assessment that can constitute a cue for for the local predators to move. Following this inference, the net dispersal of predators using "the passive dispersal" at Patch i is given by

$$\rho_i \left(y_j - y_i \right).$$

Motivated by the field work of Kiester and Slatkin (1974) on Iguanid lizards and Kummel et al. (2013) on Coccinellids, we incorporate the two dispersal strategies above into our model via a parameter $s \in [0,1]$ representing the proportion of predator population using

the passive dispersal strategy as follows:

$$
\begin{aligned}
\frac{dx_1}{dt} &= x_1\left(1-\frac{x_1}{K_1}\right)-\frac{a_1x_1y_1}{1+x_1}\\
\frac{dy_1}{dt} &= \frac{a_1x_1y_1}{1+x_1}-d_1y_1+\rho_1(1-s)\left(\underbrace{\frac{a_1x_1y_1}{1+x_1}}_{\text{attraction strength to Patch 1}}y_2-\underbrace{\frac{a_2x_2y_2}{1+x_2}}_{\text{attraction strength to Patch 2}}y_1\right)+\rho_1 s\,(y_2-y_1)\\
\frac{dx_2}{dt} &= rx_2\left(1-\frac{x_2}{K_2}\right)-\frac{a_2x_2y_2}{1+x_2}\\
\frac{dy_2}{dt} &= \frac{a_2x_2y_2}{1+x_2}-d_2y_2+\rho_2(1-s)\left(\underbrace{\frac{a_2x_2y_2}{1+x_2}}_{\text{attraction strength to Patch 2}}y_1-\underbrace{\frac{a_1x_1y_1}{1+x_1}}_{\text{attraction strength to Patch 1}}y_2\right)+\rho_2 s\,(y_1-y_2)\,.
\end{aligned}
\tag{2.3}
$$

where $r=\frac{r_2}{r_1}$.

First, we have the following theorem regarding the basic dynamical properties of Model (2.3):

Theorem 1. *Assume that all parameters are positive. Model* (2.3) *is positively invariant and bounded in* $\mathbb{R}^4_+$. *In addition, the set* $\{(x_1,y_1,x_2,y_2)\in\mathbb{R}^4_+ : x_i=0\}$ *is invariant for both* $i=1,2$.

Our main focus is to explore how the combinations of two different dispersal strategies measured by the parameter $s\in[0,1]$ affect the two patch population dynamics. Before we continue, we first provide a summary of the dynamics of the subsystems of Model (2.3) including the cases of $s=0$ and $s=1$.

In the absence of dispersal in predator, Model (2.3) is reduced to the rescaled Rosenzweig and MacArthur (1963) prey-predator single patch model (2.2) with $i=1,2$

$$
\begin{aligned}
\frac{dx_i}{dt} &= \frac{r_i}{r_1}x_i\left(1-\frac{x_i}{K_i}\right)-\frac{a_ix_iy_i}{1+x_i}\\
\frac{dy_i}{dt} &= \frac{a_ix_iy_i}{1+x_i}-d_iy_i
\end{aligned}
$$

where $\frac{r_2}{r_1} = r$. For convenience, let $\mu_i = \frac{d_i}{a_i - d_i}$, and $\nu_i = \frac{r_i(K_i-\mu_i)(1+\mu_i)}{a_i K_i}$ $i = 1,2$, then the global dynamics of the single patch model (2.2) can be summarized from the work of Liu and Chen (2003); Hsu et al. (1977); Hsu (1978) as follows:

1. Model (2.2) always has two boundary equilibria $(0,0)$, $(K_i,0)$ where the extinction $(0,0)$ is always a saddle.

2. The boundary equilibria $(K_i,0)$ is globally asymptotically stable if $\mu_i > K_i$.

3. If $\frac{K_i-1}{2} < \mu_i < K_i$, then $(K_i,0)$ becomes saddle and the unique interior equilibria (μ_i,ν_i) emerges which is globally asymptotically stable.

4. If $0 < \mu_i < \frac{K_i-1}{2}$, the boundary equilibrium $(K_i,0)$ is a saddle, and the unique interior equilibrium (μ_i,ν_i) is a source where Hopf bifurcation occurs at $\mu_i = \frac{K_i-1}{2}$. The system (2.2) has a unique stable limit cycle.

The summary on the dynamics of Model (2.3) when the dispersal of predator foraging activities is driven by local population density (i.e., $s = 1$) and when the dispersal of predator foraging activities is driven by predation strength (i.e. $s = 0$) are briefly presented in Table 2.3 (see Kang et al. (2017) for more detailed summary on the global dynamics).

2.4 Mathematical Analysis

From Theorem 1, we know that the set $\{(x_1,y_1,x_2,y_2) \in \mathbb{R}^4_+ : x_i = 0\}$, is invariant for both $i = 1,2$. Assume that $x_j = 0$, Model (2.3) is reduced to the following three species subsystem:

$$\begin{aligned}
\frac{dx_i}{dt} &= r_i x_i \left(1 - \frac{x_i}{K_i}\right) - \frac{a_i x_i y_i}{1 + x_i} \\
\frac{dy_i}{dt} &= \frac{a_i x_i y_i}{1 + x_i} - d_i y_i + \rho_i (1-s) \left(\frac{a_i x_i y_i}{1 + x_i} y_j\right) + \rho_i s (y_j - y_i) \\
\frac{dy_j}{dt} &= -d_j y_j - \rho_j (1-s) \left(\frac{a_i x_i y_i}{1 + x_i} y_j\right) - \rho_j s (y_j - y_i)
\end{aligned} \tag{2.4}$$

whose basic dynamics are provided in the following theorem:

Theorem 2. *[Basic dynamics of Model* (2.4)*] Let* $\mu_i = \frac{d_i}{a_i - d_i}$ *and* $s \in (0,1)$*, then the following statements of Model* (2.4) *are held:*

1. *Prey* x_i *is persistent with* $\limsup_{t\to\infty} x_i(t) \leq K_i$.

2. *If* $\mu_i > K_i$*, then predators in two patches go extinct, and the system* (2.4) *has global stability at* $(K_i, 0, 0)$.

3. *If* $\rho_i s < \frac{(a_i - d_i)(K_i - \mu_i)}{1+K_i}$*, then predators in the two patches are persistent.*

Notes. Model (2.4) can apply to the case where Patch i is the source patch with prey population and Patch j is the sink patch without prey population. The predator in the sink patch is migrated from the source patch. Theorem 2 indicates the follows regarding the effects of the proportion of predator using the passive dispersal on Model (2.4):

1. Prey x_i of Model (2.4) is always persistent for all $r_i > 0$. This is different than the case of $s = 1$ since prey may go extinct when $s = 1$.

2. If $\mu_i < K_i$ and $\rho_i s$ is small enough, then the inequality $\rho_i s < \frac{(a_i - d_i)(K_i - \mu_i)}{1+K_i}$ holds, hence predators persist. This result suggests that, under the condition of $\mu_i < K_i$, the large value of $\rho_i s$ could drive predator extinction in two patches at least locally.

The interior equilibria (x_1^*, y_1^*, y_2^*) of Model (2.4) is determined by first solving for y_i^* and x_i^* in $\frac{dx_i}{dt} = 0$ and $\frac{dy_j}{dt} = 0$ as follows:

$$\begin{aligned} \frac{dx_i}{dt} = 0 \quad &\Rightarrow \quad y_i^* = \frac{r_i(K_i - x_i^*)(1 + x_i^*)}{a_i K_i} \\ \frac{dy_j}{dt} = 0 \quad &\Rightarrow \quad x_i^* = \frac{-\rho_j s y_i^* + \rho_j s y_j^* + d_j y_j^*}{a_i \rho_j s y_i^* y_j^* - a_i \rho_j y_i^* y_j^* + \rho_j s y_i^* - \rho_j s y_j^* - d_j y_j^*} \end{aligned} \tag{2.5}$$

An equation of y_j^* is obtained by solving the following equation from Model (2.4):

$$\frac{dy_i}{dt}\rho_j + \frac{dy_j}{dt}\rho_i = \frac{a_i x_i y_i}{1 + x_i}\rho_j - d_i y_i \rho_j - d_j y_j \rho_i = 0 \quad \Rightarrow \quad y_j^* = \frac{\rho_j y_i^* (-a_i x_i^* + d_i x_i^* + d_i)}{d_j \rho_i (x_i^* + i)} \tag{2.6}$$

A substitution of y_i^* from (2.5) into y_j^* gives $y_j^* = \frac{r_i(K_i - x_i^*)[x_i^*(a_i - d_i) - d_i]\rho_j}{a_i K_i d_j \rho_i}$. The discussion above implies that the existence of the interior equilibrium requires $a_i > d_i$ and $\mu_i = \frac{d_i}{a_i - d_i} < x_i^* < K_i$ otherwise $y_j^* < 0$ or $y_i^* < 0$. Define

$$f_{t_i}(x_i) = K_i(1+x_i)[(a_i - d_i)(d_j + s\rho_j) - d_j s\rho_i] - K_i a_i(d_j + s\rho_j)$$

$$f_{b_i}(x_i) = [d_i - (a_i - d_i)x_i][K_i(d_j + s\rho_j) + r_i\rho_j(1-s)(1+x_i)(1+K_i)] + d_j K_i s(1+x_i)\rho_i.$$

Then we can conclude that x_i^* solving from Equation (2.5) is in term of y_i^* and y_j^*. Upon substitution of y_i^* and y_j^* into x_i^* we obtain the following nullclines:

$$\begin{aligned} x_i &= \frac{K_i(1+x_i)[(a_i - d_i)(d_j + s\rho_j) - d_j s\rho_i] - K_i a_i(d_j + s\rho_j)}{[d_i - (a_i - d_i)x_i][K_i(d_j + s\rho_j) + r_i\rho_j(1-s)(1+x_i)(1+K_i)] + d_j K_i s(1+x_i)\rho_i} = \frac{f_{t_i}(x_i)}{f_{b_i}(x_i)} \\ &\Leftrightarrow \\ x_i f_{b_i}(x_i) - f_{t_i}(x_i) &= \underbrace{[x_i^3 - (\mu_i + K_i)x_i^2 - \alpha_i x_i + \beta_i]}_{f_i(x_i)}[x_i + 1] = 0 \end{aligned} \tag{2.7}$$

with $\beta_i = \frac{\left[d_j\rho_i s + d_i(d_j + \rho_j s)\right]K_i}{r_i(a_i - d_i)(1-s)\rho_j}$ and

$$\alpha_i = \frac{[d_j s\rho_i + r_i d_i(1-s) - (a_i - d_i)(d_j + s\rho_j)]K_i}{r_i(a_i - d_i)(1-s)\rho_j} = \beta_i + \frac{[r_i d_i(1-s) - a_i(d_j + s\rho_j)]K_i}{r_i(a_i - d_i)(1-s)\rho_j}.$$

Based on the arguments above and additional analysis, we have the following proposition regarding the existence of the interior equilibria of Model (2.4):

Proposition 1. *Model* (2.4) *can have up to two interior equilibria* $E^{\ell}_{x_i,y_i,y_j} = (x_{i\ell}^*, y_{i\ell}^*, y_{j\ell}^*), \ell = 1,2$. *More specifically,*

1. *If* $a_i < d_i$ *or* $K_i < \mu_i$ *or* $(\mu_i + K_i)^2 + 3\alpha_i < 0$, *Model* (2.4) *has no interior equilibrium.*
2. *If* $\frac{3\beta_i}{\mu_i + K_i} < \alpha_i < (\mu_i + K_i)^2$, *then* $f_i(x_i)$ *has two positive roots* $x_{i\ell}^*, \ell = 1,2$. *If, in addition,* $\mu_i < x_{i\ell}^* < K_i$ *for both* $\ell = 1,2$, *then Model* (2.4) *has two interior equilibria.*

Notes. Proposition (1) implies that even if $f_i(x_i)$ has two positive real roots, Model (2.4) may have none or one interior equilibrium unless these two positive roots are in (μ_i, K_i).

Note that the interior equilibria of the subsystem Model (2.4) represent the boundary equilibria of Model (2.3) when $x_1 = 0 (i = 2)$ or $x_2 = 0 (i = 1)$. The existence of these boundary equilibria of Model (2.3) when $x_1 = 0$ or $x_2 = 0$ are hence guarantee by the conditions to obtain the interior equilibria $E^{\ell}_{x_i,y_i,y_j}$ and $E^{\ell}_{y_j,x_i,y_i}$ from Proposition (1).

In order to capture the dynamics of the interior equilibria of Model 2.4, we perform bifurcation simulations with respect to the proportion of predators using the passive dispersal, i.e., the values of s. Our analysis implies that Model (2.4) can have up to two interior equilibria $E^{\ell}_{x_1,y_1,y_2} = (x^*_{1\ell}, y^*_{1\ell}, y^*_{2\ell})$ (for $i = 1$) and $E^{\ell}_{y_1,x_2,y_2} = (\hat{y}^*_{1\ell}, \hat{x}^*_{2\ell}, \hat{y}^*_{2\ell})$ $\ell = 1, 2$ (for $i = 2$). We fix the following parameter values,

$$r_1 = 1,\ r_2 = 1.8,\ d_2 = 0.35,\ K_1 = 10,\ K_2 = 7,\ a_2 = 1.4,\ \rho_1 = 1,\ \rho_2 = 2.5.$$

These fixed values implies that at Patch 2, prey and predator coexist in the form of a unique stable limit cycle in the absence of dispersal since $\mu_2 = \frac{d_2}{a_2 - d_2} = 35/105 < (K_2 - 1)/2 = 3$. We consider the following two typical cases regarding the population dynamics of prey and predator in the absence of dispersal:

1. $d_1 = 0.85,\ a_1 = 1$: Predator and prey are persistent and have global equilibrium dynamics at Patch 1 in the absence of dispersal since $(K_1 - 1)/2 = 4.5 < \mu_1 = \frac{d_1}{a_1 - d_1} = 17/3 < 10 = K_1$.

2. $d_1 = 2,\ a_1 = 2.1$: Predator goes extinct globally at Patch 1 in the absence of dispersal since $\mu_1 = \frac{d_1}{a_1 - d_1} = 20 > K_1 = 10$.

The fixed values of parameters and the two cases above provide the following four scenarios:

1. $i = 1$ (i.e., $x_2 = 0$ for Model (2.3)) with $d_1 = 0.85,\ a_1 = 1$. In this case, Patch 1 is the source patch and Model (2.4) can have up to two interior equilibria depending on the values of s (see Figure 2.1(a)).

2. $i = 1$ (i.e., $x_2 = 0$ for Model (2.3)) with $d_1 = 2,\ a_1 = 2.1$. In this case, Patch 1 is the source patch and Model (2.4) has no interior equilibria according to Proposition (1).

3. $i = 2$ (i.e., $x_1 = 0$ for Model (2.3)) with $d_1 = 0.85,\ a_1 = 1$. In this case, Patch 2 is the source patch and Model (2.4) can have up to two interior equilibria depending on the values of s (see Figure 2.1(b)). The relative large value of s can stablize the dynamics (see the blue region of Figure 2.1(b)).

4. $i = 2$ (i.e., $x_1 = 0$ for Model (2.3)) with $d_1 = 2,\ a_1 = 2.1$. In this case, Patch 2 is the source patch and Model (2.4) can have up to two interior equilibria depending on the values of s (see Figure 2.1(c)). The relative large value of s can stablize the dynamics (see the blue region of Figure 2.1(c)).

Scenarios	$\mathbf{a_1 = 1}$ and $\mathbf{d_1 = 0.85}$				$\mathbf{a_1 = 2.1}$ and $\mathbf{d_1 = 2}$		
	$\mathbf{E^1_{x_1y_1y_2}}$	$\mathbf{E^2_{x_1y_1y_2}}$	$\mathbf{E^1_{y_1x_2y_2}}$	$\mathbf{E^2_{y_1x_2y_2}}$	$\mathbf{E^{1,2}_{x_1y_1y_2}}$	$\mathbf{E^1_{y_1x_2y_2}}$	$\mathbf{E^2_{y_1x_2y_2}}$
$s \leq 0.1$	LAS	✗	Saddle	✗	✗	Saddle	✗
$0.15 \leq s \leq 0.45$	LAS	Saddle	Saddle	✗	✗	Saddle	✗
$0.55 \leq s \leq 0.62$	✗	✗	Saddle	✗	✗	LAS	Saddle
$0.68 < s < 0.82$	✗	✗	LAS	Saddle	✗	✗	✗
$s \geq 0.82$	✗	✗	✗	✗	✗	✗	✗

Table 2.1: Summary of the Effect of the Proportion of Predators Using the Passive Dispersal on Model (2.4) From Figures 2.1(a), 2.1(b), and 2.1(c). LAS Refers to Local Asymptotical Stability And ✗ Implies the Equilibrium Does Not Exist.

The bifurcation diagrams (Figure 2.1) suggest that the proportion of predators using the passive dispersal can have huge impacts on the number of interior equilibria of Model (2.4): For the small values of s, Model (2.4) can have one interior equilibrium ($E^1_{x_1,y_1,y_2}$ or $E^1_{y_1,x_2,y_2}$); For the intermediate values of s, Model (2.4) can have two interiors $E^l_{x_1,y_1,y_2}, l = 1,2$ ($i = 1$) or $E^l_{y_1,x_2,y_2}, l = 1,2$ ($i = 2$); For the large values of s, it has no interior equilibria.

A more detail description of the effects of s on the interior equilibria of Model (2.4) is provided in Table (2.1).

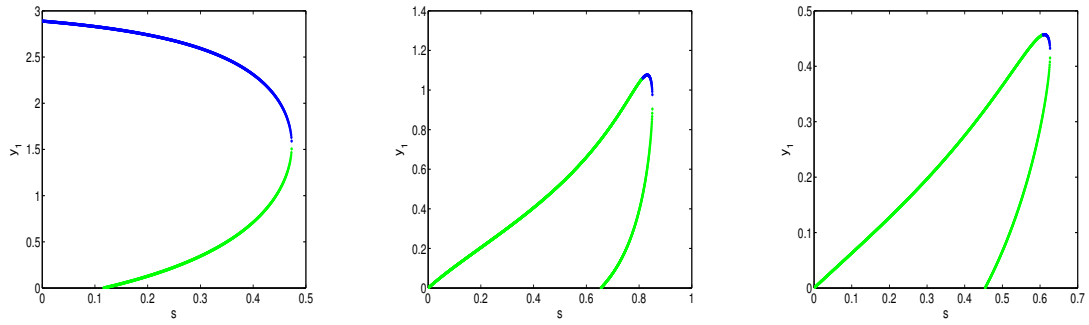

(a) Effect of dispersal strategy when $x_2 = 0, d_1 = 0.85, a_1 = 1$

(b) Effect of dispersal strategy when $x_1 = 0, d_1 = 0.85, a_1 = 1.$

(c) Effect of dispersal strategy when $x_1 = 0, d_1 = 2, a_1 = 2.1.$

Figure 2.1: One Parameter Bifurcation Diagrams of Model (2.4) with y-axis Representing the Population Size of Predator at Patch 1 and x-axis Represent the Proportion of Predator Using the Passive Dispersal. Figure 2.1(a) Describes the Number of Interior Equilibria $(\hat{x}_1^*, \hat{y}_1^*, \hat{y}_2^*)$. Figure 2.1(b) and 2.1(c) Describe the Number of Interior Equilibria (y_1^*, x_2^*, y_2^*). Blue Represents the Sink and Green Represents the Saddle.

2.4.1 Boundary Equilibria and Global Dynamics of Model (2.3)

First, we have boundary equilibria and global dynamics of Model (2.3) in the following theorem.

Theorem 3. *[Boundary equilibria and global dynamics of Model* (2.3)*] Assume that* $s \in (0,1)$. *Model* (2.3) *always has the following four boundary equilibrium*

$$E_{0000}, E_{K_1000}, E_{00K_20}, E_{K_10K_20}$$

with the first three always being saddle. $E_{K_10K_20}$ *is locally asymptotically stable if the follwoing two inequalities in* (2.8) *hold:*

$$\begin{aligned} &\sum_{i=1}^{2}\left[\frac{(a_i-d_i)(\mu_i-K_i)}{1+K_i}+s\rho_i\right]>0 \\ &\text{and} \\ &\left[\frac{(a_1-d_1)(\mu_1-K_1)}{1+K_1}\right]\left[s\rho_2+\frac{(a_2-d_2)(\mu_2-K_2)}{1+K_2}\right]+s\rho_1\left[\frac{(a_2-d_2)(\mu_2-K_2)}{1+K_2}\right]>0. \end{aligned} \tag{2.8}$$

And $E_{K_1 0 K_2 0}$ is saddle when one or both of equations (2.8) *are not satisfied. In addition,*

1. *Model* (2.3) *is globally stable at $E_{K_1 0 K_2 0}$ if $\mu_i > K_i$ for both $i = 1, 2$.*

2. *At least prey population in one patch of Model* (2.3) *is persistent, and the predator population in each patch is persistent if $\mu_i < K_i$ for both $i = 1, 2$.*

Notes. Theorem 3 indicates that the global stability of the boundary equilibrium $E_{K_1 0 K_2 0}$ does not depend on the proportion of predator population using the passive dispersal since $E_{K_1 0 K_2 0}$ is globally asymptotically stable when $\mu_i > K_i, i = 1, 2$ which is independent of s. However, the value of $s > 0$ and $\rho_i, i = 1, 2$ can stabilize $E_{K_1 0 K_2 0}$. For example, assume that $\mu_i < K_i$ and $\mu_j > K_j$, then in the absence of dispersal, the boundary equilibrium $E_{K_1 0 K_2 0}$ is a saddle. In the presence of the dispersal, according to Theorem 3, if we choose ρ_j large enough, then $E_{K_1 0 K_2 0}$ can be locally stable, thus the large dispersal at one patch may stabilize the boundary equilibrium $E_{K_1 0 K_2 0}$. However, if $s = 0$, then dispersal has no such effects.

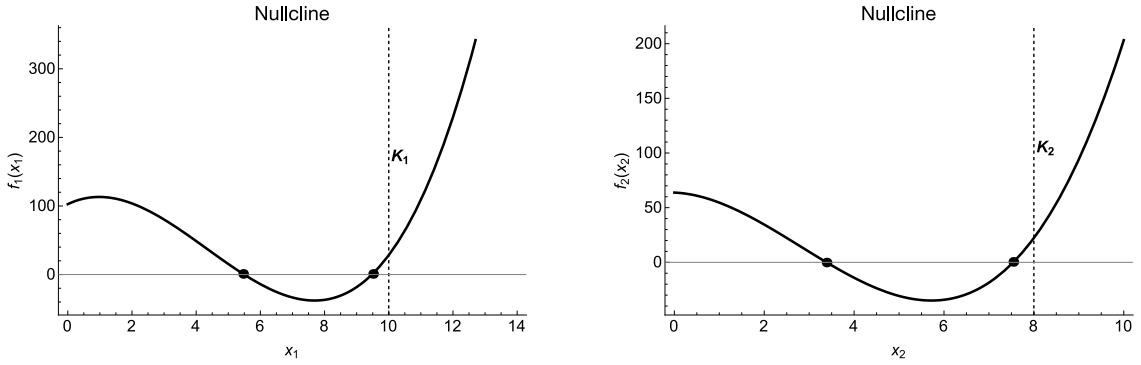

(a) Number of boundary equilibria when $x_2 = 0$

(b) Number of boundary equilibria when $x_1 = 0$

Figure 2.2: Boundary Equilibria $E^b_{1\ell} = (x^*_{1\ell}, y^*_{1\ell}, 0, y^*_{2\ell})$ and $E^b_{2\ell} = (0, \hat{y}^*_{1\ell}, \hat{x}^*_{2\ell}, \hat{y}^*_{2\ell})$. The Solid Lines are $f_1(x_1)$ and $f_2(x_2)$ While The Dashed Lines Are K_1 and K_2 Which Illustrates the Existence of Boundary Equilibria When $K_1 > x^*_{1\ell}$ or $K_2 > \hat{x}^*_{2\ell}$, $\ell = 1, 2$. The Black Dots Represent Real Positive $x^*_{1\ell}$ and $\hat{x}^*_{2\ell}$.

Recall from Proposition (1) that the interior equilibria $E^l_{x_1, y_1, y_2}$ and $E^l_{y_1, x_2, y_2}$ $l = 1, 2$ of Model (2.4) correspond to the boundary equilibria $E^b_{1\ell} = (x^*_{1\ell}, y^*_{1\ell}, 0, y^*_{2\ell})$ and $E^b_{2\ell} =$

$(0,\hat{y}^*_{1\ell},\hat{x}^*_{2\ell},\hat{y}^*_{2\ell}),\ \ell=1,2$ of Model (2.3). Based on Proposition (1) , we could conclude that Model (2.3) has four such boundary equilibria. Figures 2.2 provide such an numerical example for the existence of the four boundary equilibria $E^b_{1\ell}=(x^*_{1\ell},y^*_{1\ell},0,y^*_{2\ell})$ and $E^b_{2\ell}=(0,\hat{y}^*_{1\ell},\hat{x}^*_{2\ell},\hat{y}^*_{2\ell})$ under the following parameters:

$$s=0.65,\ r_1=1,\ r_2=0.54,\ d_1=0.45,\ d_2=0.105,\ K_1=10,\ K_2=8,\ a_1=0.6,$$

$$a_2=0.35,\ \rho_1=1.75,\ \rho_2=1.2.$$

We continue our study by analyzing the effects of s on the dynamics of the boundary equilibria $E^b_{1\ell}$ and $E^b_{2\ell}$, $\ell=1,2$ by adopting the same parameters in generating interior equilibria of Model (2.4) shown in Figure 2.1, i.e., let $d_1=0.85$,$a_1=1$ and $d_1=2,\ a_1=2.1$ and

$$r=1.8,\ d_2=0.35,\ K_1=10,\ K_2=7,\ a_2=1.4,\ \rho_1=1,\ \rho_2=2.5.$$

Under these parameter values, we have the following two cases that are shown in Figure 2.3:

1. $d_1=0.85$,$a_1=1$: In this case, Model 2.3 can have up to three boundary equilibria depending on the values of s (see Figures 2.3(a), 2.3(b) and Table 2.2).

2. $d_1=2,\ a_1=2.1$: In this case, Model 2.3 can have up to two boundary equilibria depending on the values of s (see Figures 2.3(c) and Table 2.2).

We recapitulate the following dynamics regarding the effect of s on the equilibria $E^b_{1\ell}$ and $E^b_{2\ell},\ \ell=1,2$: (1) Model (2.3) can have up to four boundary equilibria; (2) These boundary equilibria when exist are locally asymptotically stable or saddle; (3) Large s has a potential to destroy these equilibria. Also, observe the blue line for locally stable and green line for saddle in Figure 2.1(a) as oppose to only green line for saddle in Figure 2.3(a); this results suggest that the additional dimension from the three species Model (2.4) has a destabilization effect on the four species Model (2.3).

Scenarios	$\mathbf{a_1 = 1}$ and $\mathbf{d_1 = 0.85}$				$\mathbf{a_1 = 2.1}$ and $\mathbf{d_1 = 2}$		
	$\mathbf{E^b_{11}}$	$\mathbf{E^b_{12}}$	$\mathbf{E^b_{21}}$	$\mathbf{E^b_{22}}$	$\mathbf{E^b_{11,12}}$	$\mathbf{E^b_{21}}$	$\mathbf{E^b_{22}}$
$s \leq 0.1$	Saddle	✗	Saddle	✗	✗	Saddle	✗
$0.15 \leq s \leq 0.45$	Saddle	Saddle	Saddle	✗	✗	Saddle	✗
$0.55 \leq s \leq 0.62$	✗	✗	Saddle	✗	✗	Saddle	Saddle
$0.68 < s < 0.82$	✗	✗	LAS	Saddle	✗	✗	✗
$s \geq 0.82$	✗	✗	✗	✗	✗	✗	✗

Table 2.2: Summary of the Effect of the Proportion of Predators Using the Passive Dispersal on Model (2.4) From Figures 2.3(a), 2.3(b), and 2.3(c). LAS Refers to Local Asymptotical Stability and ✗ Implies the Equilibrium Does Not Exist.

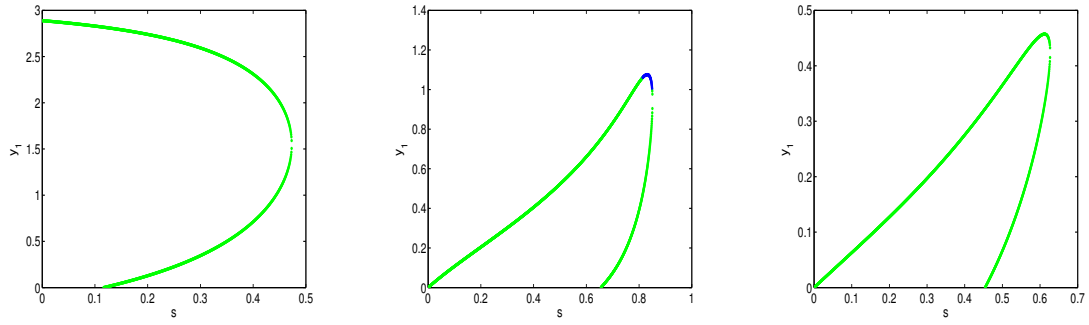

(a) Effect of dispersal strategy when $x_2 = 0, d_1 = 0.85, a_1 = 1$.

(b) Effect of dispersal strategy when $x_1 = 0, d_1 = 0.85, a_1 = 1$.

(c) Effect of dispersal strategy when $x_1 = 0, d_1 = 2, a_1 = 2.1$.

Figure 2.3: One Parameter Bifurcation Diagrams of Model (2.3) With y-axis Representing the Population Size of Predator at Patch 1 And x-axis Represent the Proportion of Predator Using the Passive Dispersal. Figure 2.3(a) Describes the Number of Boundary Equilibria $E^b_{1\ell} = (x^*_{1\ell}, y^*_{1\ell}, 0, y^*_{2\ell}), \ell = 1,2$. Figure 2.3(b) and 2.3(c) Describes the Number of Boundary Equilibria $E^b_{2\ell} = (0, \hat{y}^*_{1\ell}, \hat{x}^*_{2\ell}, \hat{y}^*_{2\ell}), \ell = 1,2$. Blue Represents the Sink and Green Represents the Saddle.

2.4.2 Interior Equilibria and Stability of Model (2.3)

Define $p_i(x) = \frac{a_i x}{1+x}$, $q_i(x) = \frac{r_i(K_i-x)(1+x)}{a_i K_i}$, and recall that $\mu_i = \frac{d_i}{a_i - d_i}$. Then from Model (2.3) we have the following equations

$$\begin{aligned}\frac{dx_i}{dt} &= r_i x_i\left(1-\frac{x_i}{K_i}\right) - \frac{a_i x_i y_i}{(1+x_i)} = \frac{a_i x_i}{1+x_i}\left[\frac{r_i(K_i-x_i)(1+x_i)}{a_i K_i} - y_i\right] \\ &= p_i(x_i)\left[q_i(x_i) - y_i\right].\end{aligned}$$

$$\begin{aligned}\rho_j\frac{dy_i}{dt} + \rho_i\frac{dy_j}{dt} &= \rho_j y_i[\frac{a_i x_i}{1+x_i} - d_i] + \rho_i y_j[\frac{a_j x_j}{1+x_j} - d_j] \\ &= \rho_j y_i[p_i(x_i) - d_i] + \rho_i y_j[p_j(x_j) - d_j]\end{aligned}$$

Consider $(x_1^*, y_1^*, x_2^*, y_2^*)$ as an interior equilibrium of Model (2.3), then the following conditions must be satisfied:

$$q_i(x_i) - y_i = 0 \quad \Leftrightarrow \quad y_i = q_i(x_i)$$

and

$$\rho_j y_i[p_i(x_i) - d_i] + \rho_i y_j[p_j(x_j) - d_j] = 0 \quad \Leftrightarrow \quad \rho_j y_i[p_i(x_i) - d_i] = -\rho_i y_j[p_j(x_j) - d_j] \tag{2.9}$$

which yields the following by substituting the expression of $p_i(x)$ and $q_i(x)$ into (2.9)

$$x_i^2 - (\mu_i + K_i)x_i + \underbrace{\mu_i K_i + \frac{a_i K_i}{a_j K_j}\frac{\rho_i r_j}{\rho_j r_i}\frac{(a_j - d_j)}{(a_i - d_i)}(x_j - \mu_j)(x_j - K_j)}_{\phi_i(x_j)} = 0 \tag{2.10}$$

The equation (3.6) gives the following nullclines:

$$x_i = \frac{(\mu_i + K_i) \pm \sqrt{(\mu_i + K_i)^2 - 4\phi_i(x_j)}}{2} = F_i(x_j),\ i, j = 1, 2,\ i \neq j. \tag{2.11}$$

The complex form of (2.11) prevents us to obtain the explicit solutions of the interior equilibria of Model (2.3). We are going to explore the symmetric interior equilibrium for the symmetric Model (2.3) where we say that Model (2.3) is symmetric if $a_1 = a_2 = a$, $d_1 = d_2 = d$, $K_1 = K_2 = K$, $r_1 = r_2 = r$. Now we have the following theorem:

Theorem 4. *[The symmetric interior equilibrium and the stability] Suppose that Model* (2.3) *is symmetric with* $r = 1$. *We denote*

$$\mu = \frac{d}{a-d}, \text{ and } \nu = \frac{(K-\mu)(1+\mu)}{aK}.$$

Then $E = (\mu, \nu, \mu, \nu)$ *is an unique symmetric interior equilibrium for Model* (2.3). *Moreover,* E *is locally asymptotically stable if* $\frac{K-1}{2} < \mu < K$ *while it is unstable if* $\mu < \frac{K-1}{2}$ *for* $s \in [0,1]$.

Notes. Theorem (4) implies the symmetric Model (2.3) has an unique symmetric interior equilibrium of the form $E = (\mu, \nu, \mu, \nu)$. The related results imply that dispersal of predators and s has no effect on the local stability of this symmetric interior equilibria when it exist since $\frac{K-1}{2} < \mu < K$ does not depend on $\rho_i, i = 1,2$ or s. We note that Model (2.3) can have two additional interior equilibria in the symmetric case which can be locally stable or saddle depending on the value of s (see green line for saddle and blue line for locally stable in Figures 2.4(a) which correspond to the additional two boundary equilibria of Model (2.3) in the symmetric case). We consider the following fixed symmetric parameters:

$$r_1 = r_2 = r = 1,\ d_1 = d_2 = d = 5,\ K_1 = K_2 = K = 10,\ a_1 = a_2 = a = 6.$$

According to the bifurcation diagrams in Figures 2.4(a) and 2.4(b), Model (2.3) can have up to three interior equilibria in the symmetric case. It seems that the larger value of s can create two additional asymmetric interior equilibria which can be saddle or locally stable, thus generate bistability between two different interior attractors (See blue lines in Figure 2.4(a) when $0.78 \leq s \leq 0.92$). The local stability of $E = (\mu, \nu, \mu, \nu)$ does not depend on s as illustrated in Theorem 4.

Define $\mu_i = \frac{d_i}{a_i - d_i}, \nu_1 = \frac{(K_1-\mu_1)(1+\mu_1)}{a_1 K_1}, \nu_2 = \frac{r(K_2-\mu_2)(1+\mu_2)}{a_2 K_2}$, $\hat{\mu}_i = \frac{\hat{d}_i}{a_i - \hat{d}_i}$, $\hat{\nu}_i = q_i(\hat{\mu}_i) = \frac{r_i(K_i-\hat{\mu}_i)(1+\hat{\mu}_i)}{a_i K_i}$, $\hat{\nu}_j^i = \frac{\rho_j \hat{\nu}_i}{d_j+\rho_j}$ where $\hat{d}_i = d_i + \frac{\rho_i d_j}{d_j+\rho_j}$ $i, j = 1,2$, $i \neq j$ and $E_{12}^{b*} = E_{\mu_1 \nu_1 K_2 0}$, $E_{22}^{b*} = E_{K_1 0 \mu_2 \nu_2}$. Then the boundary dynamics for $s = 0,1$ from the work of Jansen (2001); Kang et al. (2017) and $s \in (0,1)$ from our current work is summarize in Table 2.3

Scenarios	**Existence condition, Local and Global stability of Model** (2.3)		
	$\mathbf{s=0}$	$\mathbf{s\in(0,1)}$	$\mathbf{s=1}$
E_{0000}, E_{K_1000}, E_{00K_20}	Always exist and always saddle	Always exist and always saddle	Always exist and always saddle
$E_{K_10K_20}$	Always exist; LAS and GAS if $\mu_i > K_i$ for both $i=1,2$	Always exist; GAS if $\mu_i > K_i$ for both $i=1,2$; while LAS if Equations 2.8 are satisfied	Always exist; GAS if $\mu_i > K_i$ for both $i=1,2$; LAS if condition (1) is satisfied
$E^b_{1\ell}$ $(x_i=0)$, $\ell=1,\ 2,$ $i=1,2$	Do not exist	One or two exist if $\frac{3\beta_j}{\mu_j+K_j} < \alpha_j < (\mu_j+K_j)^2$ with $i,j=1,2,\ i\neq j$; Can be locally asymptotically stable or saddle as shown in Figures 2.3(a), 2.3(b), 2.3(c)	Exist if $0<\hat{\mu}_i<K_i$; LAS if $\frac{K_i-1}{2}<\widehat{\mu}_i<K_i$ and $r_j<a_j\hat{v}^i_j$. GAS if $\frac{K_i-1}{2}<\widehat{\mu}_i<K_i$ and $\frac{r_j(K_j+1)^2}{4a_jK_j}<\widehat{v}^j_i$, $i,j=1,2,i\neq j$.
E^{b*}_{i2}, $i,j=1,2,$ $i\neq j$	Exist if $0<\mu_i<K_i$; LAS if $\frac{K_i-1}{2}<\mu_i<K_i$ and condition (2) is satisfied	Do not exist	Do not exist
Cond. 1:	$\sum_{i=1}^{2}\left[\frac{(a_i-d_i)(\mu_i-K_i)}{1+K_i}+\rho_i\right]>0$ and $\left[\frac{(a_1-d_1)(\mu_1-K_1)}{1+K_1}\right]\left[\rho_2+\frac{(a_2-d_2)(\mu_2-K_2)}{1+K_2}\right]+\rho_1\left[\frac{(a_2-d_2)(\mu_2-K_2)}{1+K_2}\right]>0$		
Cond. 2:	$0<\frac{d_i}{a_j-d_i}<K_j<\mu_j$ and $\rho_j<\frac{d_j-K_j(a_j-d_j)}{v_i\left[K_j(a_j-d_i)-d_i\right]}$; $i,j=1,2,i\neq j$		

Table 2.3: Summary of the local and global dynamic of Model (2.3). LAS refers to the local asymptotical stability, GAS refers to the global stability, and Cond. refers to condition.

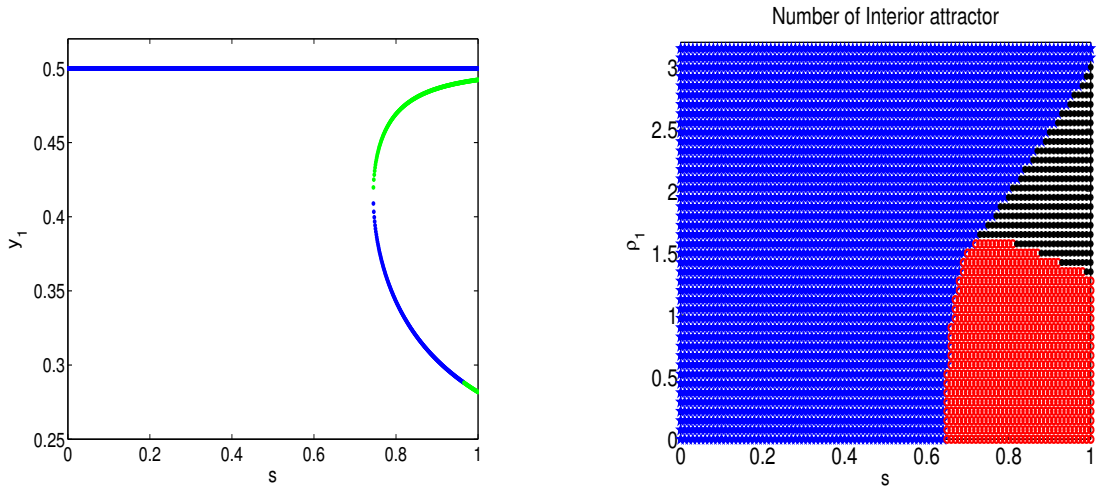

(a) s V.S. y_1 for the effect of s when Model (2.3) is symmetric with $\rho_1 = 1.72$ and $\rho_2 = 13$

(b) s V.S. ρ_1 for the number of interior equilibria when Model (2.3) is symmetric and $\rho_2 = 13$

Figure 2.4: One and Two Parameter Bifurcation Diagrams of Symmetric Model (2.3) with y-axis Representing the Population Size of Predator at Patch 1 in Figure 2.4(a). Blue Line Represents Sink and Green Line Represents Saddle Interior Equilibria in Figure 2.4(a). Black Region Have Three Interior Equilibria; Red Regions Have Two Interior Equilibria; And Blue Regions Have One Interior Equilibrium in Figure 2.4(b).

2.5 Effects of Dispersal Strategies on the Prey-predator Population Dynamics

In order to get more insights into the dynamics of Model (2.3), we perform bifurcation analysis in this section. We fixed the following parameters for most of the simulations

$$r = 1.8,\ d_2 = 0.35,\ K_1 = 10,\ K_2 = 7,\ a_2 = 1.4,\ \rho_1 = 1,\ \rho_2 = 2.5.$$

and consider these two cases: $d_1 = 0.85,\ a_1 = 1$ and $d_1 = 2,\ a_1 = 2.1$. According to the dynamics of the subsystem Model (2.2) provided in Section 2.3, we know that in the absence of dispersal, Patch 1 has global stability at $(10,0)$ if $\frac{d_1}{a_1-d_1} > 10$ (e.g., when $d_1 = 2,\ a_1 = 2.1$) and it has global stability at its unique interior $\left(\frac{d_1}{a_1-d_1}, \frac{\left(10-\frac{d_1}{a_1-d_1}\right)\left(1+\frac{d_1}{a_1-d_1}\right)}{10a_1}\right)$ if $4.5 < \frac{d_1}{a_1-d_1} < 10$ (e.g., when $d_1 = 0.85,\ a_1 = 1$); while Patch 2 has a unique stable limit cycle since $d_2 = 0.35,,\ K_2 = 7,\ a_2 = 1.4$.

We implement one and two parameters bifurcation diagrams to obtain insights into the dynamical patterns of the asymmetric two patch Model (2.3) in the following way:

1. $d_1 = 0.85$ and $a_1 = 1$:

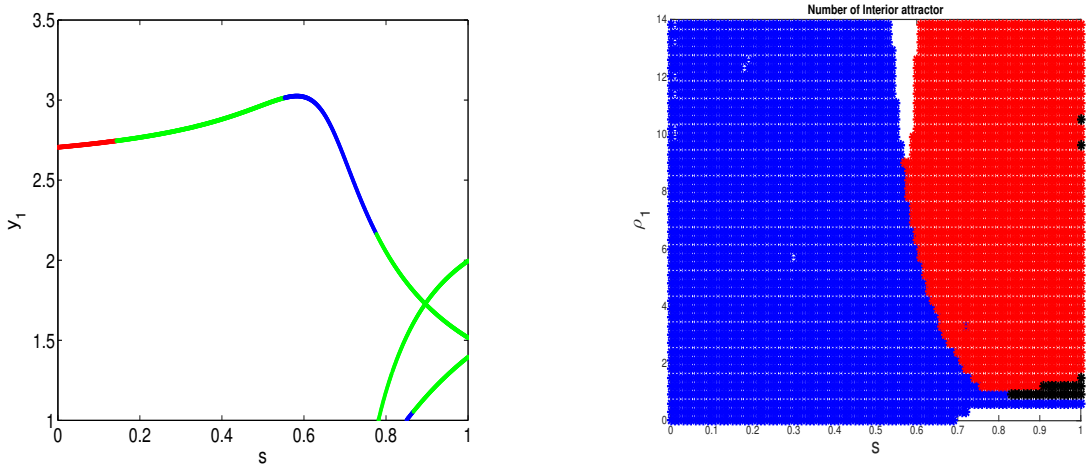

(a) s V.S. y_1 for the effect of s when $d_1 = 0.85$, $a_1 = 1$, $\rho_1 = 1$, and $\rho_2 = 2.5$

(b) s V.S. y_1 for the number of interior equilibria when $d_1 = 0.85$, $a_1 = 1$, and $\rho_2 = 2.5$

Figure 2.5: One and Two Parameter Bifurcation Diagrams of Model (2.3) with y-axis Representing the Population Size of Predator at Patch 1 in Figure 2.5(a). Blue Line Represents Sink, Green Line Represents Saddle, and Red Line Represents Source Interior Equilibria in Figure 2.5(a). Black Region Have Three Interior Equilibria; Red Regions Have Two Interior Equilibria; Blue Regions Have One Interior Equilibrium, and White Regions Have No Interior Equilibria in Figure 2.5(b).

In the absence of dispersal, the uncoupled two patch model is unstable at the interior equilibrium $(5.67, 288.89, 0.33, 80)$. However, in the presence of the dispersal, Figure 2.5(a) (blue regions) suggest that the intermediate values of s can stabilize the dynamics while the large values of s with certain dispersal strengths could generate multiple interior equilibria (up to three interior equilibria), thus lead to multiple attractors potentially. Moreover, two dimensional bifurcation diagram shown in Figure 2.5(b) suggest that the large values of s combined with the small or large dispersal strength ρ_1 in Patch 1 can destroy the interior equilibria (see white regions in Figure 2.5(b)) with consequences that prey in one patch may go extinct but predator persists

in each patch. Table (2.4) provides a more details description on the existence and stability of the interior equilibria of Model (2.3).

Scenarios	$\mathbf{a_1 = 1}$ and $\mathbf{d_1 = 0.85}$			$\mathbf{a_1 = 2.1}$ and $\mathbf{d_1 = 2}$		
	$\mathbf{E^1_{x_1y_1x_2y_2}}$	$\mathbf{E^2_{x_1y_1x_2y_2}}$	$\mathbf{E^3_{x_1y_1x_2y_2}}$	$\mathbf{E^1_{x_1y_1x_2y_2}}$	$\mathbf{E^2_{x_1y_1x_2y_2}}$	$\mathbf{E^3_{x_1y_1x_2y_2}}$
$s \leq 0.07$	Source	✗	✗	Saddle	Source	LAS
$0.9 \leq s \leq 0.15$	Source	✗	✗	Saddle	Saddle	LAS
$0.2 \leq s \leq 0.43$	Saddle	✗	✗	LAS	Saddle	Saddle
$0.55 \leq s \leq 0.68$	LAS	✗	✗	LAS	✗	✗
$0.78 \leq s \leq 0.82$	Saddle	Saddle	✗	Saddle	✗	✗
$0.83 \leq s \leq 0.84$	Saddle	Saddle	LAS	Saddle	✗	✗
$s \geq 0.84$	Saddle	Saddle	Saddle	Saddle	✗	✗

Table 2.4: Summary of The Effect of the Proportion of Predators Using the Passive Dispersal on the Interior Equilibria of Model (2.3) From Figures 2.5(a), and 2.6(a). LAS Refers to Local Asymptotical Stability, ✗ Implies the Equilibrium Does Not Exist, and $E^i_{x_1y_1x_2y_2}, i = 1,2,3$ Are the Three Possible Interior Equilibria of Model (2.3).

2. $d_1 = 2$ and $a_1 = 2.1$:

   In the absence of dispersal, the uncoupled two patch model has extinction of predator in Patch 1 and is unstable at the boundary equilibrium $(10, 0, 0.33, 80)$. However, in the presence of the dispersal, Figure 2.6(a) (blue regions) suggest that the intermediate values of s can stabilize the dynamics while the small values of s with certain dispersal strengths could generate multiple interior equilibria (up to three interior equilibria), thus lead to multiple attractors potentially. Moreover, two dimensional bifurcation diagram shown in Figure 2.6(b) suggest that the large values of s combined with the large dispersal strength ρ_1 in Patch 1 can destroy the interior equilibria (see white regions in Figure 2.5(b)) with consequences that prey in one patch may go extinct but predator persists in each patch. A more detail dynamic from Figure 2.6(b) is presented in Table (2.4).

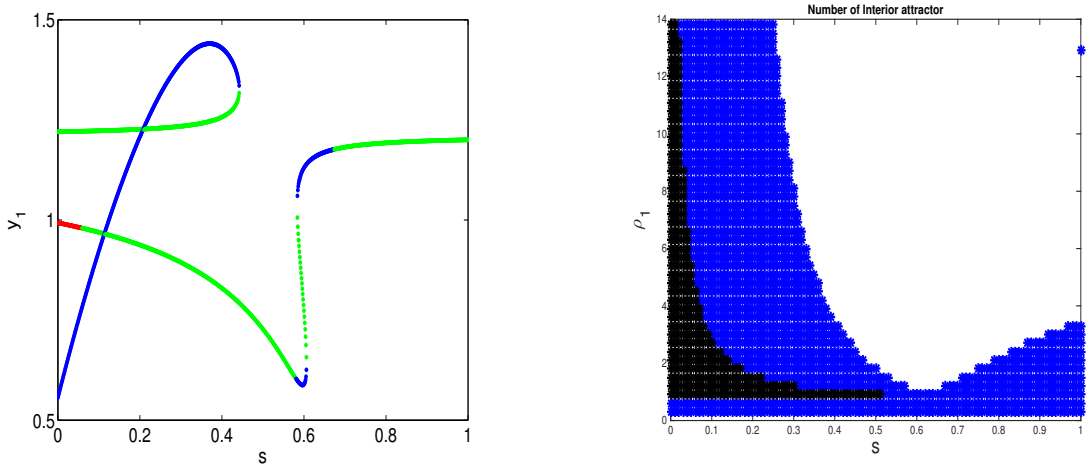

(a) s V.S. y_1 for the effect of s when $d_1 = 2$, $a_1 = 2.1$, $\rho_1 = 1$, and $\rho_2 = 2.5$

(b) s V.S. ρ_1 for the number of interior equilibria when $d_1 = 2$, $a_1 = 2.1$, and $\rho_2 = 2.5$

Figure 2.6: One and Two Parameter Bifurcation Diagrams of Model (2.3) with y-axis Representing the Population Size of Predator at Patch 1 in Figure 2.6(a). Blue Line Represents Sink, Green Line Represents Saddle, and Red Line Represents Source Interior Equilibria in Figure 2.6(a). Black Region Have Three Interior Equilibria; Red Regions Have Two Interior Equilibria; Blue Regions Have One Interior Equilibrium, and White Regions Have No Interior Equilibria in Figure 2.6(b).

3. Two parameter bifurcation diagrams of the relative dispersal rate ρ_2 versus the dispersal strategy s for both scenarios of $d_1 = 0.85,\ a_1 = 1$ (Figure 2.7(a)) and $d_1 = 2,\ a_1 = 2.1$ (Figure 2.7(b)). For both cases, the large s combined with the large dispersal strength in Patch 2, i.e., ρ_2, can destroy the interior equilibrium (see white regions in Figures 2.7(a) and 2.7(b) for $s > 0.6$); while the small s (for $d_1 = 0.85,\ a_1 = 1$) and the large value of s (for $d_1 = 2,\ a_1 = 2.1$) could generate multiple interior equilibria (see black region for three interior equilibria and red region for two interior equilibria in Figure 2.7(a) and 2.7(b)).

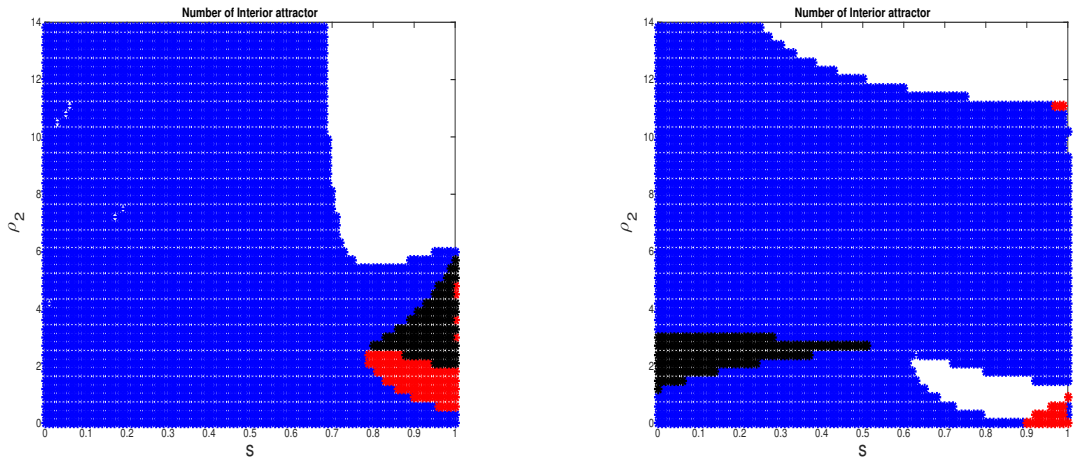

(a) s V.S. ρ_2 for the number of interior equilibria when $d_1 = 0.85$ and $a_1 = 1$

(b) s V.S. ρ_2 for the number of interior equilibria when $d_1 = 2$ and $a_1 = 2.1$

Figure 2.7: Two Parameters Bifurcation Diagrams of Model (2.3) with y-axis Representing the Relative Dispersal Rate ρ_2 and x-axis Represent the Strength of Dispersal Mode s. Black Region Have Three Interior Equilibria; Red Regions Have Two Interior Equilibria; Blue Regions Have One Interior Equilibrium, and White Regions Have No Interior Equilibria in Figures 2.7(a) and 2.7(b).

No interior equilibrium but all species coexist with fluctuating dynamics: Our discussions above suggest that the large values of s can destroy the interior equilibrium (see white regions in Figures 2.5(b), 2.6(b), 2.7(a) and 2.7(b)). Thus, the system is not permanent based on the fixed point theorem. However, our time series (e.g., Figures 2.8(a) and 2.8(b)) suggest that for almost all strictly positive initial conditions, both prey and predator can coexist through fluctuating dynamics for some white regions of Figures 2.7(a) and 2.7(b).

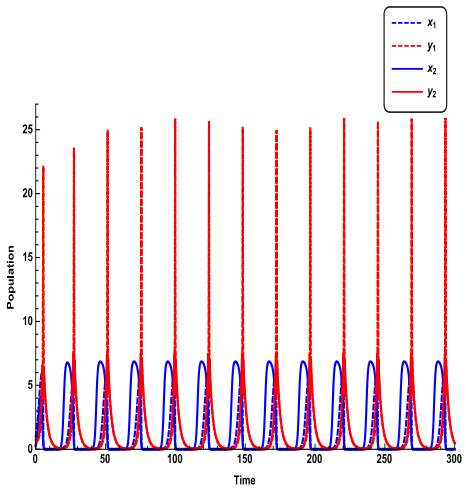

(a) Time series of Model 2.3 when $a_1 = 1$, $d_1 = 0.85$, $s = 0.55$, $\rho_1 = 13$, $x_1(0) = 1$, $y_1(0) = 0.25$, $x_2(0) = 0.3$, and $y_2(0) = 0.7$.

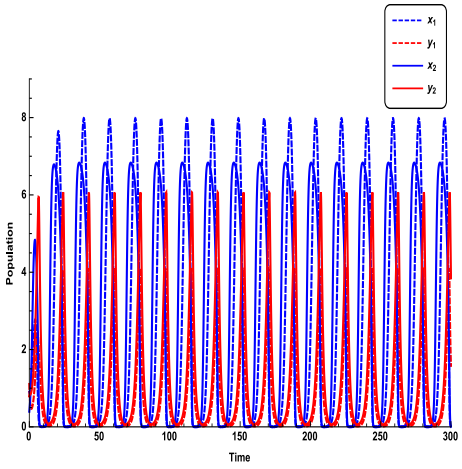

(b) Time series of Model 2.3 when $a_1 = 2.1$, $d_1 = 2$, $\rho_1 = 1$, $\rho_2 = 0.75$, $s = 0.85$, $x_1(0) = 0.9$, $y_1(0) = 1.1$, $x_2(0) = 0.4$, and $y_2(0) = 0.8$

Figure 2.8: Time Series of Model 2.3 when $r = 1.8$, $d_2 = 0.35$, $k_1 = 10$, $k_2 = 7$, and $a_2 = 1.4$. Figures 2.8(a) and 2.8(b) Illustrate the Coexistence of Prey and Predator Through Fluctuating Dynamics While Model 2.3 Has No Interior Equilibria. The Blue Dashed Lines Represent the Prey Population in Patch 1, the Dashed Red Lines Represent the Predator Population in Patch 1, the Blue Solid Lines Is the the Prey Population in Patch 2, and the Red Solid Lines Represent Predator Population in Patch 2.

The proportion of the predators population engaging in the passive dispersal, i.e., s, has profound impacts on the population dynamics of prey and predator presented by Model (2.3) which generate complicated dynamics including different types of multiple attractors.

Boundary attractor versus an interior attractor through two interior equilibria: When Model (2.3) has two interior equilibria, the typical dynamics are that Model (2.3) either converges to a boundary attractor or the interior attractor depending initial conditions. We provide an example in Figures 2.9(a), and 2.9(b) where $a_1 = 1$, $d_1 = 0.85$, $s = 0.8$ and

$$r = 1.8,\ d_2 = 0.35,\ K_1 = 10,\ K_2 = 7,\ a_2 = 1.4,\ \rho_1 = 1,\ \rho_2 = 2.5.$$

Two interior attractors through three interior equilibria: When Model (2.3) has three interior equilibria, the typical dynamics are that Model (2.3) has two interior attractors. We

provide an example in Figures 2.10(a), and 2.10(b) where $a_1 = 1$, $d_1 = 0.85$, $s = 0.8392$ and

$$r = 1.8,\ d_2 = 0.35,\ K_1 = 10,\ K_2 = 7,\ a_2 = 1.4,\ \rho_1 = 1,\ \rho_2 = 2.5.$$

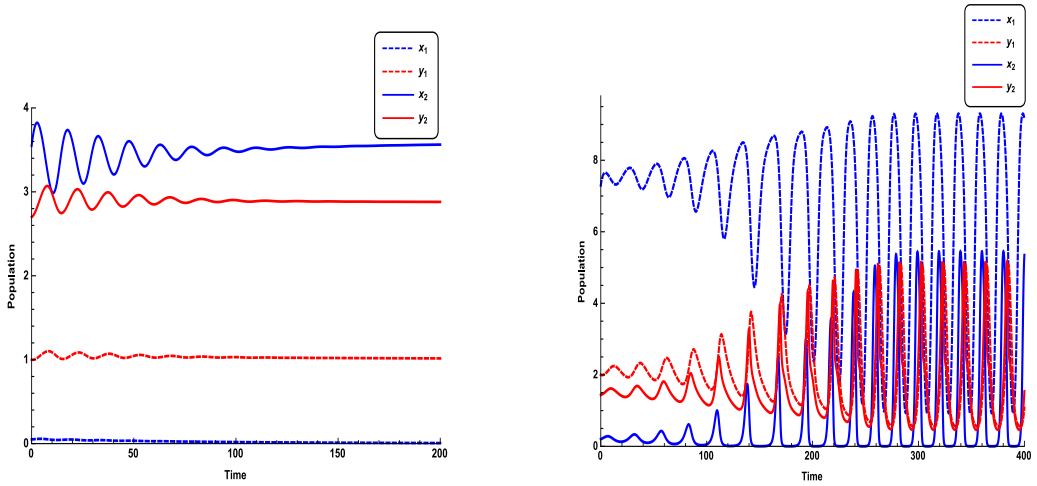

(a) Time series of Model 2.3 when $a_1 = 1$, $d_1 = 0.85$, $s = 0.8$, $x_1(0) = 0.05$, $y_1(0) = 1$, $x_2(0) = 3.55$, and $y_2(0) = 2.7$ which converges to the boundary equilibrium $(x_1, y_1, x_2, y_2) = (0, 1, 3.6, 2.9)$.

(b) Time series of Model 2.3 when $a_1 = 1$, $d_1 = 0.85$, $s = 0.8$, $x_1(0) = 0.2$, $y_1(0) = 1.15$, $x_2(0) = 2.7$, and $y_2(0) = 2.8$

Figure 2.9: Time Series of Model 2.3 When $r = 1.8$, $d_2 = 0.35$, $k_1 = 10$, $k_2 = 7$, $a_2 = 1.4$, $\rho_1 = 1$, and $\rho_2 = 2.5$. Figures 2.9(a) and 2.9(b) Represent the Dynamical Pattern Generated by Two Interior Saddles, One Boundary Sink and One Boundary Saddle. The Blue Dashed Lines Represent the Prey Population in Patch 1, the Dashed Red Lines Represent the Predator Population in Patch 1, the Blue Solid Lines Is the the Prey Population in Patch 2, and the Red Solid Lines Represent Predator Population in Patch 2.

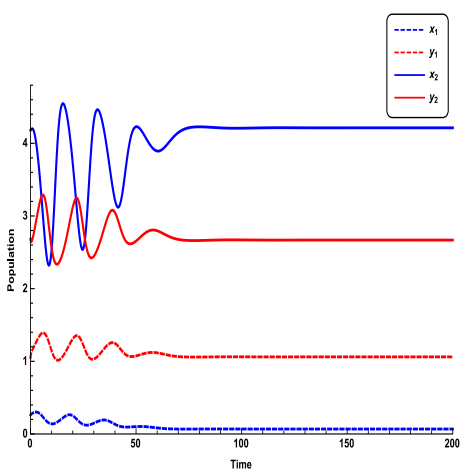

(a) Time series of Model 2.3 when $a_1 = 1$, $d_1 = 0.85$, $s = 0.8392$, $x_1(0) = 0.25$, $y_1(0) = 1.05$, $x_2(0) = 4.18$, and $y_2(0) = 2.68$ which stabilize at $(x_1, y_1, x_2, y_2) = (0.09, 1.08, 4.27, 2.64)$.

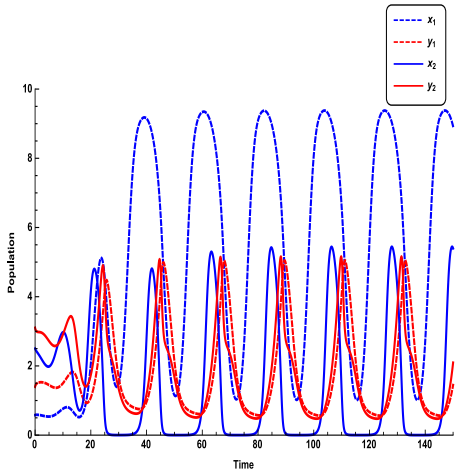

(b) Time series of Model 2.3 when $a_1 = 1$, $d_1 = 0.85$, $s = 0.8392$, $x_1(0) = 0.58$, $y_1(0) = 1.4$, $x_2(0) = 2.5$, and $y_2(0) = 3.1$

Figure 2.10: Time Series of Model 2.3 When $r = 1.8$, $d_2 = 0.35$, $k_1 = 10$, $k_2 = 7$, $a_2 = 1.4$, $\rho_1 = 1$, and $\rho_2 = 2.5$. Figures 2.10(a) and 2.10(b) Describe the Dynamical Pattern Generated by Two Interior Saddles and One Interior That Is Locally Stable. The Blue Dashed Lines Represent the Prey Population in Patch 1, the Dashed Red Lines Represent the Predator Population in Patch 1, the Blue Solid Lines Is the the Prey Population in Patch 2, and the Red Solid Lines Represent Predator Population in Patch 2.

2.6 Discussion

The model proposed in this chapter integrates two dispersal strategies in predators: (1) The passive dispersal, also called the classical foraging behavior Jansen (1995); Hanski (1999, 1998); Hastings (1983); (2) The density dependent dispersal measured through predation attraction. The linear combination of these two dispersals is linked by a parameter $s \in [0,1]$. If $s = 1$, our model reduces to the classical foraging case and when $s = 0$, our current model reduces to the recent work of Kang et al. (2017). The parameter s is proxy for the changing of dispersal strategy in predators driven by environmental conditions or other characteristics that may affect the efficiency in predator foraging activity thus it regulates the adaptive behavior of the predator. The main focus of our study is hence on the

cases when $s \in (0,1)$; however, we also provide a summary of our model's dynamics when $s = 0$ and $s = 1$ in Table (2.3). Our results address how the dispersal strategies and the related dispersal strengths affect population dynamics of prey and predator, hence generate different spatial dynamical patterns. We provide a summary of the dynamics of Model (2.3) based on mathematical analysis and bifurcation diagrams as follows:

First, we note that our model reduces to the Rosenzweig-MacArthur model in the absence of dispersal. The boundedness and positivity of the proposed model is guaranteed by the argument in Theorem 1. The analytical results are summarized in Table (2.3) along with numerical results presented throughout the paper. When there is no prey in one of the patches, our model exhibits the sink-source dynamics where no prey patch is the sink. Analytical results (Theorem 2) imply that predators could be driven to extinction locally if the product of the dispersal strength and the proportion of predator population using the passive dispersal (i.e. s) is large. Recall that for large value of s, Model (2.4) is reduced to the classical prey predator model without prey in one of the patches. Thus large values of ρ_i negatively affect the persistence of predator as in the classical prey predator model of Reeve (1988); Hanski (1999); Jansen (2001). In addition, the sink-source dynamics can pocess two interior equilibria (see Proposition (1)). Our simulations (Figure 2.1) suggest that the small values of s lead to permanence of the system which is supported by Theorem 2. For the intermediate values of s, the system can can have two interiors $E^l_{x_1,y_1,y_2}, l = 1,2$ ($i = 1$) or $E^l_{y_1,x_2,y_2}, l = 1,2$ ($i = 2$); For the large values of s, our model has no interior equilibria with the consequences that the predator goes extinct in two patches. Moreover, the intermediate values of s can stabilize the dynamics with certain dispersal strengths (see blue line in Figures 2.1(a), 2.1(b), and 2.1(c)).

Theorem (3) and Proposition (1) provide the existence of the boundary equilibria and the related local stability of our model (2.3). These results illustrate how s can potentially stabilize the basic boundary equilibria $E_{K_1 0 K_2 0}$ consequently driving predator extinct in both

patches locally. Theorem (4) provides insights into the existence and stability of a symmetric interior equilibria when Model (2.3) is symmetric (i.e. in exception of the dispersal strength and dispersal strategy, all life history parameters are the same in both patches). The analytical results indicate that the dispersal strategies do not affect the existence and stability of this symmetric interior equilibria denoted by E. However, bifurcation diagrams shown in Figures 2.4(a) and 2.4(b) suggest that the large predator population using the passive dispersal could generate two additional asymmetric interior equilibria which can be saddle or locally stable, thus generate bistability between two different attractors (see blue lines in Figure 2.4(a) when $0.78 \leq s \leq 0.92$).

Numerical simulations performed in Section 2.5 show that the dispersal strategies, i.e., the portion of predator population using the passive dispersal strategies, have huge impacts on prey and predator population dynamics in two patches. The intermediate predator population using the passive dispersal tends to stabilize the dynamics. Depending on the other life history parameters, the large or small predator population using the passive dispersal with certain dispersal strengths could generate multiple interior equilibria (up to three interior equilibria), thus lead to multiple attractors potentially. When Model (2.3) has two interior equilibria, it either converges to a boundary attractor or the interior attractor depending initial conditions (see Figures 2.9(a), and 2.9(b)); when Model (2.3) has three interior equilibria, it can have two interior equilibria (see Figures 2.10(a), and 2.10(b)). The large predator population using the passive dispersal combined with the large dispersal strength can destroy the interior equilibria with consequences that prey in one patch may go extinct but predator persists in each patch. However, there are situations when the two patch model has no interior equilibrium but all species coexist with fluctuating dynamics (see Figures 2.8(a) and 2.8(b)). These results provide an insight on the dynamics generated by social animals that encompass multiple dispersal strategy as foraging behavior and change these strategies conditioned on cues in their environments.

2.7 Concluding Remarks

In nature, many species tend to adapt to their environmental conditions and change their foraging behavior accordingly (see example of foraging behavior of Ants in Taylor (1977); Markin (1970); Traniello et al. (1984)). The study provided in this chapter is a simplification of such phenomenon, considering organisms may naturally have more than two foraging strategies and such foraging behavior could change with respect to climate conditions, population density, nutritional demands, danger resulting from predator or human interaction, etc. One limitation of this work is we do not consider climate effect or nutritional demands. The summary of the findings however illustrates how population dynamics of prey and predators (or host and parasite) are affected by changing their foraging behavior. This study gives a better understanding on how combinations of different foraging strategies used by predators favor or affect their coexistence or extinction. It will be interesting to study a two patch prey predator model with adaptive foraging behavior in which the foraging is happening in the prey rather than the predators (or in both species) and look at conditions under which dispersal can save prey from extinction. Such work is elaborated in chapter 3 where I look at one of the marvelous species of nature: Honeybee *Apis mellifera* and its parasitic mite the Varroa destructor.

Chapter 3

DISPERSAL EFFECTS ON POPULATION DYNAMICS OF THE HONEYBEE-MITE INTERACTIONS

3.1 Abstract

Honeybees are amazing and highly beneficial insect species that play important roles in undisturbed and agricultural ecosystems. Unfortunately, honeybees are increasingly threatened by numerous factors, most notably the parasitic varroa mite (*Varroa destructor* Anderson and Trueman). A recent field study showed that dispersal of mites into hives of foraging bees greatly contributes to the rapid growth of mite populations in colonies, and increases the mortality of honeybee colonies.

Motivated by this, we propose a simple two-patch honeybee-Varroa model to explore how foraging behavior of honeybees in the presence of Varroa mite infestations affect the population dynamics of honeybees and mites, respectively. We provide a full analysis on the local and global dynamics of our proposed two-patch model that incorporates mite dispersal generated by honeybee foraging activities. Our analytical and numerical studies reveals the dynamical outcomes of dispersal including: (a) Mite's extinction cannot be prevented by mite dispersal when mite population in each patch goes extinct in the absence of mite dispersal, however, mite dispersal could drive mite extinct under proper conditions. (b) Under proper conditions, large value of dispersal rate in mites could have the following effects: (1) save one honeybee colony from collapsing when honeybee colonies go extinct in both patches; (2) drive honeybee extinct in at least one patch. (c) Intermediate dispersal rate could generate multiple locally stable honeybee-mite coexistence equilibria, and drive mite's extinction under proper environments. (d) An increase in dispersal rate causes a

growth of the varroa population, which in return has a negative feedback on the colony population. (e) Increasing mite dispersal from a healthy patch to a collapsing patch could reduce the extinction time in the collapsing patch. Our results provide novel insights on the effects of foraging and Varroa dispersal on colony survival.

3.2 Introduction

Honeybees play a vital role in sustaining our planet's ecosystem. Studies have demonstrated that the majority of food consumed by human rely on bees' pollination for abundant yields and better quality Klein et al. (2007); McGregor et al. (1976); Watanabe et al. (1994). Many countries heavily rely on these food for the growth of their economy. For instance, coffee production, that heavily rely on honeybee pollination, has major economic value in rural Brazil. The work of Kruger (2007) shows that increases in the county-level value of coffee production may led to more work among middle-income boys and girls. Southwick and Southwick (1992) estimated the economic value of honey bees as agricultural pollinators in United States and pointed out that the annual social gains range between $1.6 to $5.7 billion. This efficient pollination of the honeybees is due to their systematic foraging strategy. A laboratory experiment by Greggers and Menzel (1993) shows that a foraging honeybee learns the properties of a food source so effectively that specific expectations guide the choice behavior. Waddington and Holden (1979) have also shown that honeybees maximize their net energy efficiency (net energy gained divided by energy spent) while foraging, thus their foraging is based on an optimal strategy to maximize profit or colony survival. Honeybees must hence adapt their foraging activity to a changing environment (see the work of DeGrandi-Hoffman et al. (1989)). Nevertheless, there has been a sharp decrease in honeybee population globally due to many phenomena. While the exact causes of this rapid decline is not known, some known factors may constitute a possible portal to the disorder (e.g. stressful apiculture practices, honey bee diseases, or parasitism by

mites). Infestation by Varroa destructor *(Acari: Varroidae)* has strongly been suggested to be one of the important factors causing colonies to collapse DeGrandi-Hoffman et al. (2016); Kang et al. (2015); DeGrandi-Hoffman et al. (2014); Sumpter and Martin (2004).

While Varroa reproductive rates are relatively low, DeGrandi-Hoffman et al. (2014) demonstrated that mite population can surprisingly be very large in the late fall (Fries et al., 1994; Martin, 1998) even if miticides are applied in the late summer. Sakofski et al. (1990) reported that bees robbing behavior tend to be at its peak during August and September when there is almost no nectar flow which can lead to substantial numbers of mites being transported into a colony by the robbing of highly infested colonies close to breakdown. Varroa are often attached to the abdomen of young workers which facilities their spread to other colonies and occasionally, workers from colonies infested by varroa erroneously enter foreign nest due to their bad conditions caused by the parasitism (Schmid-Hempel, 1998). These movements of Varroa among colonies could hence elucidate the rapid population growth in the late fall. This has been supported by the work of DeGrandi-Hoffman et al. (2016) in which the proportion of foragers carrying mites while entering and leaving was measured and its appropriate relationship to the growth of the Varroa population at two apiary sites was established. While there were more foragers with mites at the first site, DeGrandi-Hoffman et al. (2016) found that the degree that the mite population increased was related to the growth in the population of foragers with mites at both sites.

Mathematical models have been proven to be a great tool in the representation of an ecological system. For instance, Eberl et al. (2010) established a model to study the effect of Acute Paralysis Virus (APV) carried by parasitic Varroa mites to a healthy population of honey bees. Their results indicate that a certain number of worker bees is required for successful production of new bees in the presence of the virus (see also Ratti et al. (2012)

for the effect of APV with seasonal changes in bee colonies). Khoury et al. (2011) developed a compartment differential equation model of honey bee colony population dynamics to explore the impact of different death rates of forager bees on colony development and their model predicted that higher forager death rate than certain threshold would lead to colony failure. Kribs-Zaleta and Mitchell (2014) studied a model that accounts for healthy hive dynamics and hive extinction due to Colony Collapse Disorder (CCD) while modeling CCD via a transmissible infection brought to the hive by foragers. Other mathematical and simulated models have looked at the effect of different stresses such as nutritional or pathogenesis on colony development (Perry et al., 2015; Schmickl and Crailsheim, 2004, 2007). We acknowledge that these models give valuable insights into the population dynamics of honeybees and some cases under which their colony may collaspe. However, none of these models, to our knowledge, have been developed to explicitly analyze the foraging activities of honey bees under infestation by varroa destructor.

Motivated by the work of DeGrandi-Hoffman et al. (2016), this chapter proposes a two patch honeybee and Varroa system bees are the prey and Varroa mite represent their predators. As contrary to our work in chapter 2 where the prey is immobile but predator disperse, both the prey and predator (i.e. honeybee and mite) are mobile between the two patches in this chapter. The dispersal of the phoretic mites is done through attachment to a honey bee forager that travel in and out of the patches. For instance, the phoretic mites in patch 1 attach to honey bee forager from patch 2 when honey bee forager from patch 2 rob honey or pollen from patch 1 (see the work of (Delfinado-Baker et al., 1992; Branco et al., 1999; Kraus and Page, 1995)). We aim to study the effect of the adaptive dispersal of honey bee colonies under infestation by the Varroa mites.

3.3 Model Derivations

Let H_i and M_i be the total population of honeybees and mites in the colony (patch) i at time t respectively. Following the recent work of Kang et al. (2016), the population dynamics of varroa mites and honeybees in a single colony i could be described by the following set of nonlinear equations:

$$\begin{aligned} \frac{dH_i}{dt} &= \frac{r_i H_i^2}{K_i + H_i^2} - d_{h_i} H_i - \alpha_i H_i M_i \\ \frac{dM_i}{dt} &= c_i \alpha_i H_i M_i - d_{m_i} M_i \end{aligned} \tag{3.1}$$

where r_i is the egg laying rate of queen; $\sqrt{K_i}$ is the colony size at which the term $\frac{H_i^2}{K_i+H_i^2}$ achieves half of its maximum value; d_{h_i} and d_{m_i} are respectively the natural average death rate of the adult honey bees and mites population in colony i; α_i measures the parasitism rate of varroa mites; and c_i is the conversion rate from the parasitism of honeybees to the reproduction of newborn mites. All the parameters are positive and Kang et al. (2016) provided a great detail for the derivation of Model (3.1). The realistic ranges of these parameters can be found in Table B.4 and are used for future numerical simulations including bifurcation diagrams.

Specifically, the single patch model (3.1) has the following assumptions:

1. The successful survivability of an egg into an adult bee in colony i is represented by the term $\frac{H_i^2}{K_i+H_i^2}$, which incorporates the collaborative efforts of adult workers, via division of labor. This term assumes that successful colonies produce more brood and efficient workers, an assumption supported by the literature work (Schmickl and Crailsheim, 2007; Kang et al., 2016; Eischen et al., 1984).

2. From the reference Kang et al. (2016), Model (3.1) assumes the implicit stage structure of both the bee population and the mite population where the ratio of different stages are constants. For instance, if we define $\xi_h \in [0,1]$ the percentage of brood

population, then $(1-\xi_h)H$ is the adult honeybee population (i.e the foragers). Therefore the honeybee model in (3.1) could be described as

$$\frac{dH_i}{dt} = \frac{r_i H_i^2}{K_i + H_i^2} - d_{h_i}(1-\xi_{h_i})H_i - \alpha_i H_i M_i = \frac{r_i H_i^2}{K_i + H_i^2} - \hat{d}_{h_i} H_i - \alpha_i H_i M_i$$

with $\hat{d}_{h_i} = d_{h_i}(1-\xi_{h_i})$. Similarly, if $\xi_m \in [0,1]$ is the percentage of mites at the non-phoretic stage, then $(1-\xi_m)M$ is the phoretic mite population. Thus we denote $\hat{d}_{m_i} = d_{m_i}(1-\xi_{m_i})$ and the mite model in (3.1) becomes

$$\frac{dM_i}{dt} = c_i \alpha_i H_i M_i - d_{m_i}(1-\xi_{m_i})M_i = c_i \alpha_i H_i M_i - \hat{d}_{m_i} M_i.$$

Since $\xi_h \in [0,1]$ is the percentage of brood population and $(1-\xi_h)H$ is the adult honeybee population, then $\frac{\xi_h}{1-\xi_h}$ is the ratio of the brood to the adult honeybee in a colony. Similarly, $\frac{\xi_m}{1-\xi_m}$ is the ratio of the mites at the non-phoretic stage to the mites at the phoretic stage. We note that ξ_m and ξ_h should normally vary with time (or season). Instead of utilizing an explicit age structure model in our current manuscript, we assume ξ_m and ξ_h are constant parameters. In reality, we should expect due to seasonality that the ratio of brood to adult bees or ratio of mites at the non-phoretic stage to the mites at the phoretic stage varies. As we point out earlier, our current model is motivated by the field work of DeGrandi-Hoffman et al. (2016) and follows the recent work of Kang et al. (2016), thus our model does not include seasonality and assumes the constant ratios. In addition, the work of Harris (1980) suggests that the brood to adult bee ratio changes slightly from spring to fall; and the ratio of phoretic and non-phoretic mites changes throughout the season with the availability of brood.

3. The direct impact of the parasitism on honeybees is modeled by the term $\alpha_i H_i M_i$ that accounts for decreases in fitness due to mite parasitism; reductions on the average life span of bees. The use of Holling Type I functional response to model the direct

impact of mite on the bees population follow the fact that mites have devastating effects on bee colonies (e.g transmission of viruses or other parasitism effects from DeGrandi-Hoffman et al. (2016)). While we are only referring to parasitism here, we assume that the rate of parasitism by the mite is proportional to the rate of encounter between the varroa mites and the honeybees in order to take into account the severity of mite infestation.

4. The survival of mites depends on the honeybee population (the life of the mite is intimately connected to the life of the honeybee) with the term $c_i\alpha_i H_i M_i$ representing the successful reproduction and maturation of mites via the consumption/parasitism of honeybees.

Let $N_{h_i}^c = \frac{\frac{r_i}{d_{h_i}} - \sqrt{\left(\frac{r_i}{d_{h_i}}\right)^2 - 4K_i}}{2}$, $N_{h_i}^* = \frac{\frac{r_i}{d_{h_i}} + \sqrt{\left(\frac{r_i}{d_{h_i}}\right)^2 - 4K_i}}{2}$, $H_i^* = \frac{d_{m_i}}{c_i\alpha_i}$, and $M_i^* = \frac{1}{\alpha_i}\left[\frac{r_i H_i^*}{H_i^{*2}+K_i} - d_{h_i}\right]$

where $N_{h_i}^c$ is the critical population in order for a honeybee colony to survive in the absence of mites (could also refer to an *Allee threshold*); $N_{h_i}^*$ is the population size of a healthy honeybee colony that could attain without mites; and (H_i^*, M_i^*) are population size of honeybees and mites when they coexist in (3.1). The full dynamics of Model (3.1) can be summarized from (Kang et al., 2016) as follow:

1. Model (3.1) always has the extinction equilibrium $(0,0)$ which is always locally asymptotically stable and globally stable if $\frac{r_i}{2\sqrt{K_i}} < d_{h_i}$.

2. If $\frac{r_i}{2\sqrt{K_i}} > d_{h_i}$, then the system has additional two mite-free equilibria $(N_{h_i}^c, 0)$ and $(N_{h_i}^*, 0)$ which stability are as follow:

   - The equilibrium $(N_{h_i}^c, 0)$ is a saddle if $N_{h_i}^c < H_i^*$ and it is a source (i.e an unstable focus or an unstable node depending on parameter values) when $N_{h_i}^c > H_i^*$.

- $(N_{h_i}^*, 0)$ is a sink for $N_{h_i}^* < H_i^*$ and a saddle when $N_{h_i}^* > H_i^*$. If $N_{h_i}^* < H_i^*$, the trajectory of Model (3.1) converges to the equilibrium $(0,0)$ or $(N_{h_i}^*, 0)$ depending on the initial conditions.

3. If $N_{h_i}^c < H_i^* < N_{h_i}^*$, then the unique interior equilibrium (H_i^*, M_i^*) emerges, which is locally asymptotically stable when $H_i^* > \sqrt{K_i}$. In this case, initial conditions are important for the survival of the colony. Model (3.1) undergoes a supercritical Hopf-bifurcation at $H_i^* = \sqrt{K_i}$; and it has a unique unstable limit cycle around the co-existence equilibrium (H_i^*, M_i^*) (which is a source) when $H_i^* < \sqrt{K_i}$ where the periodic orbits expand until it touches the stable manifold of the boundary equilibrium $(\bar{H}_h^c, 0)$ which lead to the extinction of both honeybees and parasitic mites. Under this condition, extinction of honeybees and mites occurs globally independently of initial conditions. We refer to the colony in the latter case as *the collapsing colony*. To further illustrate the dynamics of the single patch Model (3.1), we provide the bifurcation diagram in Figures 3.1(a) and 3.1(b) by letting

$$r = 1500,\ c = 0.01,\ d_h = 0.15,\ dm = 0.095,\ \alpha = 0.005.$$

The scenario that we consider here is that the extinction equilibrium $(0,0)$ and the honeybee-only equilibrium $(N_h^*, 0)$ are both locally stable, i.e., they are the only two attractors of the system where the interior equilibrium (H^*, M^*) is unstable and the system (3.1) undergoes a supercritical Hopf-bifurcation at $H^* = \frac{d_m}{\alpha c} = K$. Thus, initial conditions are important as both the bees and mites could be driven to extinction or only bee population can survive depending on initial condition. Initial condition is hence important for the survival of the colony. These dynamics are illustrated in Figures 3.1(a) and 3.1(b).

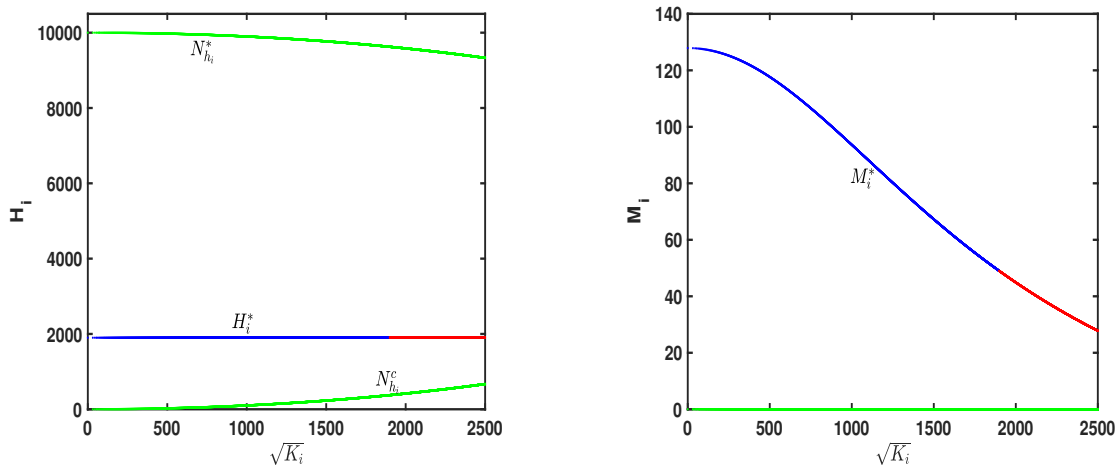

(a) H_i vs $\sqrt{K_i}$ for the effect of brood rearing coeafficient

(b) M_i vs $\sqrt{K_i}$ for the effect of brood rearing coefficient

Figure 3.1: One Parameter Bifurcation Diagrams of the Single Patch Model (3.1). The Notations H_i^* and M_i^* Represent the Population of Honeybee and Mite at Patch i, Respectively. $N^*_{h_i}$ and $N^c_{h_i}$ Are the Honeybee Population at the Boundary Equilibrium $E_{N^*_{h_i}0}$ and $E_{N^c_{h_i}0}$ Respectively. The Blue Line Represents Sink, the Green Line a Saddle, and the Red Line a Source.

Varroa mites attached to honeybee foragers could move among colonies by direct transfer between foragers or by robbing nectar and pollen from highly infested colonies. Thus, varroa mites population could increase through reproduction, parasitising honeybees or, immigrating into the colonies by attaching to honeybee foragers DeGrandi-Hoffman and Curry (2004). To incorporate the behavior of mite dispersal, we define ρ_{ij} as the average foraging rate of the honeybee foragers visiting colony j from colony i (for robbing) or the average connecting rate from colony i to colony j during the visitations of the same resource sites. More specifically, this average rate includes the potential events such as honeybee foragers from colony i rubbing colony j; honeybee foragers from both colony i and j visiting a common resource such that the mites transfer between foragers. We do not model resource dynamics explicitly, however, the likelihood of bees visiting colonies that optimize resource consumption is implicitly incorporated into ρ_{ij} thus ρ_{ij} take into account the adaptive foraging strategy of the bees. The probability of the mites M_j attaching to

forager bees H_j at colony j is modeled by $\frac{H_j}{a_j+H_j}$, where a_j is the size of the bee population at which the rate of attachment is half maximal (see the similar approach in Sumpter and Martin (2004); Betti et al. (2014)). Motivated by the importance of ensuring the "conservation of mass" in population modeling by Schmickl and Crailsheim (2007) but perhaps a bit unrealistically, our model ensures that no bees and mites are "lost". Thus, for a starting point, our model has the following net dispersal term at colony i that conserves the mass:

$$\left(\underbrace{\rho_{ji} \overbrace{\frac{H_j}{a_j+H_j}}^{\text{probability of } M_j \text{ attaching to } H_j} M_j}_{\text{mites entering colony i from colony j}} - \underbrace{\rho_{ij} \overbrace{\frac{H_i}{a_i+H_i}}^{\text{probability of } M_i \text{ attaching to } H_i} M_i}_{\text{mites leaving colony i for colony j}} \right).$$

The population dynamics of varroa destructor and honeybees in a two-patch framework can be described by the following nonlinear equations:

$$\begin{aligned}
\frac{dH_1}{dt} &= \underbrace{\frac{r_1 H_1^2}{K_1+H_1^2}}_{\text{successful reproduction at colony 1}} - \underbrace{d_{h_1} H_1}_{\text{mortality}} - \underbrace{\alpha_1 H_1 M_1}_{\text{parasitism effects}} \\
\frac{dM_1}{dt} &= c_1 \alpha_1 H_1 M_1 - d_{m_1} M_1 + \underbrace{\left(\rho_{21} \overbrace{\frac{H_2}{a_2+H_2}}^{\text{probability of } M_2 \text{ attaching to } H_2} M_2 - \rho_{12} \overbrace{\frac{H_1}{a_1+H_1}}^{\text{probability of } M_1 \text{ attaching to } H_1} M_1 \right)}_{\text{Net dispersal effects at colony 1}} \\
\frac{dH_2}{dt} &= \underbrace{\frac{r_2 H_2^2}{K_2+H_2^2}}_{\text{successful reproduction at colony 2}} - \underbrace{d_{h_2} H_2}_{\text{mortality}} - \underbrace{\alpha_2 H_2 M_2}_{\text{parasitism effects}} \\
\frac{dM_2}{dt} &= c_2 \alpha_2 H_2 M_2 - d_{m_2} M_2 + \underbrace{\left(\rho_{12} \overbrace{\frac{H_1}{a_1+H_1}}^{\text{probability of } M_1 \text{ attaching to } H_1} M_1 - \rho_{21} \overbrace{\frac{H_2}{a_2+H_2}}^{\text{probability of } M_2 \text{ attaching to } H_2} M_2 \right)}_{\text{Net dispersal effects at colony 2}}
\end{aligned} \tag{3.2}$$

where it is assumed that the single patch model (3.1) already includes the added mortality due to foraging behavior. Model (3.2) allows to address the following:

1. The dispersal effects on the population dynamics of honeybees versus Varroa mites by comparing the number of equilibria and their stability of the single patch model (3.1) to the corresponding two patch model (3.2) when $\rho_{12} = \rho_{21} = \rho$.

2. The dynamical effects of varied dispersal rates (i.e., ρ_{12}, ρ_{21}) on population outcomes of the two-patch model (3.2).

3. Identify conditions where dispersal rates could promote or suppress the collapse of a honeybee colony.

3.4 Mathematical Analysis

The state space of the proposed two patch model (3.2) is $\{(H_1, M_1, H_2, M_2) \in \mathbb{R}^4_+\}$. Recall that $N^c_{h_i} = \frac{\frac{r_i}{d_{h_i}} - \sqrt{\left(\frac{r_i}{d_{h_i}}\right)^2 - 4K_i}}{2}$, $N^*_{h_i} = \frac{\frac{r_i}{d_{h_i}} + \sqrt{\left(\frac{r_i}{d_{h_i}}\right)^2 - 4K_i}}{2}$, $H^*_i = \frac{d_{m_i}}{c_i \alpha_i}$, and $M^*_i = \frac{1}{\alpha_i}\left[\frac{r_i H^*_i}{H^{*2}_i + K_i} - d_{h_i}\right]$ for $i = 1, 2$. We start with the basic dynamical properties of Model (3.2) as the following theorem:

Theorem 5. *Assume that all parameters are strictly positive. Model* (3.2) *is positively invariant and bounded in* $\mathbb{R}^4_+$. *Moreover, we have the following dynamics regarding Model* (3.2)*:*

1. *The set* $H_i = 0$ *for* $i = 1$ *or 2 is invariant.*

2. *The honeybee population in patch* $i = 1, 2$ *is bounded by* $N^*_{h_i}$, *i.e.,*

$$\limsup_{t \to \infty} H_i(t) \leq N^*_{h_i}.$$

And the honeybee population $H_i(t)$ *approaches to 0 if its initial population is less than the critical threshold, i.e.,* $H_i(0) < N^c_{h_i}$.

3. *The extinction equilibrium* $E_{0000} = (0,0,0,0)$ *is always locally asymptotically stable, and Model* (3.2) *converges to* E_{0000} *locally if the initial honeybee population at both patches are less than the critical threshold, i.e.,* $H_i(0) < N_{h_i}^c$ $i = 1$ *and* 2.

4. *If* $\frac{r_i}{2\sqrt{K_i}} < d_{h_i}$ *for either* $i = 1,$ *or* 2*, the honeybee population* $H_i(t)$ *approaches to 0, i.e.,*

$$\limsup_{t\to\infty} H_i(t) = 0.$$

Thus if $\frac{r_i}{2\sqrt{K_i}} < d_{h_i}$ *for* $i = 1$ *and* 2*, then* (3.2) *converges to* E_{0000} *globally.*

5. *If* $N_{h_i}^* < H_i^* = \frac{d_{m_i}}{c_i\alpha_i}$ *for both* $i = 1,2$*, then the population of mites in both patches goes extinct.*

Biological Implications: Theorem 5 implies that Model (3.2) is well-defined biologically. By comparison, with the dynamics of the single patch model (3.1), we observe that Model (3.2) inherits many dynamic properties from Model (3.1) including the importance of initial honeybee population and sufficient conditions that lead to the extinction of mites. For example, if mite population in each patch goes extinct in the absence of mite dispersal, then dispersal of mites can not prevent its extinction. However, if honeybee populations go extinct in one patch and survives in the other patch, then dispersal could potentially make mites survive in both patches. On the other hand, dispersal could also drive the extinction of mites in both patches (see our one dimensional bifurcation diagrams shown in Figures 3.2(a)-3.2(c)). In the case that honeybee colonies go extinct in both patches, the large dispersal rate in mites could save one honeybee colony from collapsing (see Figures 3.14 and 3.15).

In addition, Theorem 5 indicates that honeybee population at patch i goes extinct when the inequality $\frac{r_i}{2\sqrt{K_i}} < d_{h_i}$ holds. Define $\hat{H}_j^* = \frac{\left(H_j^* - a_j + \frac{\rho_{ji}}{c_j\alpha_j}\right) + \sqrt{4a_jH_j^* + \left(H_j^* - a_j + \frac{\rho_{ji}}{c_j\alpha_j}\right)^2}}{2}$ and

$$\hat{M}_j^* = \frac{1}{\alpha_j}\left[\frac{r_j\hat{H}_j^*}{(\hat{H}_j^*)^2 + K_j} - d_{h_j}\right], \quad \hat{M}_i^* = \frac{\rho_{ji}\hat{H}_j^*\hat{M}_j^*}{d_{m_i}(a_j + \hat{H}_j^*)}$$

for $i, j = 1, 2,\ i \neq j$. Then we have the following theorem regarding the dynamics when one of the two honeybee colonies collapses:

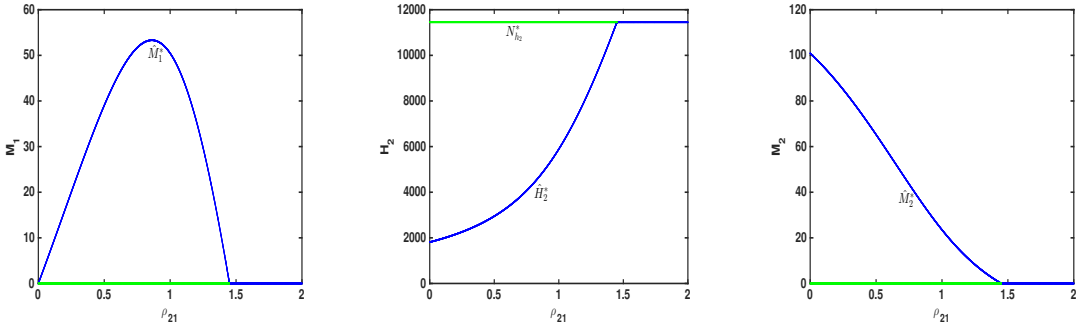

(a) M_1 vs ρ_{21} for the effect of dispersal

(b) H_2 vs ρ_{21} for the effect of dispersal

(c) M_2 vs ρ_{21} for the effect of dispersal

Figure 3.2: One Parameter Bifurcation Diagrams of the Subsystem Model (3.3) when $r_2 = 1500$, $c_2 = 0.01$, $d_{h_2} = 0.15$, $\alpha_2 = 0.005$, $a_2 = 23000$, $K_2 = 1000000$ with $(H_1^*, M_1^*) = (0,0)$, $(H_2^*, M_2^*) = (1812, 100.9)$ Without Dispersal. The Notations $\hat{H}_2^*$ and $\hat{M}_i^*$, $i = 12$ Represent the Population of Honeybee and Mite at the Unique Interior Equilibrium. $N_{h_2}^*$ is the Honeybee Population at the Boundary Equilibrium $E_{0N_{h_2}^*0}$. The Blue Line Represents Sink and the Green Line a Saddle.

Theorem 6. *[Dynamics of Model* (3.3)*] If the inequality* $\frac{r_i}{2\sqrt{K_i}} < d_{h_i}$ *holds, then Model* (3.2) *reduces to the following system:*

$$\begin{aligned}
\frac{dM_i}{dt} &= -d_{m_i}M_i + \rho_{ji}\frac{H_j}{a_j + H_j}M_j \\
\frac{dH_j}{dt} &= \frac{r_jH_j^2}{K_j + H_j^2} - d_{h_j}H_j - \alpha_jH_jM_j \\
\frac{dM_j}{dt} &= c_j\alpha_jH_jM_j - d_{m_j}M_j - \rho_{ji}\frac{H_j}{a_j + H_j}M_j
\end{aligned} \tag{3.3}$$

whose dynamics can be summarized as follows:

1. *If* $\frac{r_j}{2\sqrt{K_j}} \geq d_{h_j}$, *Model* (3.3) *has two boundary equilibria* $(0, N^c_{h_j}, 0)$ *and* $(0, N^*_{h_j}, 0)$ *where* $(0, N^c_{h_j}, 0)$ *is always saddle; and* $(0, N^*_{h_j}, 0)$ *is a sink if the following inequality holds*

$$N^*_{h_j}\left(1 - \frac{\rho_{ji}}{c_j\alpha_j(\alpha_j + N^*_{h_j})}\right) < \frac{d_{m_j}}{c_j\alpha_j} = H^*_j$$

which is equivalent to (i) $H^*_j > N^*_{h_j}$ *or (ii)* $\rho_{ji} > \frac{c_j\alpha_j(N^*_{h_j} - H^*_j)(a_j + N^*_{h_j})}{N^*_{h_j}} > 0$*; otherwise,* $(0, N^*_{h_j}, 0)$ *is a saddle.*

2. *If* $\frac{r_j}{2\sqrt{K_j}} \geq d_{h_j}$ *and* $N^c_{h_j} < \hat{H}^*_j < N^*_{h_j}$ *hold, then Model* (3.3) *has a unique interior equilibrium* $(\hat{M}^*_i, \hat{H}^*_j, \hat{M}^*_j)$ *which is locally stable if* $\hat{H}^*_j > \sqrt{K_j}$ *otherwise it is saddle.*

Biological Implications: Theorem 6 is relevant where one colony is broken. However, from dynamical point of view, the results of Theorem 6 regarding Model (3.3) capture the role of dispersal on honeybee colonies collapsing in one patch while the other is healthy. The dispersal effects could hence be summarized as follows:

1. Dispersal has no effect when $H^*_j > N^*_{h_j} > \sqrt{K_j}$ hold as Model (3.3) approaches to $(0, N^*_{h_j}, 0)$ for any value of ρ_{ji} (i.e., including $\rho_{ji} = 0$).

2. If there is no dispersal (i.e., $\rho_{ji} = 0$) and the inequalities $N^*_{h_j} > \max\left\{\sqrt{K_j}, H^*_j\right\}$ hold, then Model (3.3) approaches $(0, H^*_j, M^*_j)$ when $N^*_{h_j} > H^*_j > \max\left\{\sqrt{K_j}, N^c_j\right\}$ while it approaches extinction when $N^*_{h_j} > \sqrt{K_j} > H^*_j$. However, if there is a large dispersal rate (i.e., $\rho_{ji} > \frac{c_j\alpha_j(N^*_{h_j} - H^*_j)(a_j + N^*_{h_j})}{N^*_{h_j}} > 0$), then Model (3.3) can have locally stability at $(0, N^*_{h_j}, 0)$. This implies that the large dispersal can drive mite extinct when $N^*_{h_j} > H^*_j > \max\left\{\sqrt{K_j}, N^c_j\right\}$ hold (see Figures 3.2(a)-3.2(c) for this case); and it could also save honeybee colonies from collapsing if $N^*_{h_j} > \sqrt{K_j} > H^*_j$ hold. See bifurcation diagrams in Figures 3.3(a)-3.3(c) for this case.

3. Notice that $\hat{H}^*_j = \frac{\left(H^*_j - a_j + \frac{\rho_{ji}}{c_j\alpha_j}\right) + \sqrt{4a_jH^*_j + \left(H^*_j - a_j + \frac{\rho_{ji}}{c_j\alpha_j}\right)^2}}{2}$, an increasing function of the dispersal rate ρ_{ji}, requires the need of an intermediate value of the dispersal rate

to ensure $\max\left\{\sqrt{K_j}, N^c_{h_j}\right\} < \hat{H}^*_j < N^*_j$. In short, the proper optimal dispersal rate could save honeybee colonies from collapsing especially when $H^*_j < \sqrt{K_j} < \hat{H}^*_j$. For instance, when

$$r_2 = 1500,\ c_2 = 0.01,\ d_{h_2} = 0.15,\ \alpha_2 = 0.005,\ a_2 = 23000,$$

with $K_2 = 4000000,\ \max\left\{\sqrt{K_j}, N^c_{h_j}\right\} < \hat{H}^*_j < N^*_j \Leftrightarrow 1812 < 2000 < 5888,$ and the equilibrium $(\hat{M}^*_i, \hat{H}^*_j, \hat{M}^*_j) = (42.21, 5888.97, 19.67)$ is locally stable for $\rho_{21} = 1$ while $(0, N^*_{h_j}, 0) = (0, 11180.7, 0)$ is saddle. When $\rho_{21} = 5$ under the same parameters, then Model (3.3) has no interior equilibrium and $(0, N^*_{h_j}, 0)$ is locally stable.

The dynamics generated by dispersal in the subsystem Model (3.3) are better understood via the use of the following bifurcation diagrams (see Figures 3.2(a)-3.2(c) and Figures 3.3(a)-3.3(a)), which provide direct illustrations of the effects of dispersal on mites.

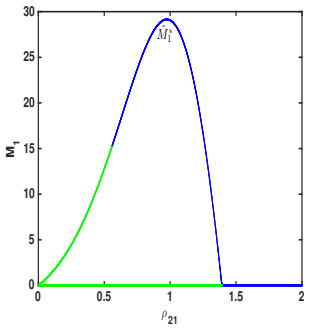

(a) M_1 vs ρ_{21} for the effect of dispersal

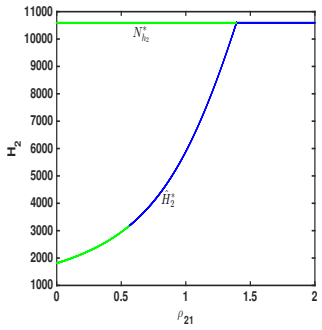

(b) H_2 vs ρ_{21} for the effect of dispersal

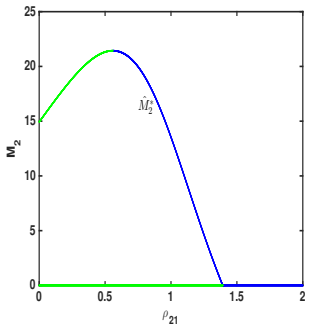

(c) M_2 vs ρ_{21} for the effect of dispersal

Figure 3.3: One Parameter Bifurcation Diagrams of the Subsystem Model (3.3) when $r_2 = 1500$, $c_2 = 0.01$, $d_{h_2} = 0.15$, $\alpha_2 = 0.005$, $a_2 = 23000$, $K_2 = 10000000$ with $(H^*_1, M^*_1) = (0,0)$, $(H^*_2, M^*_2) = (1812, 14.9)$ Without Dispersal. The Notations $\hat{H}^*_2$ and $\hat{M}^*_i,\ i = 12$ Represent the Population of Honeybee and Mite at the Unique Interior Equilibrium. $N^*_{h_2}$ is the Honeybee Population at the Boundary Equilibrium $E_{0N^*_{h_2}0}$. The Blue Line Represents Sink and the Green Line a Saddle.

3.4.1 Boundary Equilibria and Their Stability

Model (3.2) is capable of supporting the following boundary equilibria under additional conditions:

$$E_{0000} = (0,0,0,0), \quad E_{N^c_{h_1}000} = (N^c_{h_1},0,0,0), \quad E_{N^*_{h_1}000} = (N^*_{h_1},0,0,0), \quad E_{00N^c_{h_2}0} = (0,0,N^c_{h_2},0)$$

$$E_{00N^*_{h_2}0} = (0,0,N^*_{h_2},0), \quad E_{N^c_{h_1}0N^c_{h_2}0} = (N^c_{h_1},0,N^c_{h_2},0), \quad E_{N^*_{h_1}0N^c_{h_2}0} = (N^*_{h_1},0,N^c_{h_2},0),$$

$$E_{N^c_{h_1}0N^*_{h_2}0} = (N^c_{h_1},0,N^*_{h_2},0), \quad E_{N^*_{h_1}0N^*_{h_2}0} = (N^*_{h_1},0,N^*_{h_2},0),$$

$$E_{H_1,M_1,0,M_2} = (\hat{H}^*_1,\hat{M}^*_1,0,\hat{M}^*_2), \quad E_{0,M_1,H_2,M_2} = (0,\check{M}^*_1,\check{H}^*_2,\check{M}^*_2).$$

where $\check{H}^*_j = \frac{\left(H^*_j - a_j + \frac{\rho_{ji}}{c_j\alpha_j}\right) + \sqrt{4a_jH^*_j + \left(H^*_j - a_j + \frac{\rho_{ji}}{c_j\alpha_j}\right)^2}}{2}$ and $\check{M}^*_j = \frac{1}{\alpha_j}\left[\frac{r_j\check{H}^*_j}{(\check{H}^*_j)^2+K_j} - d_{h_j}\right]$, $\check{M}^*_i = \frac{\rho_{ji}\check{H}^*_j\hat{M}^*_j}{d_{m_i}(a_j+\check{H}^*_j)}$ for $i,j = 1,2,\ i \neq j$. It would be interesting to explore how dispersal rates affect the local stability of the following boundary equilibria:

$$E_{N^*_{h_1}000},\ E_{00N^*_{h_2}0},\ E_{N^*_{h_1}0N^*_{h_2}0},\ E_{H_1,M_1,0,M_2} \text{ and } E_{0,M_1,H_2,M_2}.$$

The conditions on the existence and stability of these boundary equilibria are illustrated in the following theorem:

Theorem 7. *[Boundary equilibria of Model* (3.2)*] Let $i,\ j = 1,2$ and $i \neq j$. The existence and stability conditions of the boundary equilibria of Model* (3.2) *are provided below:*

1. *Model* (3.2) *always have the extinction equilibrium E_{0000} which is always locally asymptotically stable.*

2. *If $\frac{r_i}{2\sqrt{K_i}} \geq d_{h_i}$, Model* (3.2) *has the boundary equilibria with $H_j = M_i = M_j = 0$ while $H_i = N^*_{h_i}$ or $H_i = N^c_{h_i}$. The boundary equilibrium with $H_i = N^*_{h_i}$ (i.e., $E_{N^*_{h_1}000}$ or $E_{00N^*_{h_2}0}$) is locally stable if one of the following two conditions hold: (i) $H^*_i > N^*_{h_i}$ or (ii) $H^*_i < N^*_{h_i}$ and $\rho_{ij} > \frac{c_i\alpha_i(N^*_{h_i}-H^*_i)(a_i+N^*_{h_i})}{N^*_{h_i}}$; and saddle otherwise.*

3. *If* $\frac{r_i}{2\sqrt{K_i}} \geq d_{h_i}$ *for both* $i = 1$ *and 2 hold, then Model* (3.2) *has the boundary equilibria of* $E_{N^*_{h_1}0N^*_{h_2}0}$, $E_{N^*_{h_1}0N^c_{h_2}0}$, *and* $E_{N^c_{h_1}0N^*_{h_2}0}$ *where* $E_{N^*_{h_1}0N^*_{h_2}0}$ *is locally stable if one of the following conditions hold*

   (a) $H^*_i > N^*_{h_i}$ *for both* $i = 1,2$

   (b) $H^*_i < N^*_{h_i}$, $H^*_j > N^*_{h_j}$ *and*

$$\frac{\rho_{ij}N^*_{h_i}}{a_i + N^*_{h_i}} + \frac{\rho_{ji}N^*_{h_j}}{a_j + N^*_{h_j}} + c_j\alpha_j(H^*_j - N^*_{h_j}) > c_i\alpha_i(N^*_{h_i} - H^*_i)$$

   and

$$\frac{\rho_{ij}c_j\alpha_j N^*_{h_i}(H^*_j - N^*_{h_j})}{a_i + N^*_{h_i}} > c_i\alpha_i c_j\alpha_j(N^*_{h_i} - H^*_i)(H^*_j - N^*_{h_j}) + \frac{\rho_{ji}c_i\alpha_i N^*_{h_j}(N^*_{h_i} - H^*_i)}{a_j + N^*_{h_j}}.$$

4. *If* $\frac{r_i}{2\sqrt{K_i}} \geq d_{h_i}$ *and* $N^c_{h_i} < \hat{H}^*_i < N^*_{h_i}$ *hold, then Model* (3.2) *has the boundary equilibrium with* $H_j = 0$, $H_i = \hat{H}^*_i$, $M_i = \hat{M}^*_i$, $M_j = \hat{M}^*_i$ *which is locally stable if* $\hat{H}^*_j > \sqrt{K_j}$.

5. *If the boundary equilibrium* $E_{N^*_{h_1}0N^c_{h_2}0}$, *or* $E_{N^c_{h_1}0N^*_{h_2}0}$, *or* $E_{N^c_{h_1}000}$ *or* $E_{00N^c_{h_2}0}$ *exists, it is always saddle.*

Biological Implications: Theorem 7 provides sufficient conditions on the existence and stability of all possible boundary equilibria of Model (3.2). These theoretical results provide cases under which dispersal can promote local extinction or coexistence of honeybee in both patches when mite population is extinct in at least one patch. We note the following points regarding the dispersal effects on the local stability of the boundary equilibria:

1. If $\frac{r_i}{2\sqrt{K_i}} \geq d_{h_i}$ and $H^*_i < N^*_{h_i}$, then in the absence of mite dispersal, the population of honeybee at Patch i could approach H^* when $\max\left\{N^c_{h_i}, \sqrt{K_i}\right\} < H^*_i < N^*_{h_i}$ or the honeybee colony collapses when $H^*_i < \sqrt{K_i}$. However, in the presence of mite dispersal, the large dispersal rate from Patch i to Patch j, i.e., ρ_{ij}, can stabilize the boundary equilibrium $H_j = M_i = M_j = 0$, $H_i = N^*_{h_i}$ (i.e., $E_{N^*_{h_1}000}$ or $E_{00N^*_{h_2}0}$) of Model

(3.2) such that the honeybee colony could survive locally. This implies that the large dispersal rate from Patch i to Patch j could increase the honeybee population at Patch i or prevent its collapsing under certain conditions. See our bifurcation diagrams on the case of the honeybee colony collapsing in one patch (Figures 3.3(a)-3.3(c)).

2. The phenomenon mentioned above also applies to the case when $\frac{r_i}{2\sqrt{K_i}} \geq d_{h_i}$ for both $i = 1,2$ and $H_i^* < N_{h_i}^*, H_j^* < N_{h_j}^*$. Figures 3.14 and 3.15 on the cases that honeybee colonies collapse in both patches without dispersal illustrate that the large mite dispersal rate could save the honeybee colony.

3.4.2 Interior Equilibria and the Stability

We note the following regarding Model (3.2) :

$$\frac{dH_i}{dt} = \frac{r_i H_i^2}{K_i + H_i^2} - d_{h_i} H_i - \alpha_i H_i M_i = H_i \left(\frac{r_i H_i}{K_i + H_i^2} - d_{h_i} - \alpha_i M_i \right)$$

$$\frac{dM_i}{dt} + \frac{dM_j}{dt} = c_i \alpha_i H_i M_i + c_j \alpha_j H_j M_j - d_{m_i} M_i - d_{m_j} M_j$$

with $i, j = 1,2,\ i \neq j$. Consider $(\hat{H}_1^*, \hat{M}_1^*, \hat{H}_2^*, \hat{M}_2^*)$ an interior equilibrium of Model (3.2), then the following conditions must be satisfied:

$$\frac{r_i H_i}{K_i + H_i^2} - d_{h_i} - \alpha_i M_i = 0 \quad \Leftrightarrow \quad M_i = \frac{1}{\alpha_i} \left[\frac{r_i H_i^*}{H_i^{*2} + K_i} - d_{h_i} \right] \tag{3.4}$$

$$c_i \alpha_i H_i M_i + c_j \alpha_j H_j M_j - d_{m_i} M_i - d_{m_j} M_j = 0 \tag{3.5}$$

By substituting M_i and M_j from (3.4) into (3.5), we obtain:

$$\frac{dM_i}{dt} + \frac{dM_j}{dt} = \underbrace{\frac{[d_{h_i}(K_i + H_i^2) - r_i H_i](d_{m_i} - c_i \alpha_i H_i)}{(K_i + H_i^2)\alpha_i}}_{\phi_i(H_i)} + \underbrace{\frac{[d_{h_j}(K_j + H_j^2) - r_j H_j](d_{m_j} - c_j \alpha_j H_j)}{(K_j + H_j^2)\alpha_j}}_{\phi_j(H_j)} = 0 \tag{3.6}$$

The complexity of Model (3.2) prevents us to obtain the explicit solutions of the interior equilibria, thus we explore the symmetric interior equilibria for Model (3.2). We say that Model (3.2) is symmetric if $c_1 = c_2 = c,\ \alpha_1 = \alpha_2 = \alpha,\ r_1 = r_2 = r,\ K_1 = K_2 = K,\ a_1 = a_2 = a,\ d_{m_1} = d_{m_2} = d_m,\ d_{h_1} = d_{h_2} = d_h$, and $\rho_{12} = \rho_{21} = \rho$. The symmetric model is hence presented as follow:

$$\begin{aligned}
\frac{dH_i}{dt} &= \underbrace{\frac{rH_i^2}{K+H_i^2}}_{\text{successful reproduction in colony } i} - \underbrace{d_h H_i}_{\text{natural death}} - \underbrace{\alpha H_i M_i}_{\text{parasitism effects}} \\
\frac{dM_i}{dt} &= c\alpha H_i M_i - d_m M_i + \underbrace{\rho\left(\frac{H_j}{a+H_j}M_j - \frac{H_i}{a+H_i}M_i\right)}_{\text{dispersal effect in colony } i}
\end{aligned} \tag{3.7}$$

with $i, j = 1, 2,\ i \neq j$. We present both the analytical and numerical results of the symmetric Model (3.7). We first provide the following theorem regarding the dynamics:

Theorem 8. *[The symmetric interior equilibria and the stability] Suppose that Model* (3.2) *is symmetric and is reduced to Model* (3.7)*. Let* $H^* = \frac{d_m}{c\alpha},$ *and* $M^* = \frac{1}{\alpha}\left[\frac{rH^*}{H^{*2}+K} - d_h\right]$*. Then* $E = (H^*, M^*, H^*, M^*)$ *is a symmetric interior equilibrium for Model* (3.7)*. Moreover, E is locally asymptotically stable if* $H^* > \sqrt{K}$ *and one of the following conditions holds:*

1. $M^* \leq \frac{rH^*(a+H^*)[(H^*)^2-K]}{a\alpha[(H^*)^2+K]^2}$
2. $M^* > \frac{rH^*(a+H^*)[(H^*)^2-K]}{a\alpha[(H^*)^2+K]^2}$ *and* $\rho < \frac{c\alpha^2 M^*(a+H^*)^2[(H^*)^2+K]^2}{2\left(a\alpha M^*[(H^*)^2+K]^2 - rH^*(a+H^*)[(H^*)^2-K]\right)}$.

Otherwise, E is a saddle.

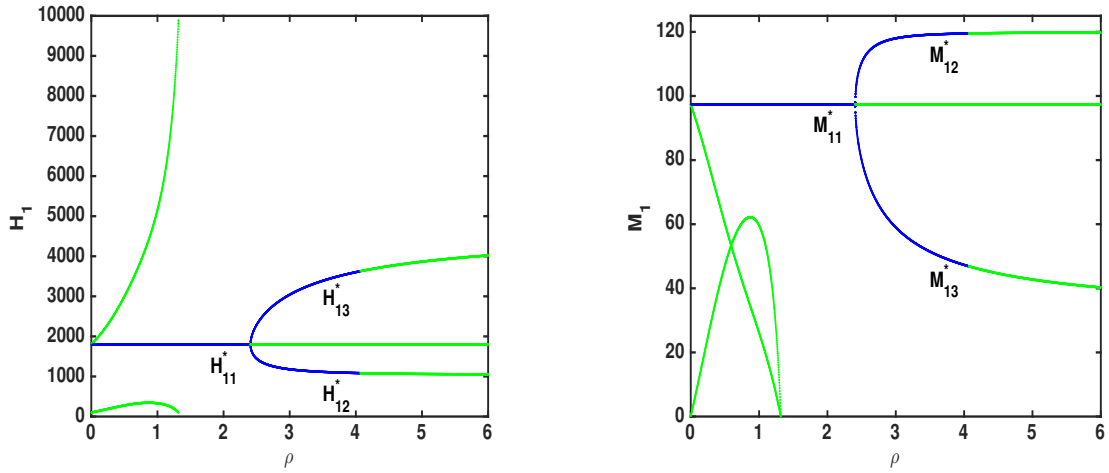

(a) H_1 vs ρ for the effect of dispersal

(b) M_1 vs ρ for the effect of dispersal

Figure 3.4: One Parameter Bifurcation Diagrams of the Symmetric Model (3.7). $(H^*, M^*) = (1800, 97.36)$ is a Sink for Both Patches Without Dispersal. The Notations H^*_{ij} and M^*_{ij} Represent the Population of Honeybee and Mite of the j^{th} Interior Equilibrium at Patch i, Respectively. The Blue Line Represents Sink and the Green Line a Saddle.

Biological Implications: Theorem (8) implies that if (H^*, M^*) is an interior equilibrium of the single patch model, (3.1), then $E = (H^*, M^*, H^*, M^*)$ is also an interior equilibrium of the symmetric model (3.7). In addition, Theorem (8) indicates that the large dispersal rate may have destabilizing effects on population dynamics. In the absence of dispersal, the two uncoupled honeybee colonies in the identical environment have local stability at the honeybee-mite coexistence equilibrium (H^*, M^*, H^*, M^*) if the following conditions hold

$$\frac{r}{2\sqrt{K}} > d_h, \text{ and } \max\left\{N_h^c, \sqrt{K}\right\} < H^* < N_h^*.$$

However, in the presence of dispersal, if $M^* > \frac{rH^*(a+H^*)[(H^*)^2-K]}{a\alpha[(H^*)^2+K]^2}$ holds, then the symmetric model (3.7) being locally stable at (H^*, M^*, H^*, M^*) needs additional restriction on the dispersal rate ρ, i.e.,

$$\rho < \frac{c\alpha^2 M^*(a+H^*)^2[(H^*)^2+K]^2}{2\left(a\alpha M^*[(H^*)^2+K]^2 - rH^*(a+H^*)[(H^*)^2-K]\right)}.$$

Otherwise, the symmetric equilibrium $E = (H^*, M^*, H^*, M^*)$ is a saddle. To further illustrate the potential effects of dispersal, we provide the bifurcation diagrams on the honeybee/mite population versus the dispersal rate ρ (see Figures 3.4(a) and 3.4(b)) by letting

$$r_1 = r_2 = r = 1500,\ c_1 = c_2 = c = 0.01,\ d_{h_1} = d_{h_2} = d_h = 0.15,$$

$$\alpha_1 = \alpha_2 = \alpha = 0.005,\ K_1 = K_2 = K = 1000000.$$

Under this set of parameter values, we have $M^* > \frac{rH^*(a+H^*)[(H^*)^2-K]}{a\alpha[(H^*)^2+K]^2}$. We provide a brief summary on the dynamical effects of dispersal as follows:

1. Large dispersal rate could destabilize the interior equilibria such that the honeybee colony collapses. This has been illustrated in the bifurcation diagram of Figure 3.4.

2. Intermediate value of dispersal rate could generate multiple locally stable honeybee-mite coexistence equilibria.

3.5 Effects of Dispersal Rates on Population Dynamics of Honeybees and Mites

To further explore the role of mite dispersal on the population of varroa mites and bees due to the honeybee foraging behavior, we perform one and two parameter bifurcation analysis of Model (3.2) by choosing the typical parameter values from Table (B.4):
$r_1 = r_2 = 1500,\ c_1 = c_2 = 0.01,\ d_{h_1} = 0.15,\ d_{h_2} = 0.13,\ \alpha_1 = \alpha_2 = 0.005,\ a_1 = 22000,\ a_2 = 23000$.

Colonies infested by varroa mites are typically faced with infection by viruses such as Deformed Wing Virus or Israeli Acute Paralysis Virus (DeGrandi-Hoffman et al. (2016)) and the level of infection drive the strength of the colonies. Similarly nutrition is another factor that contribute to the strength of a colony. These two factors are however not taken into account in our model so we consider multiple scenarios in order to implicitly model the variation that occur in colonies due to disease dynamics or nutritional factors.

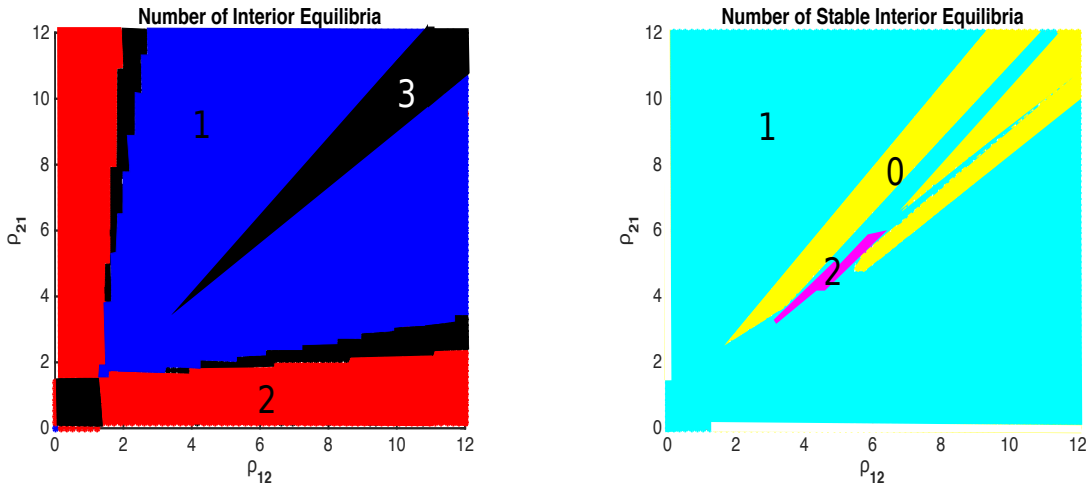

(a) ρ_{21} vs ρ_{12} for the number of interior equilibria.

(b) ρ_{21} vs ρ_{12} for the number of stable interior equilibria.

Figure 3.5: Two Parameter Bifurcation Diagrams of Model (3.2). $(H_1^*, M_1^*) = (1900, 93.6)$ and $(H_2^*, M_2^*) = (1812, 101.9)$ are Both Sink in the Absence of Dispersal. Black Region Have Three Interior Equilibria; Red Regions Have Two Interior Equilibria; Blue Regions Have One Interior Equilibrium; and white regions have no interior equilibria in Figure 3.5(a). Cyan Regions Have One Stable Interior Equilibria; Magenta Regions Have Two Stable Interior Equilibria; Yellow Regions Have No Stable Interior Equilibria, and White Regions Have No Interior Equilibria in Figure 3.5(b).

Specifically, we investigate the following two scenarios of patch dynamics in the absence of dispersal:

Case one: Honeybees and mites can coexist in both patches (non-symmetric case).

Case two: Honeybees and mites can coexist in one patch while the honeybee colony collapses in the other patch that has a highly mite infested colony or a potential colony collapsing event.

3.5.1 Case One

Let $d_{m_1} = 0.095$, $d_{m_2} = 0.0906$ and $K_1 = K_2 = 1000000$. In the absence of dispersal, the uncoupled two colonies of Model (3.1) are locally asymptotically stable at $(H_1^*, M_1^*) =$

$(1900, 93.6)$ and $(H_2^*, M_2^*) = (1812, 101.9)$, respectively.

In the presence of dispersal, we first perform two dimensional bifurcation diagrams to explore how dispersal rates affect the number of interior equilibria (see Figure 3.5(a)) and their stability (see Figure 3.5(b)). These two dimensional bifurcation diagrams suggest that: (1) Intermediate values of dispersal rates of ρ_{12} and ρ_{21} could generate multiple attractors: two stable interior equilibria and two boundary attractors $E_{N_{h_1}^* 000}, E_{00N_{h_2}^* 0}$ (see the purple regions in Figure 3.5(a)). (2) Large values of dispersal rates of ρ_{12} and ρ_{21} could destabilize the dynamics leading to the extinction of honeybee and mite in at least one patch (see the overlapping regions of black in Figure3.5(a) and yellow in Figure 3.5(a)). Additional simulations show that small values of dispersal can generate one interior attractor where $E_{N_{h_1}^* 000}$ and/or $E_{00N_{h_2}^* 0}$ are either saddle or locally stable depending on the dispersal rate (e.g., $\rho_{12} < 1.29$ leads to $E_{N_{h_1}^* 000}$ being saddle while $\rho_{21} < 1.45$ lead to $E_{00N_{h_2}^* 0}$ being saddle); and the two-patch model (3.2) has only two boundary attractors $E_{N_{h_1}^* 000}, E_{00N_{h_2}^* 0}$ when it has only one stable interior equilibrium (see the cyan regions of Figure 3.5(a)).

To explore how dispersal rates affect the dynamical patterns, we perform one dimensional bifurcation diagrams for the following two subcases, where the dispersal rates, not having data on which to base them, are given hypothetical, perhaps even biologically unrealistic, toy values, to provide some guidelines on their dynamical effects:

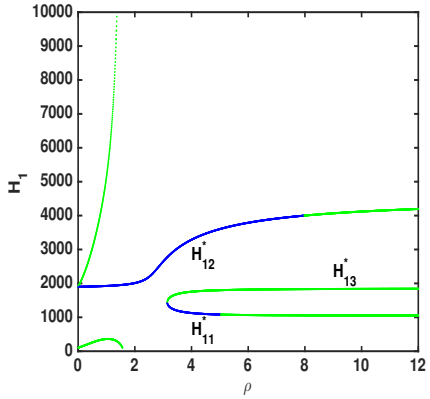

(a) H_1 vs ρ for the effect of dispersal

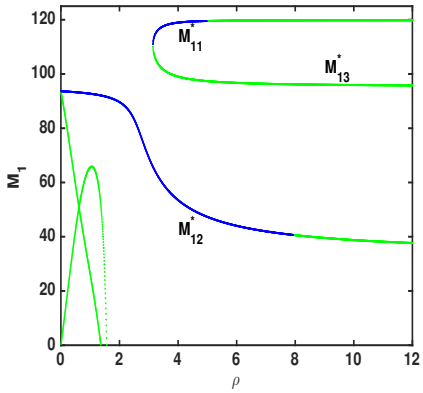

(b) M_1 vs ρ for the effect of dispersal

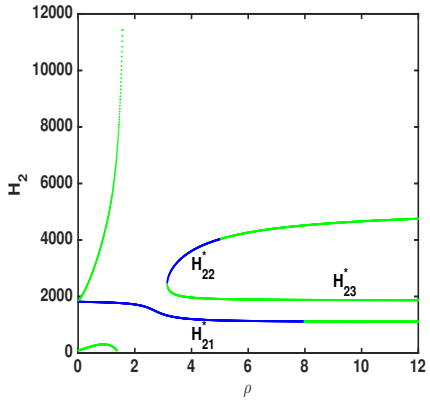

(c) H_2 vs ρ for the effect of dispersal

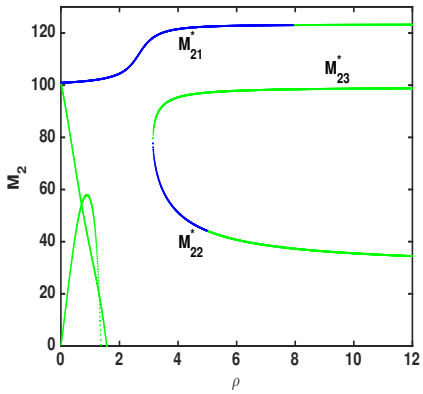

(d) M_2 vs ρ for the effect of dispersal

Figure 3.6: One Parameter Bifurcation Diagrams of Model (3.2). $(H_1^*, M_1^*) = (1900, 93.6)$ and $(H_2^*, M_2^*) = (1812, 101.9)$ are Stable Without Dispersal. The Notations H_{ij}^* and M_{ij}^* Represent the Population of Honeybee and Mite of the j^{th} Interior Equilibrium at Patch i, Respectively. The Blue Line Represents Sink and the Green Line a Saddle.

1. **Same dispersal rates between two patches:** $\rho_{12} = \rho_{21} = \rho$. One dimensional bifurcation diagrams (see Figures 3.6(a), 3.6(b), 3.6(c), and 3.6(d)) show that: (1) small values of dispersal rate could generate three interior equilibria where two are saddle and one is locally stable; (2) intermediate values of dispersal could generate multiple stable interior equilibria that lead to the bistability between interior attractors;

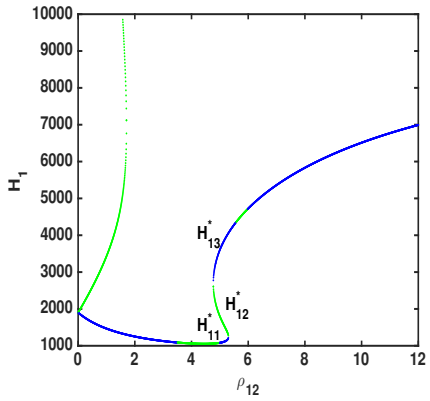

(a) H_1 vs ρ_{12} for the effect of dispersal

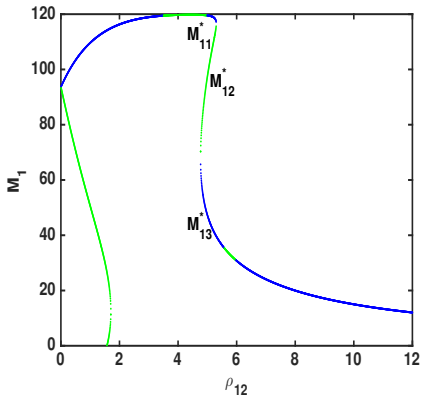

(b) M_1 vs ρ_{12} for the effect of dispersal

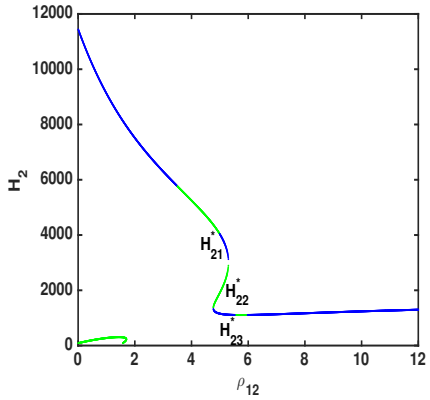

(c) H_2 vs ρ_{12} for the effect of dispersal

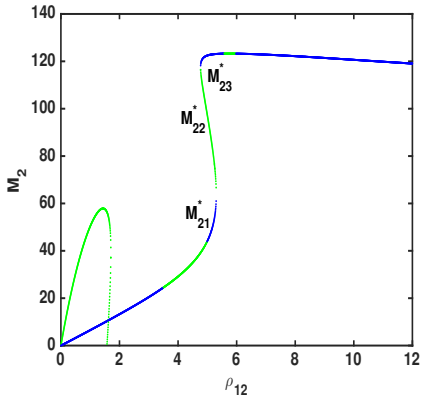

(d) M_2 vs ρ_{12} for the effect of dispersal

Figure 3.7: One parameter bifurcation diagrams of Model (3.2) when $\rho_{21} = 5$. $(H_1^*, M_1^*) = (1900, 93.6)$ and $(H_2^*, M_2^*) = (1812, 101.9)$ are Stable Without Dispersal. The Notations H_{ij}^* and M_{ij}^* Represent the Population of Honeybee and Mite of the j^{th} Interior Equilibrium at Patch i, Respectively. The Blue Line Represents Sink and the Green Line a Saddle.

and (3) large values of dispersal could destabilize the system such that dynamics converging to the boundary attractors $E_{N_{h_1}^* 000}$ or $E_{00N_{h_2}^* 0}$ depending on initial conditions. This phenomenon can lead to the collapsing of at least one honeybee colony. We also note from Figures 3.6(a) - 3.6(d) that depending on the initial conditions, when dispersal is in the intermediate value range, an increase in the mite dispersal rate yields a growth of the varroa population which in return have a negative feedback on

honeybee population in both patches. This result is supported by the field work of DeGrandi-Hoffman et al. (2016); Sakofski et al. (1990).

2. **Different dispersal rates:** $\rho_{12} \neq \rho_{21}$. We perform one dimensional bifurcation diagrams on $\rho_{12} \in [0,12]$ by fixing $\rho_{21} = 5$. Note that when $\rho_{12} = 0$, Model (3.2) is stabilized at the equilibrium $(H_1, M_1, H_2, M_2) = (1900, 93.64, 11451.1, 0)$ which corresponds to the case when foraging of honeybee is occurring in one way. Our bifurcation diagrams (Figures 3.7(a)-3.7(d)) suggest that the intermediate values of dispersal rates in mites (i.e., the value of the ratio $\frac{\rho_{21}}{\rho_{12}}$ is close to 1) could generate multiple interior/boundary attractors; and the large values of dispersal rates tend to make Model (3.2) have one stable interior equilibrium. In addition, we note that when the values of dispersal rates are small (i.e., the value of the ratio $\frac{\rho_{21}}{\rho_{12}} < 1$), an increase in the mite dispersal rate yields a rapid growth of the varroa population which in return have a negative feedback on honeybee population in both patches. This result is supported by the field work of DeGrandi-Hoffman et al. (2016); Sakofski et al. (1990).

3.5.2 Case Two

Let $d_{m_1} = 0.317$, $d_{m_2} = 0.095$, $K_1 = 1000000$ and $K_2 = 4000000$. In the absence of dispersal, Model (3.1) is locally asymptotically stable at $(H_1^*, M_1^*) = (6340, 16.17)$ at Patch 1, and has its interior equilibrium being a source at $(H_2^*, M_2^*) = (1900, 48.9)$ in Patch 2 that has a highly mite infested colony such that both honeybees and mites go extinct (i.e., Patch 2 is the collapsing colony).

In the presence of dispersal, we first perform two dimensional bifurcation diagrams to explore how dispersal rates affect the number of interior equilibria (see Figure

3.8(a)) and their stability (see Figure 3.8(b)). These two dimensional bifurcation diagrams (Figure 3.8) suggest that the large ratio of $\frac{\rho_{21}}{\rho_{12}}$ (i.e., the dispersal rate from the collapsing colony at Patch 2 to the healthy colony at Patch 1 is larger than the other direction) can save the collapsing colony such that both honeybees and mites could coexist at both patches (see the cyan regions in Figure 3.8(b)). On the other hand, when the values of the ratio of $\frac{\rho_{21}}{\rho_{12}}$ are less than 1, Model (3.2) has no stable interior equilibrium with dynamics converging to the two boundary attractors $E_{N^*_{h_1}000}, E_{00N^*_{h_2}0}$ depending on initial conditions (see yellow regions in Figure 3.8(b)). This is the case suggesting that dispersal could indeed lead to the extinction of mites.

To explore how dispersal rates affect the dynamical patterns, we perform one dimensional bifurcation diagrams 3.9 by letting $\rho_{12} = \rho_{21} = \rho \in [0,6]$ based on two dimensional bifurcation diagrams 3.8. Figures 3.9(a), 3.9(b), 3.9(c), and 3.9(d) suggest that for small dispersal rates, Model (3.2) converges to one of the boundary attractors (i.e., $E_{\hat{H}^*_1\hat{M}^*_1 0\hat{M}^*_2}$ or $E_{0\check{M}^*_1\check{H}^*_2\check{M}^*_2}$) where honeybee population goes extinct in one patch. In addition, it seems that intermediate and large values of dispersal rates (when $\rho_{12} = \rho_{21}$) could stabilize the dynamics such that both honeybees and mites are able to coexist in both patches.

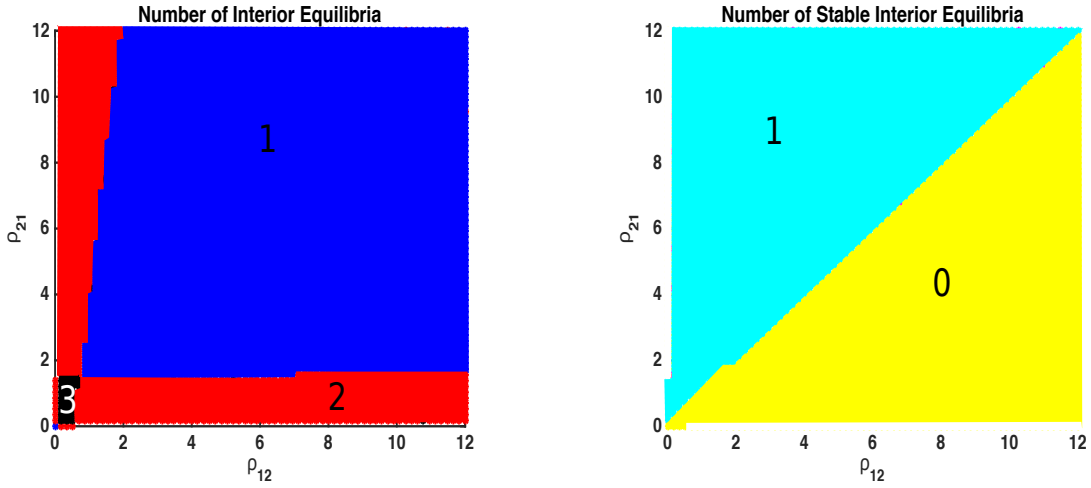

(a) ρ_{21} vs ρ_{12} for the number of interior equilibria.

(b) ρ_{21} vs ρ_{12} for the number of stable interior equilibria

Figure 3.8: Two Parameter Bifurcation Diagrams of Model (3.2). $(H_1^*, M_1^*) = (6340, 16.17)$ is sink and $(H_2^*, M_2^*) = (1900, 48.9)$ is a Source in the Absence of Dispersal. Black Region Have Three Interior Equilibria; Red Regions Have Two Interior Equilibria; Blue Regions Have One Interior Equilibrium; and white regions have no interior equilibria in Figure 3.8(a). Cyan Regions Have One Stable Interior Equilibria; Magenta Regions Have Two Stable Interior Equilibria; Yellow Regions Have No Stable Interior Equilibria; and White Regions Have no Interior Equilibria in Figure 3.8(b).

To further explore the effects of dispersal rates in mites on population dynamics, let $K_1 = 1000000$, $K_2 = 4000000$, $d_{m_1} = 0.095$ and $d_{m_2} = 0.0906$ such that, in the absence of dispersal, Model (3.2) has local stability at $(H_1^*, M_1^*) = (1900, 93.6)$ for Patch 1 (i.e., the healthy patch) while $(H_2^*, M_2^*) = (1812, 48.6)$ is a source at Patch 2 (i.e., the collapsing patch). We perform one dimensional bifurcation diagrams (Figure 3.10(a), 3.10(b), 3.10(c), and 3.10(d)) by fixing $\rho_{21} = 12$ and letting $\rho_{12} \in [0, 12]$ which is less than ρ_{21}. Our bifurcation diagrams 3.10 show that not large values of dispersal rates from the healthy patch to the collapsing patch, e.g., $\rho_{12} < 9$, could stabilize the system such that both honeybees and mites could coexist. While the larger values of ρ_{12} could not have coexistence of both honeybees and mites, and the dynamics of Model (3.2) converge to one of the two boundary

attractors $E_{N^*_{h_1}000}$ or $E_{00N^*_{h_2}0}$ depending on initial conditions. This implies that the proper values of the mite dispersal rate could save the honeybee colony from collapsing.

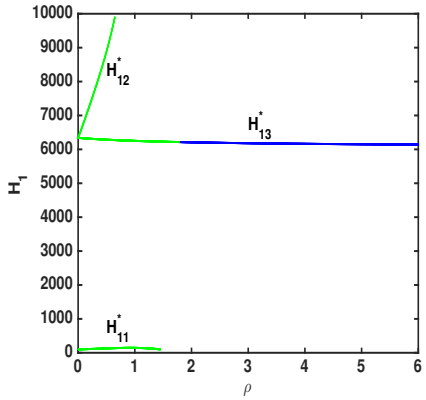

(a) H_1 vs ρ for the effects of dispersal

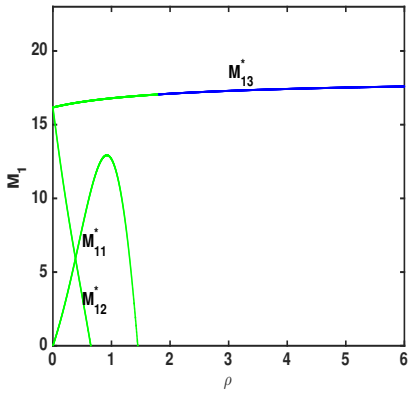

(b) M_1 vs ρ for the effect of dispersal

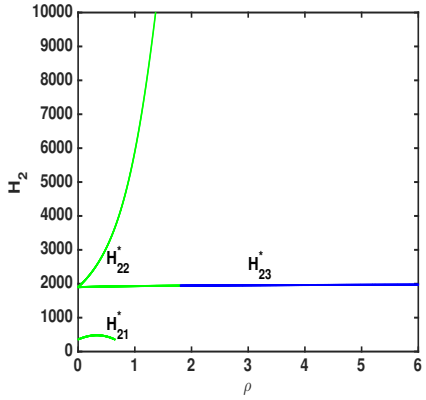

(c) H_2 vs ρ for the effect of dispersal

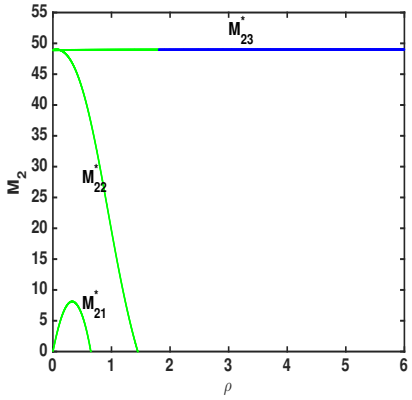

(d) M_2 vs ρ for the effect of dispersal

Figure 3.9: One Parameter Bifurcation Diagrams of Model (3.2). $(H_1^*, M_1^*) = (6340, 16.17)$ is a Sink and $(H_2^*, M_2^*) = (1900, 48.9)$ is a Source Without Dispersal. The Notations H_{ij}^* and M_{ij}^* Represent the Population of Honeybee and Mite of the j^{th} Interior Equilibrium at Patch i, Respectively. The Blue Line Represents Sink and the Green Line a Saddle.

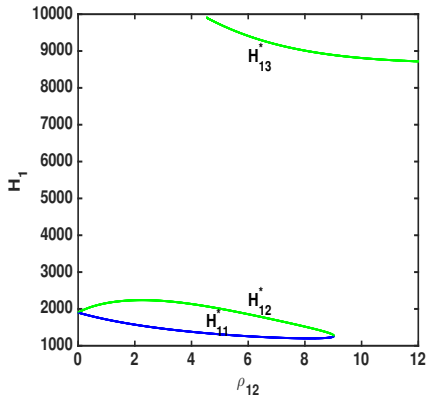

(a) H_1 vs ρ_{12} for the effect of dispersal

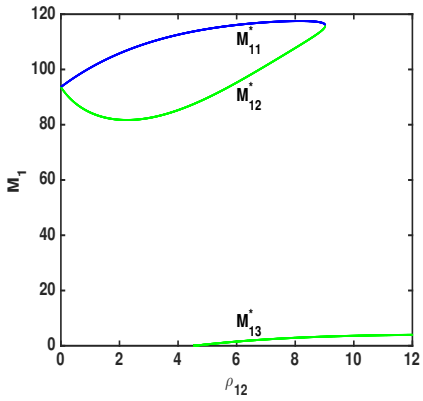

(b) M_1 vs ρ_{12} for the effect of dispersal

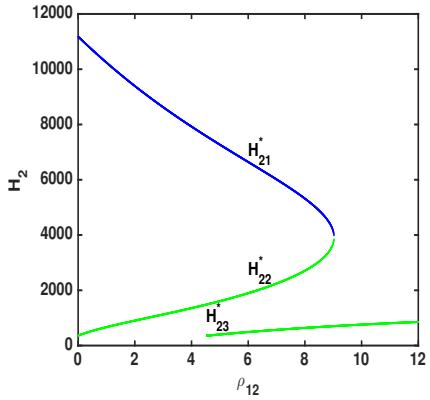

(c) H_2 vs ρ_{12} for the effect of dispersal

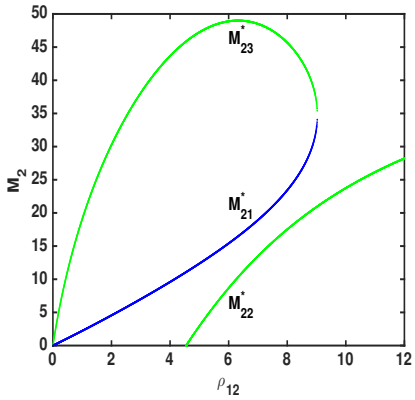

(d) M_2 vs ρ_{12} for the effect of dispersal

Figure 3.10: One parameter bifurcation diagrams of Model (3.2) when $\rho_{21} = 12$. $(H_1^*, M_1^*) = (1900, 93.6)$ is Sink and $(H_2^*, M_2^*) = (1812, 48.6)$ is a Source Without Dispersal. The Notations H_{ij}^* and M_{ij}^* Represent the Population of Honeybee and Mite of the j^{th} Interior Equilibrium at Patch i, Respectively. The Blue Line Represents Sink and the Green Line a Saddle.

One interesting observation is that when the dispersal rates from the healthy patch (i.e patch 1) to the collapsing patch (patch 2), ρ_{12} is less than 9, **an increasing dispersal rate could result in the growth of mite population and the decline of honeybee population** (see the blue lines in Figures 3.10(a)-3.10(d)). This fits in the field work of DeGrandi-Hoffman et al. (2016); Sakofski et al. (1990). On the other hand, if we decrease the dispersal rates from the healthy patch to the collapsing patch ρ_{12}, we could also observe the similar patterns. As an example, we provide time series of honeybee and mite population at

two patches by letting $c_1 = c_2 = .01$, $K_1 = 1000000$, $K_2 = 4000000$, $d_{h_1} = 0.15$, $d_{h_2} = 0.13$, $\alpha_1 = \alpha_2 = .005$, $a_1 = 22000$, $a_2 = 230000$, $d_{m_1} = 0.095$, $d_{m_2} = .0906$. Under this set of parameter values, Model (3.2) has (H_1^*, M_1^*) being a sink at Patch 1 and (H_2^*, M_2^*) being a source at Patch 2 when $\rho_{12} = \rho_{21} = 0$. However, if we take $\rho_{12} = 3$ or 7 (see the blue lines for $\rho_{12} = 3$ and black lines for $\rho_{12} = 7$ in Figures 3.11(b) and 3.11(a)) while keeps $\rho_{21} = 12$, we could observe that increasing the value of ρ_{12} results in the rapid growth of mite population and the decline of honeybee population (i.e. For $\rho_{12} = 3$, the population converge to $(H_1, M_1, H_2.M_2) = (1464.8, 109.7, 8625.4, 7)$ and for $\rho_{12} = 7$ the population stabilize at $(H_1, M_1, H_2.M_2) = (1220.9, 117, 6013, 18.9)$).

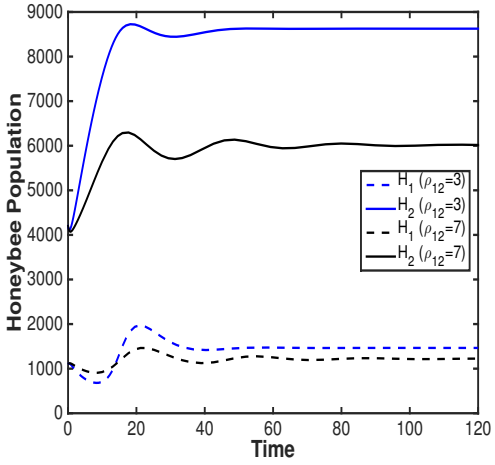

(a) Dispersal effect on honeybee populations in patch 1 and patch 2 when $H_1(0) = 1100$, $M_1(0) = 100$, $H_2(0) = 4200$, $M_2(0) = 56$.

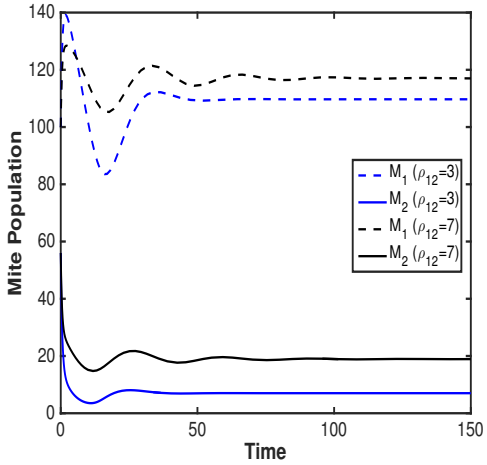

(b) Dispersal effect on mite populations in patch 1 and patch 2 when, $H_1(0) = 1100$, $M_1(0) = 100$, $H_2(0) = 4200$, $M_2(0) = 56$.

Figure 3.11: Time Series of Model (3.2) when $\rho_{21} = 12$, $r_1 = r_2 = 1500$, $c_1 = c_2 = 0.01$, $d_{h_1} = 0.15$, $d_{h_2} = 0.13$, $\alpha_1 = \alpha_2 = 0.005$, $a_1 = 22000$, $a_2 = 23000$, $d_{m_1} = 0.095$, $d_{m_2} = 0.0906$, $K_1 = 1000000$, $K_2 = 4000000$. $(H_1^*, M_1^*) = (1900, 93.6)$ is a Sink and $(H_2^*, M_2^*) = (1812, 48.6)$ is a source Without Dispersal. Figure 3.11(a) and 3.11(b) Represent Respectively the Population of Honeybees and Mites in Both Patches When $\rho_{12} = 3$ (see the blue lines) or $\rho_{12} = 7$ (see the black lines) while $\rho_{21} = 12$.

3.5.3 Dispersal Effects on Colony Extinction Time

In this subsection, we use time series simulations to illustrate how dispersal in mites may affect the extinction time of collapsing event for two cases. As mentioned in the simulations with no dispersal, the half saturation constanst a_1 and a_2 are here given two hypothetical values that differ by one order of magnitude, because there are no data on which to base these estimates. The latter might perhaps be biologically unrealistic, but are meant to be understood as toy values, to help assessing their effect on the dynamical behavior of the ecosystem. Perhaps a possible justification for this huge difference could be given by observing that some colonies may have disease dynamics due to parasitism behavior, that are not taken into account in our model. Furthermore, there may be a large variations in these parameters due to nutrition, disease dynamics, and other factors. In order to incorporate these factors, we allow large variations in these coefficients. In addition, this variation reflects the fact that there are usually many colonies in the natural habitat, facing different ecological situations; the ability of mites to attach to the bees differs from colony to colony.

1. Let $c_1 = c_2 = .01$, $K_1 = 1000000$, $K_2 = 4000000$, $d_{h_1} = 0.15$, $d_{h_2} = 0.13$, $\alpha_1 = \alpha_2 = .005$, $a_1 = 22000$, $a_2 = 230000$, $d_{m_1} = 0.095$, $d_{m_2} = .0906$. Under this set of parameter values, in the absence of dispersal, Model (3.2) has (H_1^*, M_1^*) being a sink at Patch 1 and (H_2^*, M_2^*) being a source at Patch 2, i.e., Patch 1 is a healthy colony while Patch 2 colony dies at time 59.61 when its honeybee population drops below 1.

   (a) Fix $\rho_{21} = 12$ and let $\rho_{12} = 10$ or 16 (see Figure 3.12): Figure 3.12 shows that increasing dispersal rate from the healthy colony to the collapsing colony (i.e., ρ_{12}) decreases the extinction time in Patch 2 with only honeybee surviving in Patch 1 (i.e., no mites survive at neither patch). In addition, the population of

honeybee at Patch 1 increases as ρ_{12} increases. This implies that large mite dispersal of ρ_{12} may lead to the earlier colony death event in Patch 2, however, it may increase honeybee population at Patch 1 and drive the extinction of mites in both patches.

(b) Fix $\rho_{12} = 12$ and let $\rho_{21} = 10$ or 16 (see Figure 3.13): Figure 3.13 shows similar patterns as Figure 3.12, the difference is that increasing mite dispersal rate from the collapsing colony to the healthy colony (i.e., ρ_{21}) leads to the later death event in Patch 2 but still earlier than the case when no dispersal at all (i.e., $\rho_{21} = \rho_{12} = 0$).

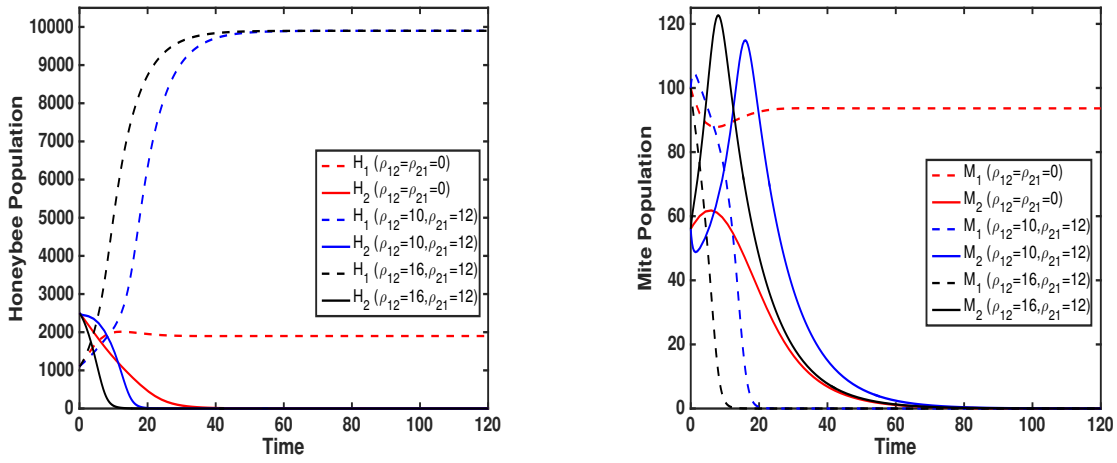

(a) dispersal effect on honeybee population when $H_1(0) = 1100$, $M_1(0) = 100$, $H_2(0) = 2500$, $M_2(0) = 56$.

(b) dispersal effects on honeybee population when $H_1(0) = 1100$, $M_1(0) = 100$, $H_2(0) = 2500$, $M_2(0) = 56$.

Figure 3.12: Time Series of Model (3.2) when $r_1 = r_2 = 1500$, $c_1 = c_2 = 0.01$, $d_{h_1} = 0.15$, $d_{h_2} = 0.13$, $\alpha_1 = \alpha_2 = 0.005$, $a_1 = 22000$, $a_2 = 23000$, $d_{m_1} = 0.095$, $d_{m_2} = 0.0906$, $K_1 = 1000000$, $K_2 = 4000000$. $(H_1^*, M_1^*) = (1900, 93.6)$ is a sink and $(H_2^*, M_2^*) = (1812, 48.6)$ is a Source Without Dispersal. Dash Lines Represent Population of Honeybees and Mites in Patch 1 and Solid Lines Represent Population of Honeybees and Mites in Patch 2. Red Lines Indicate the Population of Mites and Honeybees when $\rho_{12} = \rho_{21} = 0$; Blue Lines Indicate the Population of Honeybees and Mites when $\rho_{12} = 10$, $\rho_{21} = 12$; and Black Lines Indicates the Population of Honeybees and Mites when $\rho_{12} = 16$, $\rho_{21} = 12$.

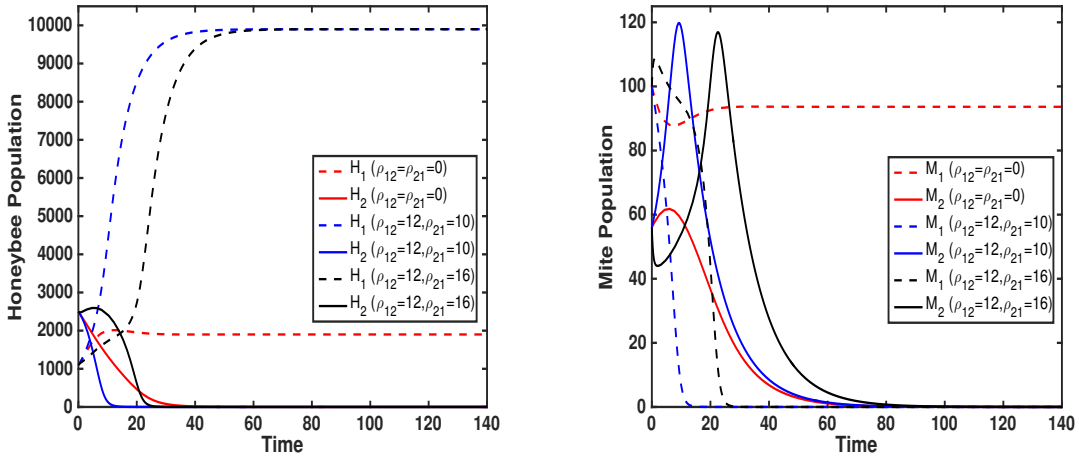

(a) Dispersal effect on honeybee population when $H_1(0) = 1100$, $M_1(0) = 100$, $H_2(0) = 2500$, $M_2(0) = 56$.

(b) Dispersal effects on honeybee population when $H_1(0) = 1100$, $M_1(0) = 100$, $H_2(0) = 2500$, $M_2(0) = 56$.

Figure 3.13: Time Series of Model (3.2) when $r_1 = r_2 = 1500$, $c_1 = c_2 = 0.01$, $d_{h_1} = 0.15$, $d_{h_2} = 0.13$, $\alpha_1 = \alpha_2 = 0.005$, $a_1 = 22000$, $a_2 = 23000$, $d_{m_1} = 0.095$, $d_{m_2} = 0.0906$, $K_1 = 1000000$, $K_2 = 4000000$. $(H_1^*, M_1^*) = (1900, 93.6)$ is a sink and $(H_2^*, M_2^*) = (1812, 48.6)$ is a Source Without Dispersal. Dash Lines Represent Population of Honeybees and Mites in Patch 1 and Solid Lines Represent Population of Honeybees and Mites in Patch 2. Red Lines Indicate the Population of Mites and Honeybees when $\rho_{12} = \rho_{21} = 0$; Blue Lines Indicate the Population of Honeybees and Mites when $\rho_{21} = 10$, $\rho_{12} = 12$; and Black Lines Indicates the Population of Honeybees and Mites when $\rho_{21} = 16$, $\rho_{12} = 12$.

2. Let $c_1 = c_2 = .01$, $K_1 = K_2 = 4000000$, $d_{h_1} = 0.15$, $d_{h_2} = 0.13$, $\alpha_1 = \alpha_2 = .005$, $a_1 = 22000$, $a_2 = 230000$, $d_{m_1} = 0.095$, $d_{m_2} = .0906$. Under this set of parameter values, in the absence of dispersal, Model (3.2) has the interior equilibrium (H_1^*, M_1^*) at Patch 1 and (H_2^*, M_2^*) at Patch 2, being source. More specifically, both Patch 1 and 2 colony die (i.e., the population of honeybee drops below 1) at times 19.85, 58.52, respectively.

   (a) Fix $\rho_{21} = 10$ and let $\rho_{12} = 2$ or 10 (see Figure 3.14): Figure 3.14 shows that: (1) mite dispersal can save Patch 1 from collapsing such that its honeybee colony survives; (2) mite dispersal may not be able to save mites from extinction; and

(3) increasing dispersal rate from Patch 1 to Patch 2 (i.e., ρ_{12}) can increase the extinction time to the collapse of Patch 2.

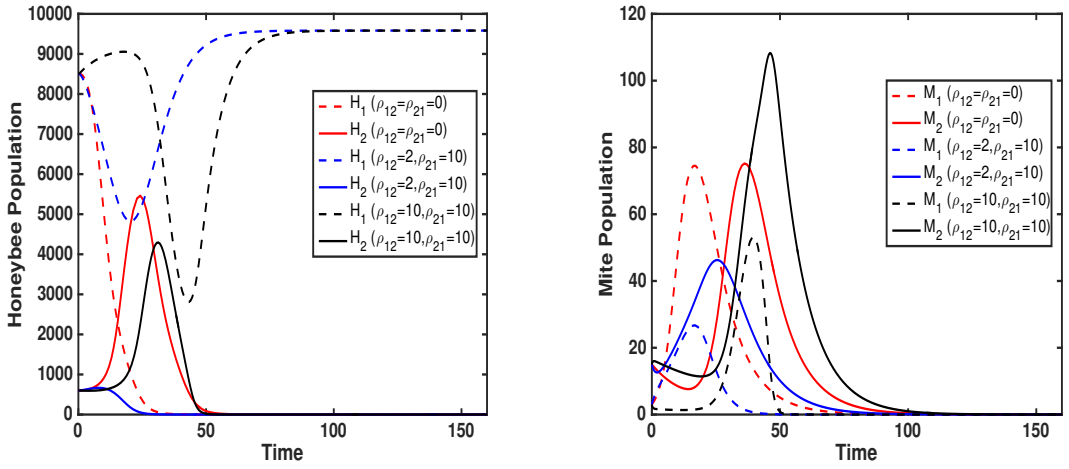

(a) Dispersal effects on honeybee populations when $H_1(0) = 8500$, $M_1(0) = 3$, $H_2(0) = 600$, $M_2(0) = 15$.

(b) Dispersal effects on honeybees populations when $H_1(0) = 8500$, $M_1(0) = 3$, $H_2(0) = 600$, $M_2(0) = 15$.

Figure 3.14: Time Series of Model (3.2) when $r_1 = r_2 = 1500$, $c_1 = c_2 = 0.01$, $d_{h_1} = 0.15$, $d_{h_2} = 0.13$, $\alpha_1 = \alpha_2 = 0.005$, $a_1 = 22000$, $a_2 = 23000$, $d_{m_1} = 0.095$, $d_{m_2} = 0.0906$, $K_1 = K_2 = 4000000$. (H_1^*, M_1^*) and (H_2^*, M_2^*) are Both Source Without Dispersal. Dash Lines Represent Population of Honeybees and Mites in Patch 1 and Solid Lines Represent Population of Honeybees and Mites in Patch 2. Red Lines Indicate the Population of Mites and Honeybees when $\rho_{12} = \rho_{21} = 0$; Blue Lines Indicate the Population of Honeybees and Mites when $\rho_{12} = 2$, $\rho_{21} = 10$; and Black Lines Indicates the Population of Honeybees and Mites when $\rho_{12} = 10$, $\rho_{21} = 10$.

(b) Fix $\rho_{12} = 10$ and Let $\rho_{21} = 2$ or 10 (see Figure 3.15): Figure 3.15 shows the similar patterns as Figure 3.15 with difference in increasing dispersal rate from Patch 2 to Patch 1 (i.e., ρ_{21}) can decrease the extinction time to collapsing event in Patch 2.

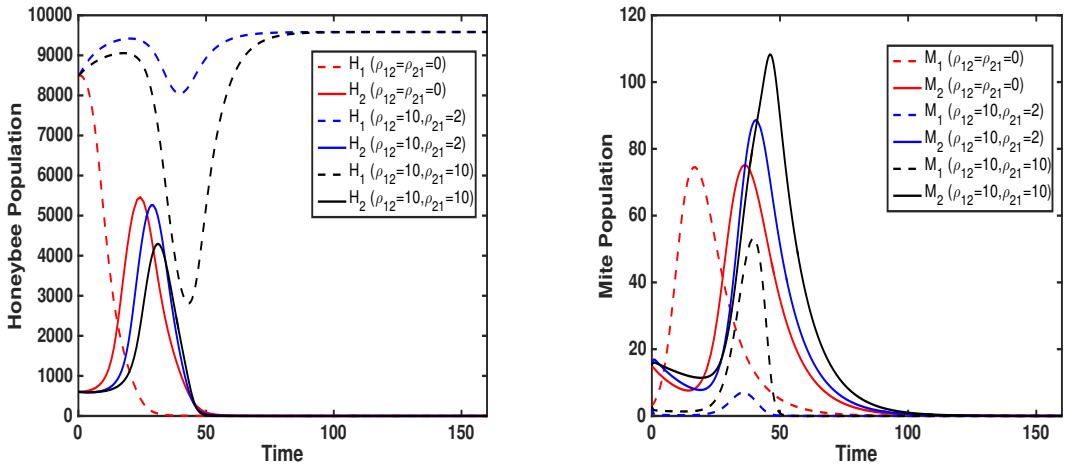

(a) Dispersal effects on honeybee populations when $H_1(0) = 8500$, $M_1(0) = 3$, $H_2(0) = 600$, $M_2(0) = 15$.

(b) Dispersal effects on honeybee populations when $H_1(0) = 8500$, $M_1(0) = 3$, $H_2(0) = 600$, $M_2(0) = 15$.

Figure 3.15: Time Series of Model (3.2) when $r_1 = r_2 = 1500$, $c_1 = c_2 = 0.01$, $d_{h_1} = 0.15$, $d_{h_2} = 0.13$, $\alpha_1 = \alpha_2 = 0.005$, $a_1 = 22000$, $a_2 = 23000$, $d_{m_1} = 0.095$, $d_{m_2} = 0.0906$, $K_1 = K_2 = 4000000$. (H_1^*, M_1^*) and (H_2^*, M_2^*) are both Source Without Dispersal. Dash Lines Represent Population of Honeybees and Mites in Patch 1 and Solid Lines Represent Population of Honeybees and Mites in Patch 2. Red Lines Indicate the Population of Mites and Honeybees when $\rho_{12} = \rho_{21} = 0$; Blue Lines Indicate the Population of Honeybees and Mites when $\rho_{21} = 2$, $\rho_{12} = 10$; and Black Lines Indicates the Population of Honeybees and Mites when $\rho_{21} = 10$, $\rho_{12} = 10$.

3.6 Discussion

This chapter proposed a nonlinear system of ordinary differential equations that describes the interactions between honeybees and mites in a two patch framework. The two patches are connected through the adaptive dispersal of the adult honeybee foragers and the phoretic mites are mobile due to their attachment to the bees. The effect of nutritional demands and honeybee diseases are not explicitly included in our model but these are implicitly included in our system via some of the life history parameter of the honeybee. For example, different values with difference of one order of magnitude of a (which represent the size of the bee population at which the rate of attachment is half the maximum) were chosen. We note that small value of a yield large probability of mites attaching to bees

thus a was used to measure the suitability of environmental conditions (i.e. availability of resource, disease, etc.). We provide boundedness and positivity of the proposed model in Theorem (5). In the absence of dispersal, our proposed model is reduced to Model (3.1) extensively studied in Kang et al. (2015) and its dynamics are summarized in Section 3.3 of this manuscript. Using analytical and numerical techniques, we study the effect of dispersal on honeybee population dynamics under infestation by the Varroa mites and its congruence to the colony collapse phenemonon.

Theorem (7) provides the existence and stability of the boundary equilibria of Model (3.2). These results reveal how the optimal dispersal of honeybees can potentially stabilize the boundary equilibria $E_{N^*_{h_1}000}$, $E_{00N^*_{h_2}0}$, or $E_{N^*_{h_1}0N^*_{h_2}0}$ consequently driving the varroa mites extinct in at least one of the patches. Theorem (8) presents the existence and stability conditions of the symmetric interior equilibrium for the symmetric Model (3.7). The analytical results suggest that large dispersal of honeybees may have destabilizing effects on the dynamics. Furthermore, bifurcation analysis of the symmetric model indicate that intermediate and large dispersal could generate two additional asymmetric interior equilibria which can be saddle or sink, thus generating bistability dynamics (see blue lines for sink and green lines for saddle in Figures 3.4(a) and 3.4(b)). When the population of honeybee goes extinct in one of the patches, our model displays a sink-source dynamics with the honeybee patch being the sink. From the analytical studies presented in Theorem (6), dispersal has no effect on the global extinction of honeybees and mites in both patches. However, large dispersal of honeybees could drive mites extinct in both patches or even prevent the extinction of honeybee locally. In addition, intermediate value of dispersal may prompt the coexistence of mites in both patches and honeybees in the sink patch.

Numerical results of the system suggest that an increase in dispersal rate of honeybees entering and leaving the colonies yield a growth of the Varroa population which in return have a negative feedback on honeybee population in at least one of the patches. These results are supported by the field work of DeGrandi-Hoffman et al. (2016). Depending on the initial population sizes, large dispersal may have destabilizing effects on the dynamics from the results presented in Figures 3.4(a) and 3.4(b) or 3.6(a)-3.6(d). Small and intermediate dispersal values could also stabilize the dynamics (see blue line in Figures 3.9(a)-3.9(d) and Figures 3.10(a)-3.10(d)). We note that when Model (3.2) has three interior equilibria that are all saddle, the system typically converges to a boundary attractor leading to the collapse in at least one of the patches. Moreover, increasing dispersal in honeybees may decrease the time until extinction of honeybees and mites when the interior equilibrium of one colony is stable while the interior equilibrium of the other colony is a source without dispersal. Nevertheless, increasing dispersal increases the time until extinction of species when the interior equilibrium of both patches are source.

3.7 Concluding Remarks

The findings from this chapter illustrate how population dynamics of honeybees and mites are affected by the adaptive foraging behavior of bees when healthy colonies are surrounded by the infested ones. While our proposed model neglects some of the environmental features that may promote colonies to collapse such as honeybee diseases (e.g. American and European foulbrood, Chalkbrood, Stonebrood, etc.), poor nutrition, or exposure to pesticides, we implicitly incorporated this into the life history parameter of the bees and study the subsequent dynamics. In addition, this study gives us a better understanding on dispersal of honeybees and its relatedness to the colony collapse phenomenon. The results provided in this chapter answers our question initially stated in chapter 1 regarding conditions under which dispersal or an adaptive dispersal could favor coexistence of social

animals. Martin (1994); Ifantidis (1988) noted that the reproduction of mites occurs only within a sealed drone or worker brood cell. The reproduction of mites therefore require the presence of brood in the colony which constitute one limitation of our model as we do not explicitly consider a stage structure model. Rather, both brood and adult honeybees are grouped into a single stage in the study presented in this chapter. It will be interesting to investigate a stage structure model, where one can measure not only the optimal foraging of the bees but also other important life history parameters that may be affecting the population size of the colony. Such work is presented in chapter 4 where I study the population dynamics only at a single patch level.

Chapter 4

THE ROLE OF VARROA ON THE HONEYBEE POPULATION DYNAMICS: A MODELING APPROACH AND THE EFFECT OF BROOD-MITE INTERACTIONS

4.1 Abstract

Honeybees play an important role in the sustainability of our ecosystem. However, the rapid decline of honeybee population have sparked a great concern worldwide. Many field and theoretical studies have shown that the collapsing of colonies may be due to the infestation by the parasitic Varroa mite (*Varroa destructor* Anderson and Trueman). Noting that reproduction of mites only occur within a sealed drone and brood cells, this project investigates the population dynamics of honeybee colonies under infestation by the Varroa mite. I propose a single patch brood-adult bee-mite interaction model in which I incorporate the time lag from brood to adult bee. My model is validated by field data and I provide full analysis on the dynamics generated by the presence of mite in a colony. The analytical and numerical studies reveal the following: (a) Large mite natural death rate could drive the mite population extinct and leave the colony with healthy brood and adult bees; (b) Small infestation by the Varroa mite could stabilize all the three population at the unique interior equilibrium while intermediate infestation rate promote coexistence of all species through fluctuating dynamics; (c) Large infestation rate however can destabilize the dynamic leading to extinction of all species dependent on initial population size. The results of my sensitivity analysis also indicate that the queen's eggs laying may be have the greatest effect on colony population size and other important parameters affecting the population size of all species are also disclosed.

4.2 Introduction

The dynamics within a honeybee colony is a complex phenomenon characterize by many behaviors including reproduction by the queen bee, brood rearing and foraging activities by the workers, diseases dynamics (e.g American and Euro- pean foulbrood, Chalkbrood, Stonebrood, etc.), parasitic effects, etc. Brood rearing and colony growth depend on queen's eggs laying activity which in return rely upon successful foraging activity by the workers making the dynamics a feedback system of interdependent elements DeGrandi-Hoffman et al. (1989). Honeybees often go through an optimal collective-decision making process in order to sustain its colony. Several field and laboratory experiments including Zimmerman (1982); Wells and Wells (1986); Fewell and Winston (1992) have illustrated the adaptive process bees generally utilize to search the most profitable food source in an explored environment. Fewell and Winston (1992) also found a direct relationship between pollen storage levels and colony brood production, demonstrating the potential for cumulative changes in individual foraging decisions to affect colony fitness. As a part of this intelligence collective decision making process, honeybees often defend their colonies against many hazard including robber bees, diseases, or parasitism Evans and Spivak (2010); Boecking and Spivak (1999). Unfortunately, honeybees are still increasingly threatened by numerous factors, most notably the parasitic Varroa mite.

As described in chapter 3 of this dissertation, the dispersal of the phoretic mites is done through attachment to a honey bee forager that travel in and out of the colonies. I highlight that reproduction of mite occur only within a brood cell thus making the honeybee brood population an important component in the reproduction cycle of the Varroa mite Martin (1994); Ifantidis (1988). Theoretical works have been proposed to study the role of mite infestation in honeybee colonies (see the work of Ratti et al. (2012); Kribs-Zaleta and Mitchell (2014); Ratti et al. (2015)). While these theoretical works provide valuables

insights on the degradation effects of mites in bess' colonies, the existing relationship between the brood, adult bee, and mite population has not fully been explored. I point out that brood population is often modeled implicitly thus the role of the brood population on the colony dynamics is de-emphasize. And so, there is a need to develop models that take into account the brood, adult bee, and mite interaction relationship in order to gain insight on the impacts of mite infestation on the health and survival of honeybee colonies.

The computer model proposed in DeGrandi-Hoffman et al. (1989) simulated the interactions of parameters that influence honeybee colony population dynamics by incorporating colony population size, weather, and the queen's reproductive state. The model was constructed using literature values for developmental rates of workers and drones, brood production cycles, average worker age before becoming a forager, average spermatozoa per drone, and spermatozoa holding capacity of a queen's spermatheca. Motivated by the work of DeGrandi-Hoffman et al. (1989), this chapter propose a single patch stage structure delay differential equation model that consider the time lag from brood to adult bee. My model is use to assess the life history parameters affecting the population size of a colony. I study the subsequent dynamics caused by these important parameters.

4.3 Model Derivation

Let B, H, and M be the total population of brood, adult honeybee, and mite at time t respectively.

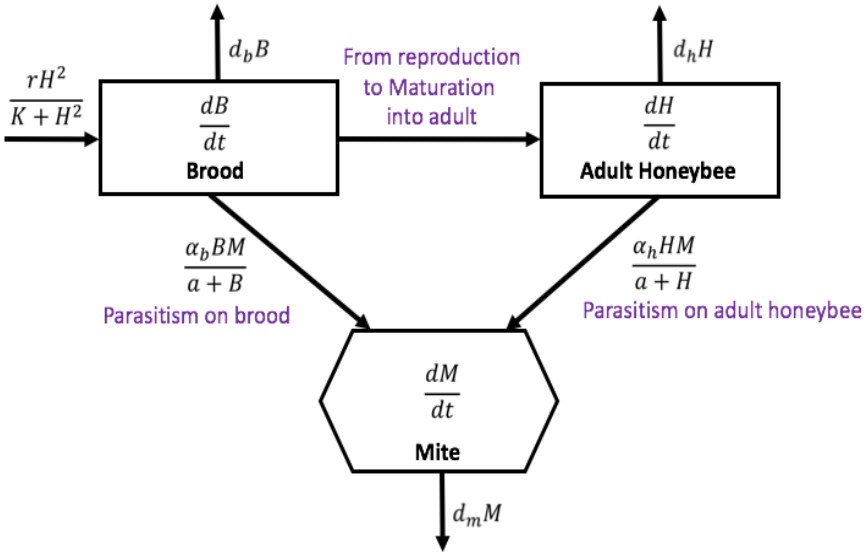

Figure 4.1: Schematic Diagram for the Honeybee-mite Parasitic Interaction.

Following the schematic diagram in Figure (4.1), our model has the following assumptions:

1. The successful survivability of an egg into a pupae stage of brood is represented by the term $\frac{H_i^2}{K_i+H_i^2}$, which incorporates the collaborative efforts of adult workers, via division of labor. This term assumes that successful colonies produce more brood and efficient workers, an assumption supported by the literature work (Schmickl and Crailsheim, 2007; Kang et al., 2016; Eischen et al., 1984). In addition, the parameters r is the egg laying rate of queen and $\sqrt{K}$ is the colony size at which the term $\frac{H_i^2}{K_i+H_i^2}$ achieves half of its maximum value.

2. The positive parameters d_b, d_h, and d_m are respectively the natural average death rate of the brood, adult bee, and mite population. The probability of the mites attaching to the brood and the adult honeybee is modeled by the terms $\frac{B}{a+B}$ and $\frac{H}{a+H}$ respectively where a is the size of the bee population at which the rate of attachment is half maximal (see the similar approach in Sumpter and Martin (2004); Betti et al. (2014)). α_b and α_h measure the parasitism rate of mites on the brood and adult honey bees

respectively. The work of STEINER et al. (1994); Garrido and Rosenkranz (2003); Boot et al. (1997) suggest that initiation of oocyte development in *Varroa jacobsoni* depends on whether the female enters the brood cell of Apis mellifra before operculation thus the term $\frac{c\alpha_b B}{a+B}$ accounting for the production of new mites where c is the conversion factor from brood to mite population. The mite model could hence be described by:

$$\frac{dM}{dt} = \frac{c\alpha_b BM}{a+B} - d_m M \tag{4.1}$$

3. The life cycle of the female Varroa mite is normally subdivided into a phoretic phase in which she lives on adult bees and a reproductive phase occurring within worker or drone brood cells thus the two life stages should be modeled explicitly. However, from the work of Kang et al. (2016); Messan et al. (2017), I assume an implicit age structures for the mite population where the ratio of different stages are constant. For example, consider $\xi \in [0,1]$ the percentage of mites at the non-phoretic stage, then $(1-\xi)M$ is the phoretic mite population. We can then denote by $\hat{d_m} = d_m(1-\xi)$ and the phoretic mite becomes

$$\frac{dM}{dt} = \frac{c\alpha_b BM}{a+B} - d_{m_i}(1-\xi)M = \frac{c\alpha_b BM}{a+B} - \hat{d}_m M.$$

Simialr approach can be follow to find the reproductive mite population and by grouping the reproductive and phoretic mites together, we obtain the mite model defines in (4.1).

4. There is a maturation mechanism that describe how brood becomes an adult honey bee. The parameter τ_b assumed to be constant is the time spent as an egg before maturing into a larvae stage. Following similar approach in Aiello and Freedman (1990), we formulate our model by considering the generation of initial data where

the past history of the brood (from egg laying) and the adult bees are prescribed over the brood incubation period and obtain the following:

(a) We define $B_0(t)$ the brood population at time t ($-\tau_b \leq t \leq 0$), which have already been incubated for time $0 < t \leq \tau_b$. For biological purposes it is assumed that $B_0(t)$ is positive and continuous for all t. In addition, we note that maturation during this period of $0 < t \leq \tau_b$ is due exclusively to brood in the initial state.

(b) When all the brood have matured at time $t > \tau_b$ however, the maturation of the brood is now due to the brood that have been generated after time equal to zero.

Moreover, the number of brood at times t is equal to the number of brood that were born at time $t - \tau_b$ and that is $\frac{rH(t-\tau_b)^2}{K+H(t-\tau_b)^2}$. The survival of the brood population depends on if they outlive the mite infestation and their natural death, so the probability of survival is $e^{-\int_{t-\tau}^{t}\left(d_b+\frac{\alpha_b M(s)}{a+B(s)}\right)ds}$ for when $0 < t \leq \tau_b$ and $t > \tau_b$. The maturation from the brood to the adult bee population is hence

$$B_0(t-\tau_b)e^{-\int_{t-\tau_b}^{t}\left(d_b+\frac{\alpha_b M(s)}{a+B(s)}\right)ds} \qquad \text{when} \qquad 0 < t \leq \tau_b$$

and

$$\frac{rH(t-\tau_b)^2}{K+H(t-\tau_b)^2}e^{-\int_{t-\tau_b}^{t}\left(d_b+\frac{\alpha_b M(s)}{a+B(s)}\right)ds} \qquad \text{when} \qquad t > \tau_b.$$

My model formulation, which has one form on the interval $0 < t \leq \tau_b$ and a second form on the interval $t > \tau_b$ is as follow:

- **Time between 0 and τ_b ($0 < t < \tau_b$)**

$$\begin{aligned}
\frac{dB}{dt} &= \underbrace{\frac{r_1 H^2}{K+H^2}}_{\text{reproduction from queen}} - \underbrace{\alpha_b \overbrace{\frac{B}{a+B}}^{\text{probability of } M \text{ attaching to } B} M}_{\text{parasitism on brood}} - \underbrace{d_b B}_{\text{brood natural death}} - \underbrace{e^{-\int_{t-\tau_b}^{t}\left[d_b+\frac{\alpha_b M(s)}{a+B(s)}\right]ds} B_0(t-\tau_b)}_{\text{from reproduction to mature into adult}} \\
\frac{dH}{dt} &= \underbrace{e^{-\int_{t-\tau_b}^{t}\left[d_b+\frac{\alpha_b M(s)}{a+B(s)}\right]ds} B_0(t-\tau_b)}_{\text{transition from brood}} - \underbrace{\alpha_h \overbrace{\frac{H}{a+H}}^{\text{probability of } M \text{ attaching to } H} M}_{\text{parasitism on adult bee}} - \underbrace{d_h H}_{\text{adult bee natural death}} \\
\frac{dM}{dt} &= \underbrace{cM\alpha_b \frac{B}{a+B}}_{\text{newborns from parasitism brood}} - \underbrace{d_m M}_{\text{mite natural death}}
\end{aligned} \tag{4.2}$$

- **Time larger than τ_b ($t > \tau_b$)**

$$\begin{aligned}
\frac{dB}{dt} &= \underbrace{\frac{r_1 H^2}{K+H^2}}_{\text{reproduction from queen}} - \underbrace{\alpha_b \overbrace{\frac{B}{a+B}}^{\text{probability of } M \text{ attaching to } B} M}_{\text{parasitism on brood}} - \underbrace{d_b B}_{\text{brood natural death}} - \underbrace{\frac{e^{-\int_{t-\tau_b}^{t}\left[d_b+\frac{\alpha_b M(s)}{a+B(s)}\right]ds} r_2 H(t-\tau_b)^2}{K+H(t-\tau_b)^2}}_{\text{from reproduction to mature into adult}} \\
\frac{dH}{dt} &= \underbrace{\frac{e^{-\int_{t-\tau_b}^{t}\left[d_b+\frac{\alpha_b M(s)}{a+B(s)}\right]ds} r_2 H(t-\tau_b)^2}{K+H(t-\tau_b)^2}}_{\text{transition from brood}} - \underbrace{\alpha_h \overbrace{\frac{H}{a+H}}^{\text{probability of } M \text{ attaching to } H} M}_{\text{parasitism on adult bee}} - \underbrace{d_h H}_{\text{adult bee natural death}} \\
\frac{dM}{dt} &= \underbrace{cM\alpha_b \frac{B}{a+B}}_{\text{newborns from parasitism brood}} - \underbrace{d_m M}_{\text{mite natural death}}
\end{aligned} \tag{4.3}$$

with $r_1 = r_2 = r$.

4.4 Mathematical Analysis

I start with the basic dynamical properties of Models (4.2) and (4.3) in the following theorem

Theorem 9. *Assume that all parameters are strictly positive with $B(0) > 0$, $H(0) > 0$, $M(0) > 0$, and $\frac{c\alpha_b}{d_m} > 1$. Then $B(t) > 0$, $H(t) > 0$, and $M(t) > 0$ for all $t > 0$ in Model* (4.2) *and* (4.3)*, that is Model* (4.2) *and* (4.3) *is positively invariant in $\mathbb{R}^3_+$. Moreover, our systems* (4.2) *and* (4.3) *are bounded in $\mathbb{R}^3_+$.*

Biological Implications: Theorem 9 implies that our system in Model (4.2) and (4.3) is well-defined biologically.

4.4.1 Boundary Equilibria and Their Stability

I now look at the equilibria and their stability of Model (4.3). The equilibria of the system is determine by setting $\frac{dB}{dt} = \frac{dH}{dt} = \frac{dM}{dt} = 0$ in Model (4.3) and we obtain the subsequent equations:

$$\frac{rH^2}{K+H^2} - \frac{\alpha_b BM}{a+B} - d_b B - \frac{rH^2}{K+H^2} e^{-\left(d_b + \frac{\alpha_b M}{a+B}\right)\tau_b} = 0 \tag{4.4a}$$

$$\frac{rH^2}{K+H^2} e^{-\left(d_b + \frac{\alpha_b M}{a+B}\right)\tau_b} - \frac{\alpha_h HM}{a+H} - d_h H = 0 \tag{4.4b}$$

$$\frac{c\alpha_b BM}{a+B} - d_m M = 0 \tag{4.4c}$$

From equations (4.4a) - (4.4c), I determine the following positive boundary equilibria of our population Model (4.2) and (4.3) which depend on the parameters specified:

$$E_{0,0,0} = (0,0,0), \quad E_{B_1^*,H_1^*,0} = (B_1^*, H_1^*, 0), \quad \text{and} \quad E_{B_2^*,H_2^*,0} = (B_2^*, H_2^*, 0)$$

where

$$B_1^* = \left[\frac{r(H_1^*)^2}{K+(H_1^*)^2}\right]\left[\frac{1-e^{-d_b\tau_b}}{d_b}\right], \quad H_1^* = \left(\frac{re^{-d_b\tau_b}}{2d_h}\right) + \sqrt{\left(\frac{re^{-d_b\tau_b}}{2d_h}\right)^2 - K}$$

$$B_2^* = \left[\frac{r(H_2^*)^2}{K+(H_2^*)^2}\right]\left[\frac{1-e^{-d_b\tau_b}}{d_b}\right], \quad H_2^* = \left(\frac{re^{-d_b\tau_b}}{2d_h}\right) - \sqrt{\left(\frac{re^{-d_b\tau_b}}{2d_h}\right)^2 - K}$$

The conditions on the existence and stability of these boundary equilibria are illustrated in the following theorem:

Theorem 10. *[Boundary equilibria of Model* (4.3)*] . The existence and stability condition of the boundary equilibria of Model* (4.2) *and* (4.3) *are provided below:*

1. *Model* (4.3) *always have the extinction equilibrium* E_{000} *which is always locally asymptotically stable.*

2. *If* $d_h < \frac{re^{-d_b\tau_b}}{2\sqrt{K}}$ *Model* (4.3) *has additional two boundary equilibria* $E_{B_1^*H_1^*0}$ *and* $E_{B_2^*H_2^*0}$ *where* $E_{B_1^*H_1^*0}$ *is always unstable. The equilibrium* $E_{B_2^*H_2^*0}$ *is however locally asymptotically stable when* $d_m > \frac{c\alpha_b B_2^*}{a+B_2^*}$ *and* $E_{B_2^*H_2^*0}$ *is unstable when* $d_m < \frac{c\alpha_b B_2^*}{a+B_2^*}$.

Biological Implications: Theorem 10 provides sufficient conditions for the existence and stability of the boundaries equilibria of Model (4.2) and (4.3). Note that all species could be driven extinct independently of the delay. In addition, large natural death of the mite population could drive mite extinct while the brood and adult bee coexist when the condition $d_m > \frac{c\alpha_b B_2^*}{a+B_2^*}$ is satisfied.

4.4.2 Interior Equilibrium of Model (4.2) and (4.3)

I now continue our study with the interior equilibria of Model (4.3). See from Equation (4.4c) that $\hat{B}^* = \frac{a}{\frac{c\alpha_b}{d_m}-1}$. Now from Equation (4.4a) and (4.4b), we obtain

$$\begin{aligned}\frac{rH^2}{K+H^2}e^{-\left(d_b+\frac{\alpha_b M}{a+B}\right)\tau_b} &= \frac{rH^2}{K+H^2} - \frac{\alpha_b BM}{a+B} - d_b B \\ \frac{rH^2}{K+H^2}e^{-\left(d_b+\frac{\alpha_b M}{a+B}\right)\tau_b} &= \frac{\alpha_h HM}{a+H} + d_h H\end{aligned}$$

which gives

$$\frac{rH^2}{K+H^2} - \frac{\alpha_b BM}{a+B} - d_b B = \frac{\alpha_h HM}{a+H} + d_h H. \tag{4.5}$$

From equation (4.5), we have $\hat{M}^* = \frac{\frac{r(\hat{H}^*)^2}{K+(\hat{H}^*)^2} - d_h\hat{H}^* - d_b\hat{B}^*}{\frac{\alpha_b\hat{B}^*}{a+\hat{B}^*} + \frac{\alpha_h\hat{H}^*}{a+\hat{H}^*}} = F_1(\hat{H}^*)$. The substitution of $\hat{M}^* = F_1(\hat{H}^*)$ in equation (4.4b) for M gives

$$F_2(\hat{H}^*) = \frac{rH^2}{K+H^2}e^{-\left(d_b+\frac{\alpha_b F_1(\hat{H}^*)}{a+B}\right)\tau_b} - \frac{\alpha_h HF_1(\hat{H}^*)}{a+H} - d_h H = 0 \tag{4.6}$$

The positive real solution of $F_2(\hat{H}^*) = 0$ when $\hat{M}^* > 0$ and $\hat{B}^* > 0$ guarantee the existence of an interior equilibrium for Model (4.2) and (4.3). The complex form of (4.6) prevents us to obtain the explicit solutions of the interior equilibria of Model (4.2) and (4.3) thus we proceed numerically as illustrated in figures 4.2(a) and 4.2(b) by choosing the following fixed parameters:

$r = 1500,\ c = 2.1,\ d_b = 0.0025,\ d_h = 0.075,\ d_m = 0.0309,\ \alpha_h = 0.005,\ \alpha_b = 0.0252,\ K = 49500000,\ \tau_b = 21$

with $\frac{c\alpha_b}{d_m} = \frac{2.1\times 0.0252}{0.0309} = 1.71262 > 1$ thus $\hat{B}^* = \frac{a}{\frac{c\alpha_b}{d_m} - 1} > 0$ for all $a \in \mathbb{R}^+$.

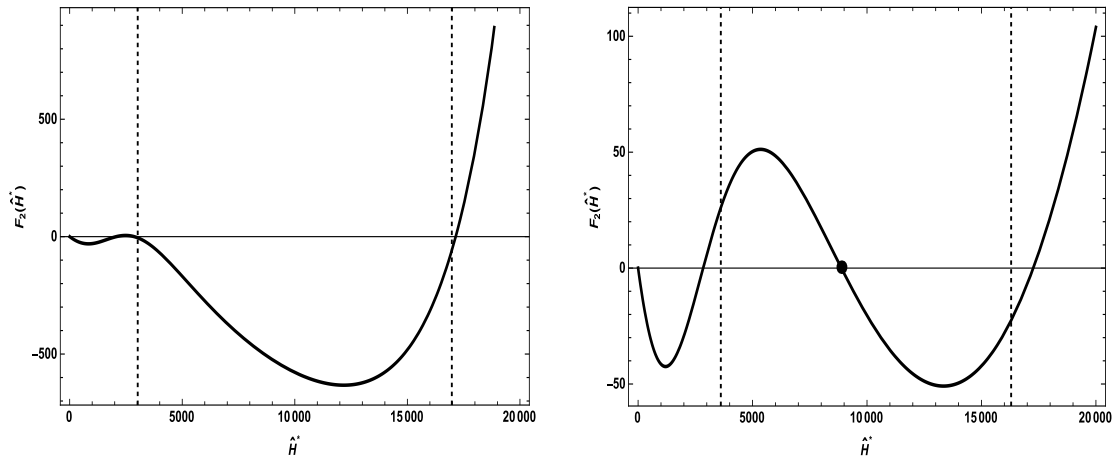

(a) No interior equilirum with $a = 2000$ (b) One interior equilibrium with $a = 12000$

Figure 4.2: Interior Equilibria of Model (4.3) Where $\hat{B}^* = \frac{a}{\frac{c\alpha_b}{d_m} - 1} = \frac{a}{\frac{2.1\times 0.0252}{0.0309} - 1} > 0$ and the Dashed Lines Represent the Positive Interval Values of $\hat{H}^*$ Where the Equilibrium $\hat{M}^*$ is Positive. The Black Dots Represent the Real Positive Equilibrium $\hat{H}^*$ in $F_2(\hat{H}^*) = 0$ Which Satisfy the Existence of an Interior Equilibrium when $\hat{M}^* > 0$. Figure 4.2(a) Show the Existence of No Interior Equilibrium While Figures 4.2(b) Show the Existence of One Unique Interior Equilibrium.

4.5 Materials and Data Description

The data consist of colonies of honeybees, varroa mites, and brood collected collected in Casa Grande, at the University of Arizona West Agricultural Facility (20 colonies). The data were established in desert climate of Arizona where temperatures are favorable for bees foraging activity especially during April until November when the data were collected.

All colonies initially had 9000 package bees with a queen and miticide treatment was used to control the varroa population in the nearby apiaries at the beginning of the experiment (April of 2014). The data used in this manuscript consist of population data (of bees, brood, and mite in the colonies).

In order to approximate the honeybee and brood population data in the colonies, frames of bees were measured monthly from May to November using a method from DeGrandi-Hoffman et al. (2008). This method consist of estimating brood and bees on an area of the frames using a 5 cm $\times$ 5 cm grid that cover the entire side of the comb. Note that one frame of bees contain approximatively 2506 bees and 5200 brood cells DeGrandi-Hoffman et al. (2008) and maximum availability of brood on frame occur at 80% (i.e. only 80% of frames are cover with brood at the maximum). Thus the colony of bees are estimating by doing: frames of bees $\times$ 2506 and colony of brood are estimating by doing: frames of brood $\times$ 0.8 $\times$ 5200. The varroa mite population density in the colonies were also collected from May until November. During the experiment season (i.e. May to November), 300 bees were brushed into a jar then the number of mites on the 300 bees were counted monthly and these constitute the phoretic mites. The population of the reproductive mites were also estimated by counting the total number of mites per sampled cells. The total mite population in a colony is hence the sum of the phoretic and reproductive mite. We proceed as follow to find the estimated mite population in colonies. Recall that the number of phoretic mites obtain is the mites per 300 bees. Then, the calculation of the phoretic mite population per colony are estimating by: $\frac{\text{mites per 300 bees}}{300} \times$ population of bees per colony. I calculated the reproductive mite per colony by performing $\frac{\text{total number of mites} \times 5200}{\text{number of cells sampled}}$. The addition of the phoretic mites and reproductive yield the total population per colonies. DeGrandi-Hoffman et al. (2016) follow similar approaches to estimate the population of bees, brood, and mite per colony.

Now I point out that the number of eggs laying by the queen bee is a function of the ambient temperature, photoperiod, adult population in the colony, and it is also noted that the total number of eggs lay each day by the queen is decreasing function of the number of days the queen has been laying eggs DeGrandi-Hoffman et al. (1989). The eggs laying rate must hence be described by a periodic function and it is known that any periodic function can be represented as an infinite sum of sines and cosines Feng et al. (2011). In order to keep the model simple and tractable, I combine these factors and adapt the first order harmonic function presented in Feng et al. (2011) to the egg laying rate r_1 and r_2 in Model (4.2) and (4.3) to obtain:

$$r_1 = r\left[1 + cos\left(\frac{2\pi(t-\Phi))}{365}\right)\right] \quad \text{and} \quad r_2 = r\left[1 + cos\left(\frac{2\pi(t-\tau_b-\Phi))}{365}\right)\right] \tag{4.7}$$

where Φ denote the day of the year with the maximum eggs laying rate, r is the baseline egg laying rate from (Sumpter and Martin, 2004; Eberl et al., 2010), and t is the time measure in days. Using Equation (4.7), the number of eggs laid by the queen over a period of a year as depicted in Figure 4.3 is obtained.

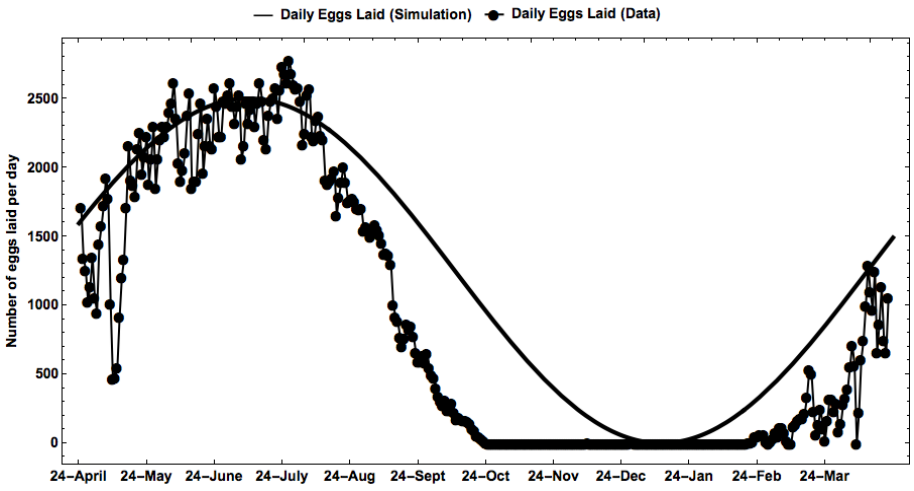

Figure 4.3: Number of Eggs Laying by a Strong Full Matted Queen Without a Constraint over a Period of One Year Following Equation (4.7) with $r = 1250$ and $\Phi = 75$. The Data Was Simulated Using the BEEPOP Model from DeGrandi-Hoffman et al. (1989) by Taking into Account Daily Temperature, Photoperiod, and Adult Population in the Colony.

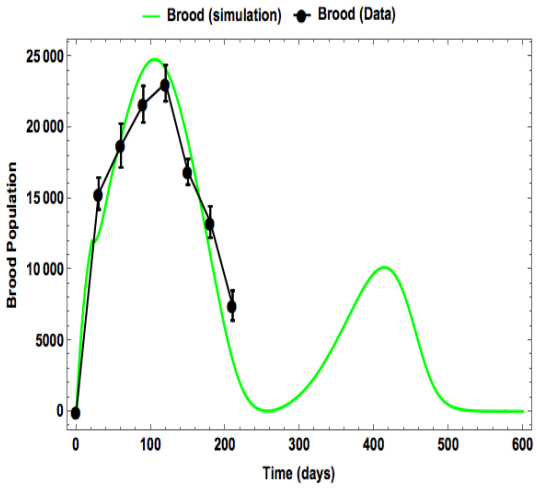

(a) Average brood population in colonies on site 1

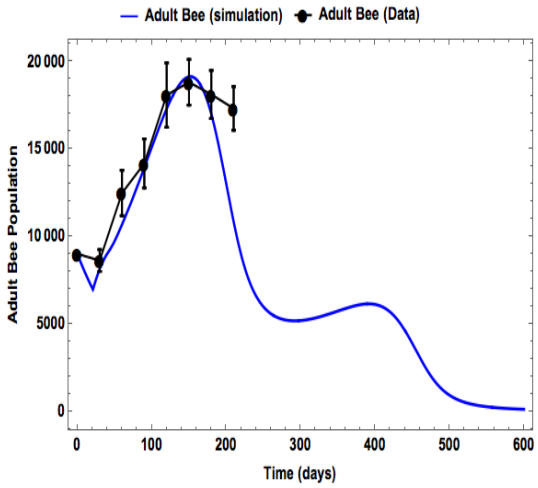

(b) Average bee population in colonies on site 1

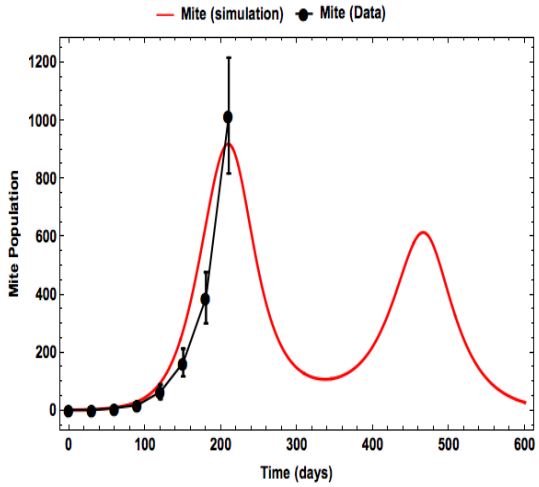

(c) Average mite population in colonies on site 1

Figure 4.4: Time Series of the Brood, Adult Bee, and Mite Simulation and Average Population Data in Casa Grande "site 1". Figures 4.4(a) Represents the Average Brood Population of 20 Colonies with Its Standard Error on Site 1 Using $r^* = 1500$, $K = 95000000$, $d_b = 0.051$, $d_h = 0.0121$, $d_m = 0.027$, $\alpha_b = 0.0447$, $\alpha_h = 0.8$, $c = 1.9$, $a = 8050$, $\Phi = 65$, $\tau_b = 21$, $B_0(t) = B(0) = 0$, $H(0) = 9000$, and $M(0) = 3$. Figures 4.4(b) Represents the Mean Adult Bee Population of 20 Colonies with Its Standard Error on Site 1. Figures 4.4(b) Represents the Mean Mite Population of 20 Colonies on Site 1. Time 0 Corresponds to April 24th for the Figures 4.4(a), 4.4(b), and 4.4(c).

4.6 Uncertainty and Sensitivity Analysis

Data fitting and parameter estimation of α_b, α_h, and a are provided in section 4.5 using data from DeGrandi-Hoffman et al. (2008) (see Figures 4.4(a), 4.4(b), and 4.4(c)) while all

other parameters are obtained from the literature as listed in Table B.4. It is often noted in mathematical biology that natural variation, error in measurements may cause a variation in the parameter of the system Marino et al. (2008). This section measures and quantify the effect of parameter sensitivity on the population size of brood, adult bee, and mite respectively. In this regard, we focus on the time corresponding to the largest population size in Figures 4.4(a), 4.4(b), and 4.4(c) as output. We note that there exist a numerous global sensitivity method in the literature, however this study will focus on two main methdology: (1) Latin Hypercube Sampling and Partial Rank Correlation Coefficient Analysis (LHS/PRCC) and (2) Extended Fourier amplitude sensitivity test (eFAST). The LHS/PRCC is a sampling method that provides a measure of the strength of a linear association between an input and an output thus it assumes a linear relationship between the output and the input while the eFAST is a variance decomposition method that quantify how strongly a parameter's frequency propagates from input, through the model, to the output Marino et al. (2008). We note the output of interest in this section are the population size while the input are the parameters. Following the method illustrated by Marino et al. (2008) I obtain results presented in Figures 4.5, 4.6, and 4.7.

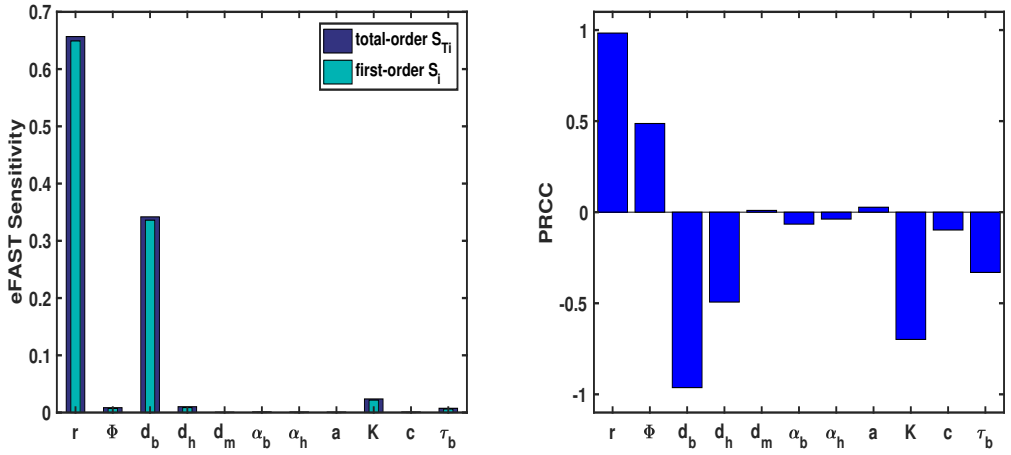

(a) eFAST sensitivity at time = 96

(b) PRCC sensitivity at time = 96

Figure 4.5: eFAST and PRCC Sensitivity Analysis on Model (4.2) and (4.3) Using Parameter from Figures 4.4 Where Time Point Chosen Correspond to the Highest Population Point from the Brood Population in Figure 4.4(a). Figures 4.5(a) Is Showing the eFAST Results with Resampling and Search Curves Were Resampled Five times $(N_R = 5)$, for a Total of 3575 Model Evaluations $(N_S = 65)$. First-order S_i and Total-order S_{Ti} are Shown for Each Parameter as Shown in the Legend. Figures 4.5(b) is Illustrating the Result of the PRCC with $N = 1000$.

The PRCC results show how the parameters r which is the queen's egg laying rate is significant across all three time period chosen (see Figures 4.5, 4.6, and 4.7). This confirm the result of DeGrandi-Hoffman et al. (1989) where it was indicated that the queen's egg-laying potential has the greatest effect on colony population size. In addition to r, it is also observable that parameter such as the natural death rate of brood and adult bee (i.e. d_b and d_h) may be the second most important parameters affecting the population size of the colony. The conversion factor from brood to mite (i.e. c) are shown to have a great effect on the mite population size in Figure 4.7(b). The infestation on the adult bee is shown not to be significant across all three time period while the infestation on brood is highly significant on the mite and adult bee population size which indicate the importance of brood's maintenance for colony growth.

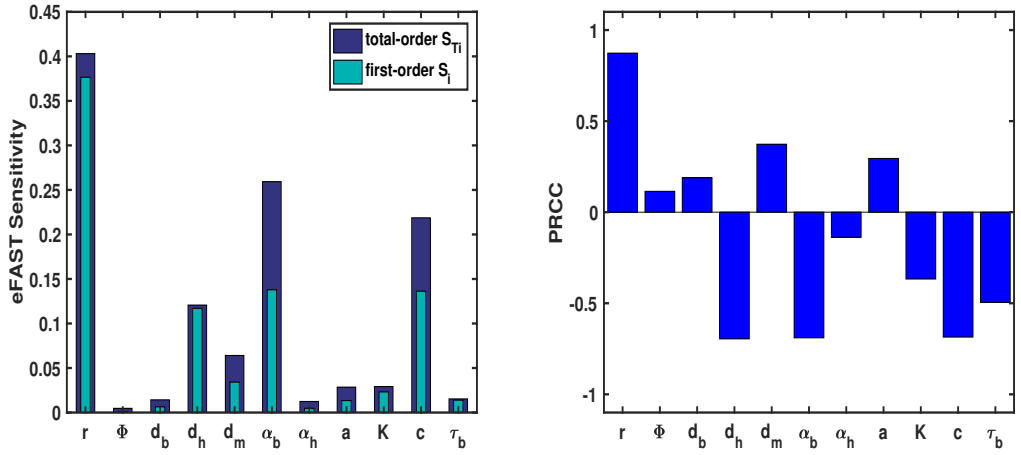

(a) eFast sensitivity at time = 132 (b) PRCC sensitivity at time = 132

Figure 4.6: eFAST and PRCC Sensitivity Analysis on Model (4.2) and (4.3) Using Parameter from Figures 4.4 Where Time Point Chosen Correspond to the Highest Population Point from the Adult Bee Population in Figure 4.4(b). Figures 4.6(a) Is Showing the eFAST Results with Resampling and Search Curves Were Resampled Five times $(N_R = 5)$, for a Total of 3575 Model Evaluations $(N_S = 65)$. First-order S_i and Total-order S_{Ti} are Shown for Each Parameter as Shown in the Legend. Figures 4.6(b) is Illustrating the Result of the PRCC with $N = 1000$.

eFast results confirm that the queen's eggs laying rate r is the most sensitive parameter affecting the population size of the colony. The natural death rate of brood, adult bee, and mite is also shown to be the most sensitive parameter affecting the population size respectively (see Figure 4.5(a), 4.6(a), 4.7(a)). All then sensitivityu results is consistent for both the PRCC and eFAST as shown in Figures 4.5, 4.6 and 4.7.

In order to test for monotonicities between the parameters and the output (i.e. colony population size), scatter plots of the ranked outputs versus the rank inputs were produced in Figures B.1, B.2, and B.3 in appendix B (see Tables B.1, B.2, and B.3 for sensitivity indexes and p-values corresponding to the figures B.1, B.2, and B.3 respectively) corresponding to time points 96, 132, and 183 respectively. A monotonic relationship can be observe from all input parameters when time is 96 from the result in Table B.1, B.2, and B.3. Marino et al. (2008) indicated that using a sample size of 65 guarantee an accuracy of the sensitivity indexes provided by eFAST. The eFAST results presented in this section use a

sample size of 200 thus this shows the accuracy of the first-order S_i and total-order S_{Ti}. In addition, these results indicates that the variability of the colony population size is not mostly accounted by the parameters a and α_h. I continue the study by exploring the effect of brood infestation rate on the population dynamics .

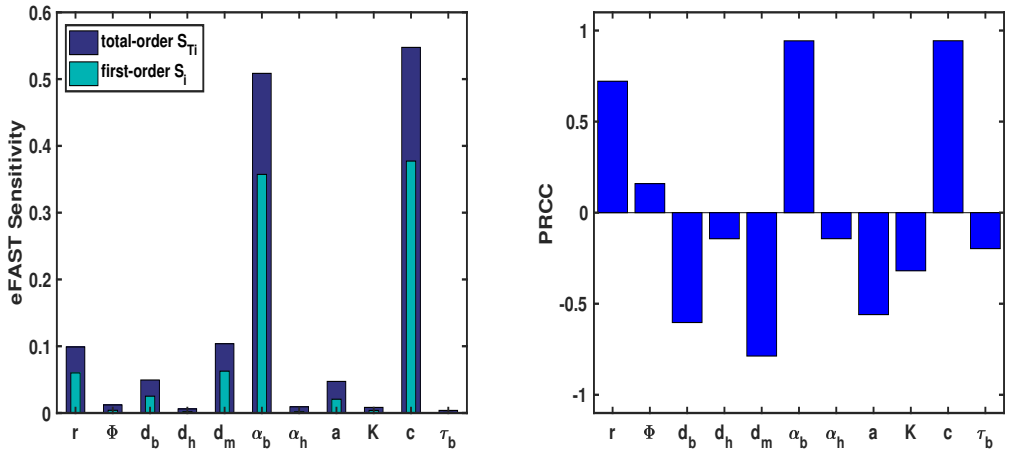

(a) eFast sensitivity at time = 183 (b) PRCC sensitivity at time = 183

Figure 4.7: eFAST and PRCC Sensitivity Analysis on Model (4.2) and (4.3) Using Parameter from Figures 4.4 Where Time Point Chosen Correspond to the Highest Population Point from the Mite Population in Figure 4.4(c). Figures 4.7(a) Is Showing the eFAST Results with Resampling and Search Curves Were Resampled Five times $(N_R = 5)$, for a Total of 3575 Model Evaluations $(N_S = 65)$. First-order S_i and Total-order S_{Ti} are Shown for Each Parameter as Shown in the Legend. Figures 4.7(b) is Illustrating the Result of the PRCC with $N = 1000$.

4.7 Effects of brood's infestation on the population dynamics

In this subsection, I use time series simulations to illustrate how the infestation of brood (i.e. α_b) may affect the population dynamics at a colony level. Note that there may be a large variations in these parameters due to disease dynamics or other mechanism. Thus, to incorporate these factors, I allow slight variations which deviate from the value estimated in Section 4.5 (See estimated value of α_b in Table B.4).

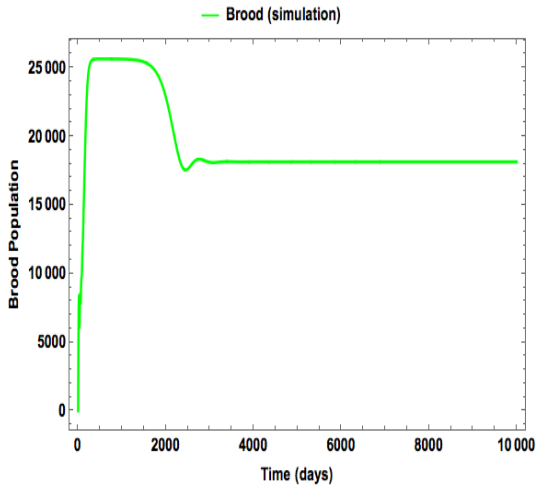

(a) Brood population for $\alpha_b = 0.0222$

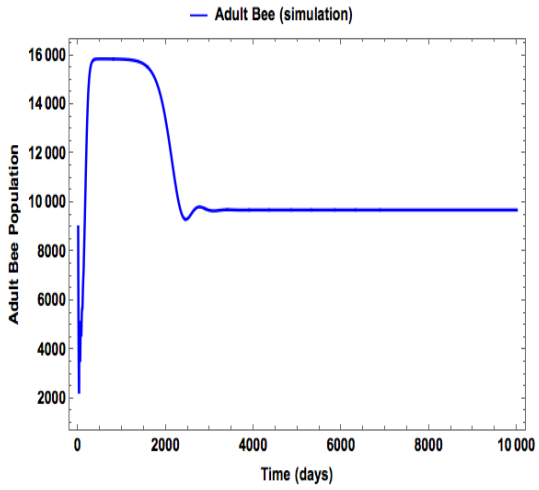

(b) Bee population for $\alpha_b = 0.0222$

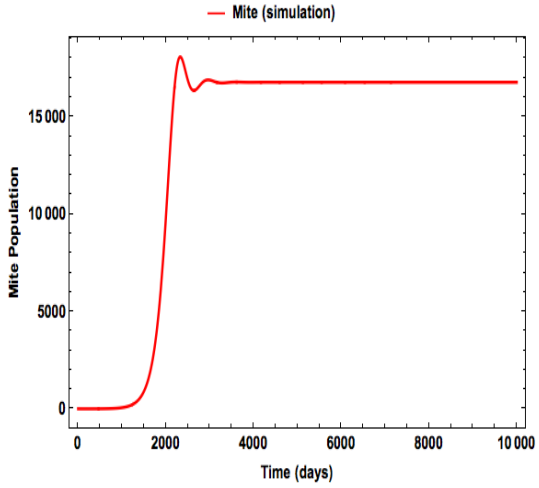

(c) Mite population for $\alpha_b = 0.0222$

Figure 4.8: Time Series of the Brood, Adult Bee, and Mite Simulation Using $r = 1500$, $K = 49500000$, $d_b = 0.0025$, $d_h = 0.075$, $d_m = 0.0309$, $\alpha_h = 0.005$, $c = 2.1$, $a = 19000$, $\tau_b = 21$, $B_0(t) = B(0) = 0$, $H(0) = 9000$, and $M(0) = 3$ When the Queen's Eggs Laying Rate is Constant. Figures 4.8(a), 4.8(b), and 4.8(c) Showing Stability of All Population at the Unique Equilibrium.

Figure 4.8 illustrate the existence of an interior equilibrium that is locally stable when the infestation rate on the brood population is sufficiently small. The parameter were chosen such that the boundary equilibrium $E_{B_2^* H_2^* 0}$ exist and is locally stable. The result obtained from such dynamic suggest that population could converge to the interior or the

boundary leaving the colony of healthy brood and adult honeybee depending on initial conditions.

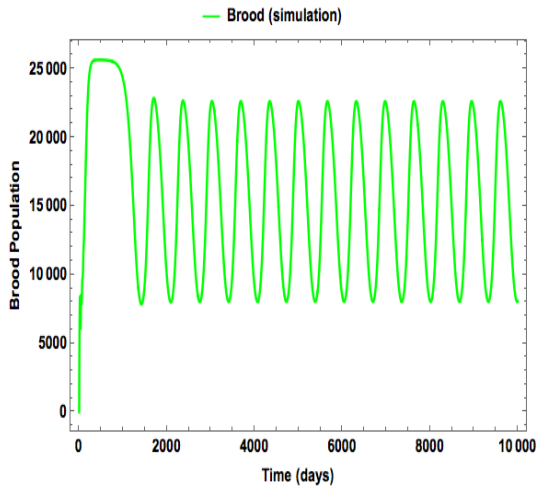

(a) Brood population for $\alpha_b = 0.0252$

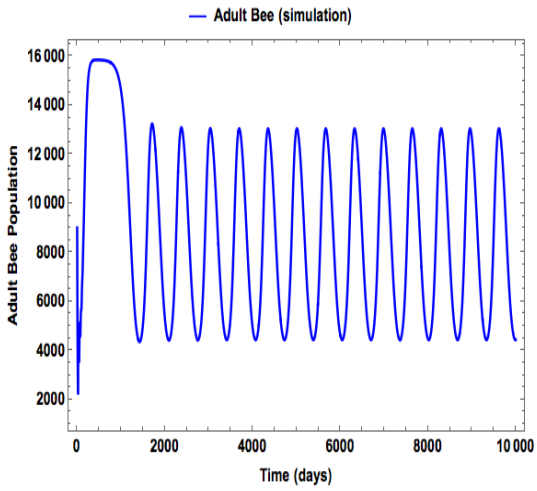

(b) Bee population for $\alpha_b = 0.0252$

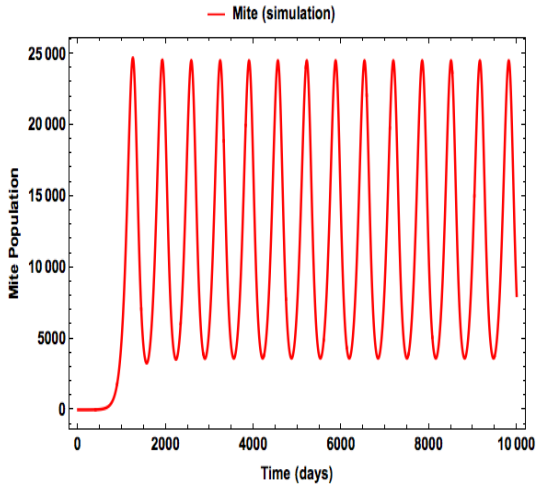

(c) Mite population for $\alpha_b = 0.0252$

Figure 4.9: Time Series of the Brood, Adult Bee, and Mite Simulation Using $r = 1500$, $K = 49500000$, $d_b = 0.0025$, $d_h = 0.075$, $d_m = 0.0309$, $\alpha_h = 0.005$, $c = 2.1$, $a = 19000$, $\tau_b = 21$, $B_0(t) = B(0) = 0$, $H(0) = 9000$, and $M(0) = 3$ When the Queen's Eggs Laying Rate is Constant. Figures 4.8(a), 4.8(b), and 4.8(c) Showing Coexistence of All Population Through Fluctuating Dynamics.

Intermediate value of the infestation rate (α_b) has the potential to drive the population into a fluctuating dynamics as illustrated in Figure 4.9. When α_b is sufficiently large, the

population of brood, adult bee, and mite converge to the extinction equilibrium thus the colony collapse as shown in Figure 4.10.

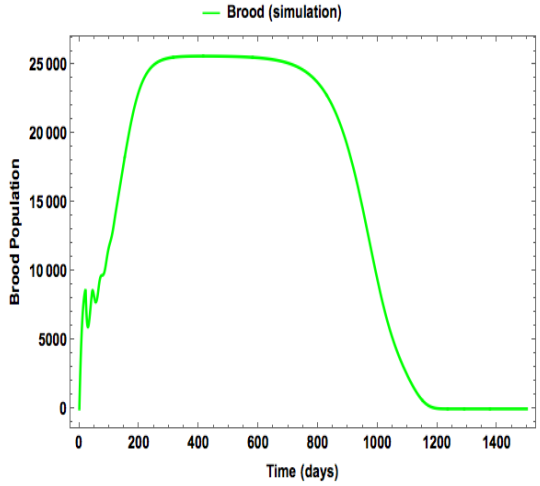

(a) Brood population for $\alpha_b = 0.0272$

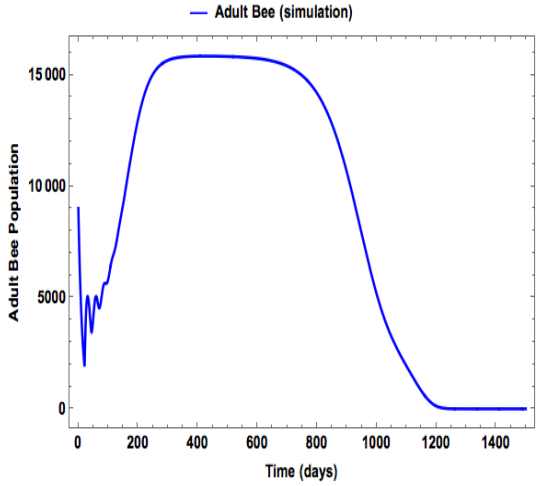

(b) Bee population for $\alpha_b = 0.0272$

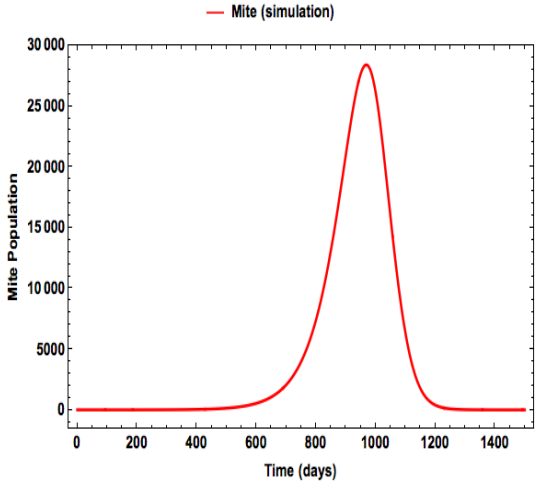

(c) Mite population for $\alpha_b = 0.0272$

Figure 4.10: Time Series of the Brood, Adult Bee, and Mite Simulation Using $r = 1500$, $K = 49500000$, $d_b = 0.0025$, $d_h = 0.075$, $d_m = 0.0309$, $\alpha_h = 0.005$, $c = 2.1$, $a = 19000$, $\tau_b = 21$, $B_0(t) = B(0) = 0$, $H(0) = 9000$, and $M(0) = 3$ When the Queen's Eggs Laying Rate is Constant. Figures 4.8(a), 4.8(b), and 4.8(c) Showing All Population Driven Extinct.

4.8 Discussion

Colonies of honeybee have starting to see a sudden decline since 2006 Le Conte et al. (2010). While the cause of this collapsing of colonies is not trivial, many scientists argue that there are are a combination of stresses involve in the loss of colonies worldwide Le Conte et al. (2010); Hayes Jr et al. (2008). The presence of Varroa mite was strongly shown to be one of the causing phenomena behind the collapse of the colonies (this was illustrated in chapter 3 of this dissertation and also presented in Kang et al. (2016); DeGrandi-Hoffman and Curry (2004); Messan et al. (2017)). I proposed a nonlinear stage structure delay differential equations that describes the interactions between brood, honeybees and mites in a single patch framework where we take into account the maturation from brood to adult honeybee. The theoretical results combined with numerical simulations provide us useful insights on how the presence of mites affect the dynamical outcome of the adult honeybee and brood population respectively. More specifically, the theoretical works suggest the following:

Theorem (9) provides the positivity and boundedness condition of Model (4.2) and (4.3) is well posed. In addition analytical solution from Theorem (10) provide sufficient conditions for the existence and stability of all the boundary equilibria of our system. It follows from this result that initial population size play an important role in sustaining the bee's colony. Moreover, large natural death of the mite population could yield the boundary equilibrium to be stable leading to the death of the mite population where the colony is left with healthy brood and honeybee.

The results from the sensitivity analysis show that the queen's egg laying reproduction rate has the highest impact on the colony population. Both our PRCC and eFAST method agree with the later result. Other important parameters affecting the population size of the brood, adult bee, and mite can also be observed. Results from time serie simulation

illustrate the dynamics generated by the mite to brood infestation rate on the population dynamics. Small infestation on the brood could promote coexistence of all species at the interior equilibrium, intermediate infestation rate could yield the coexistence of all species through fluctuating dynamics, and large infestation rate could drive the collapse of the colony. These findings show the existing relationship between the brood, adult bee, and mite when colonies are infested by Varroa due to dispersal. It will be interesting to study a similar dynamics when honeybee population are prone to use a defensive mechanism such as a grooming behavior. This will be subject to a future study.

Chapter 5

FINAL REMARKS AND RECOMMENDATIONS FOR FUTURE WORK

5.1 Final Remarks

Due to habitat fragmentation, accelerating deterioration of our ecosystem, global species extinctions, fast spread of diseases, proliferation of invasive species, etc., the role of dispersal in a host-parasite environment is becoming important. Studies regarding dispersal and space related problems have sparked great attention in the past two decades (see (Kareiva et al., 1990) for literature review). As illustrated throughout this dissertation, dispersal could destabilize population dynamics of social animals leading to global or local extinction. An introduction of dispersal in populations that were subdivided could also reduce the risk of extinction and increase the probability of persistence of species.

A divers mode of dispersal has been of ecological interest in metapopulation studies (e.g random movement (Jansen, 1995; Lengyel and Epstein, 1991), movement base on attraction, or benefit of assessment (Ghosh and Bhattacharyya, 2011; Cressman and Křivan, 2013), and adaptive dispersals Greggers and Menzel (1993); Waddington and Holden (1979), etc.). Metapopulation models are often used to study the dynamics of population groups from the same or different species that interact through dispersal. Many existing dispersal mechanisms in theoretical studies have not paid a close attention to certain species that adapt their foraging movement according to a changing environment. This existing gap between ecological observations and theoretical works reside on the fact that models become increasingly difficult to analyze as more reality is included. However, recalling Albert Einstein's famous assertion: *"a model should be as simple as possible but no simpler"*, it is crucial to cover some aspects of reality in order to get valuable insights on the dynamics

of interacting species in heterogenous environment. This dissertation covers these aspects by proposing models derived from ordinary and delay differential equations that study the role of adaptive dispersal in social animals. I point out that the work completed throughout this dissertation was motivated by field experiments and the proposed model in chapter 4 was properly validated by empirical data thus the results obtained gave great insights on the dynamics generated by adaptive dispersal in host-parasite interaction. Nevertheless, more work remains to be done regarding other adaptive dispersal mechanisms that explicitly incorporate climate, weather conditions, nutritional demands, predator avoidance, multi-patch, patch quality, etc.

In order for individual colonies to efficiently manage environmental fluctuations and disturbances, the foraging process of many social animals is adaptive and robust (Schmickl and Crailsheim, 2004; Dall et al., 2005; Galef and Laland, 2005). Social animals often take into account the quality of their resources, distance to the food source, danger resulting from other predators, climate conditions in order to obtain an energetically optimal diet. In addition, the two patch-patch models proposed in chapter 2 and 3 of this dissertation are simplification of reality as species would normally forage in a multi-patch environment rather than among two patches. It will be beneficial to build a more realistic model that account for the animal's complex society by taking into consideration all these attributes (i.e. climates, multi-patch, patch quality, stochastic variation, etc.) using an agent base modeling approach and study the role of adaptive dispersal on the population dynamics. This dissertation represents the first step in that direction.

5.2 Recommendations for Future Work

While the dispersal in prey-predator has been extensively studied (see the work of Lengyel and Epstein (1991); Pascual (1993); Jansen (1995); Briggs and Hoopes (2004); Cressman and Křivan (2013); Chewning (1975)), the research presented in this dissertation

clearly demonstrate the need of more robust models that take into account adaptive dispersal of social animals in heterogenous environment. For instance, Kummel et al. (2013) showed through their field work that the foraging behavior of Coccinellids are governed not only by the conspecific attraction but also through the passive diffusion and retention on plants with high immobile aphids number thus the foraging process is adaptive. Throughout this dissertation, I take into account these attributes and construct models that account for the ability of species to properly chose dispersal strategy depending on their population need.

The model introduce in the second chapter illustrate the existing relationship between a prey-predator (or host and parasite) interacting in a heterogenous environment where the predator is mobile while the prey is immobile. The predator has the ability to choose between two dispersal strategies: (1) the classical foraging behavior where predator is driven to the patch with the lower predator population density; (2) the density dependent dispersal measured through the predation attraction. The combination of these two dispersal mechanisms is linked through a parameter denoted "s", whose value is between 0 and 1 measuring the proportion of the predator population using the passive dispersal strategy. The later parameter is hence a proxy variable for different cues occurring in social animals' environment (e.g. weather or climate conditions, predation pressure, availability of resource, etc.) prompting them to change their dispersal strategy. It will be interesting to define an explicit function depending on temperature for the parameter "s" and explore the role of climate on population dynamics of prey-predator with adaptive dispersal in predator. Such is a limitation of the model presented in chapter 2.

In the light of recent studies on honeybees swarming behavior, it was discovered that in order for colonies to efficiently manage environmental fluctuations and disturbances, the foraging process of bees is adaptive and robust (Schmickl and Crailsheim, 2004). The foraging behavior of honeybees must take into account the quality of the resource (nectar

and pollen), distance to the food source, and danger resulting from other predators in order to obtain an energetically optimal diet. Chapter 3 of this dissertation study the role of such foraging on population of honeybees under infestation by Varroa mites. Aside from the fact that my current dispersal in honeybees denoted "ρ_{ij}" (i.e. dispersal from patch i to patch j) does not explicitly take into account temperature, patch quality, or distance from the food source, I do not incorporate any defensive behavior bees generally exhibit (see the work of Boecking and Spivak (1999); Evans and Spivak (2010)). In addition, the model propose in chapter 3 where I study the dynamics within a colony by looking at the interaction between the broods, adult bees, and mites did not take into account the defensive behavior of bees nor the preference of mite preying on nurse bees as illustrated in the work of Kraus (1993). The effect of these behaviors is however study through the life history parameter of both the honeybees and mites population. While I acknowledge that my models have some limitations, the work presented in this dissertation represent the first step on understanding the role of adaptive dispersal prompt by environmental factors such as temperature or climate conditions which may have a big impact on the conservation of the ecosystem. Thus, future work should focus more on explicitly modeling temperature (or climate change) when constructing system with adaptive dispersal in organisms.

Psalms 23:6 *Surely goodness and mercy shall follow me all the days of my life, and I shall dwell in the house of the Lord forever.*

Bibliography

Aarssen, L. and Turkington, R. (1985). Biotic specialization between neighbouring genotypes in lolium perenne and trifolium repens from a permanent pasture. *The Journal of Ecology*, pages 605–614.

Aiello, W. G. and Freedman, H. (1990). A time-delay model of single-species growth with stage structure. *Mathematical biosciences*, 101(2):139–153.

Auger, P. and Poggiale, J.-C. (1996). Emergence of population growth models: fast migration and slow growth. *Journal of Theoretical Biology*, 182(2):99–108.

Bascompte, J. (2009). Disentangling the web of life. *Science*, 325(5939):416–419.

Betti, M. I., Wahl, L. M., and Zamir, M. (2014). Effects of infection on honey bee population dynamics: a model. *PloS one*, 9(10):e110237.

Boecking, O. and Spivak, M. (1999). Behavioral defenses of honey bees against varroa jacobsoni oud. *Apidologie*, 30(2-3):141–158.

Boot, W. J., Tan, N. Q., Dien, P. C., Van Huan, L., Van Dung, N., Beetsma, J., et al. (1997). Reproductive success of varroa jacobsoni in brood of its original host, apis cerana, in comparison to that of its new host, a. mellifera (hymenoptera: Apidae). *Bulletin of entomological research*, 87(02):119–126.

Bowler, D. E. and Benton, T. G. (2005). Causes and consequences of animal dispersal strategies: relating individual behaviour to spatial dynamics. *Biological Reviews*, 80(02):205–225.

Branco, M. R., Kidd, N. A., and Pickard, R. S. (1999). Development of varroa jacobsoni in colonies of apis mellifera iberica in a mediterranean climate. *Apidologie*, 30(6):491–503.

Branco, M. R., Kidd, N. A., and Pickard, R. S. (2006). A comparative evaluation of sampling methods for varroa destructor (acari: Varroidae) population estimation. *Apidologie*, 37(4):452.

Briggs, C. J. and Hoopes, M. F. (2004). Stabilizing effects in spatial parasitoid–host and predator–prey models: a review. *Theoretical population biology*, 65(3):299–315.

Cantrell, R. and Cosner, C. (2004). *Spatial ecology via reaction-diffusion equations*. John Wiley & Sons, Ltd.

Chewning, W. C. (1975). Migratory effects in predator-prey models. *Mathematical Biosciences*, 23(3):253–262.

Cressman, R. and Křivan, V. (2013). Two-patch population models with adaptive dispersal: the effects of varying dispersal speeds. *Journal of mathematical biology*, 67(2):329–358.

Dall, S. R., Giraldeau, L.-A., Olsson, O., McNamara, J. M., and Stephens, D. W. (2005). Information and its use by animals in evolutionary ecology. *Trends in ecology & evolution*, 20(4):187–193.

Debenedictis, A. (2014). *Evolution or Creation?: A Comparison of the Arguments*. Xlibris Corporation.

DeGrandi-Hoffman, G., Ahumada, F., Curry, R., Probasco, G., and Schantz, L. (2014). Population growth of varroa destructor (acari: Varroidae) in commercial honey bee colonies treated with beta plant acids. *Experimental and Applied Acarology*, 64(2):171–186.

DeGrandi-Hoffman, G., Ahumada, F., Zazueta, V., Chambers, M., Hidalgo, G., and Watkins deJong, E. (2016). Population growth of varroa destructor (acari: Varroidae) in honey bee colonies is affected by the number of foragers with mites. *Experimental and Applied Acarology*, 69(1):21–34.

DeGrandi-Hoffman, G. and Curry, R. (2004). A mathematical model of varroa mite (varroa destructor anderson and trueman) and honeybee (apis mellifera l.) population dynamics. *International Journal of Acarology*, 30(3):259–274.

DeGrandi-Hoffman, G., Roth, S. A., Loper, G., and Erickson, E. H. (1989). Beepop: a honeybee population dynamics simulation model. *Ecological modelling*, 45(2):133–150.

DeGrandi-Hoffman, G., Wardell, G., Ahumada-Segura, F., Rinderer, T., Danka, R., and Pettis, J. (2008). Comparisons of pollen substitute diets for honey bees: consumption rates by colonies and effects on brood and adult populations. *Journal of apicultural research*, 47(4):265–270.

Delfinado-Baker, M., Rath, W., and Boecking, O. (1992). Phoretic bee mites and honeybee grooming behavior. *International journal of acarology*, 18(4):315–322.

Duffey, E. (1998). Aerial dispersal in spiders. In *Proceedings of the 17th European Colloquium of Arachnology, Edinburgh*, volume 1997, pages 187–191.

Eberl, H. J., Frederick, M. R., and Kevan, P. G. (2010). Importance of brood maintenance terms in simple models of the honeybee-varroa destructor-acute bee paralysis virus complex. *Electronic Journal of Differential Equations*, 19:85–98.

Eischen, F. A., Rothenbuhler, W. C., and Kulinčević, J. M. (1984). Some effects of nursing on nurse bees. *Journal of Apicultural Research*, 23(2):90–93.

Evans, J. D. and Spivak, M. (2010). Socialized medicine: individual and communal disease barriers in honey bees. *Journal of invertebrate pathology*, 103:S62–S72.

Feng, Z., Towers, S., and Yang, Y. (2011). Modeling the effects of vaccination and treatment on pandemic influenza. *The AAPS journal*, 13(3):427–437.

Fewell, J. H. and Winston, M. L. (1992). Colony state and regulation of pollen foraging in the honey bee, apis mellifera l. *Behavioral Ecology and Sociobiology*, 30(6):387–393.

Fraser, D. F. and Cerri, R. D. (1982). Experimental evaluation of predator-prey relationships in a patchy environment: consequences for habitat use patterns in minnows. *Ecology*, pages 307–313.

Fries, I., Camazine, S., and Sneyd, J. (1994). Population dynamics of varroa jacobsoni: a model and a review. *Bee world*, 75(1):5–28.

Fries, I., Imdorf, A., and Rosenkranz, P. (2006). Survival of mite infested (varroa destructor) honey bee (apis mellifera) colonies in a nordic climate. *Apidologie*, 37(5):564.

Fukuda, H. and Sakagami, S. F. (1968). Worker brood survival in honeybees. *Researches on Population Ecology*, 10(1):31–39.

Galef, B. G. and Laland, K. N. (2005). Social learning in animals: empirical studies and theoretical models. *AIBS Bulletin*, 55(6):489–499.

Garrido, C. and Rosenkranz, P. (2003). The reproductive program of female varroa destructor mites is triggered by its host, apis mellifera. *Experimental & applied acarology*, 31(3-4):269–273.

Ghosh, S. and Bhattacharyya, S. (2011). A two-patch prey-predator model with food-gathering activity. *Journal of Applied Mathematics and Computing*, 37(1-2):497–521.

Graham, J. M. (1992). The hive and the honey bee. Technical report, Dadant & Sons Hamilton, IL.

Greggers, U. and Menzel, R. (1993). Memory dynamics and foraging strategies of honeybees. *Behavioral Ecology and Sociobiology*, 32(1):17–29.

Grünbaum, D. and Veit, R. R. (2003). Black-browed albatrosses foraging on antarctic krill: density-dependence through local enhancement? *Ecology*, 84(12):3265–3275.

Hanski, I. (1998). Metapopulation dynamics. *Nature*, 396(6706):41–49.

Hanski, I. (1999). *Metapopulation Ecology*. Oxford University Press Oxford.

Hansson, L. (1991). Dispersal and connectivity in metapopulations. *Biological journal of the Linnean Society*, 42(1-2):89–103.

Harpur, B. A., Kent, C. F., Molodtsova, D., Lebon, J. M., Alqarni, A. S., Owayss, A. A., and Zayed, A. (2014). Population genomics of the honey bee reveals strong signatures of positive selection on worker traits. *Proceedings of the National Academy of Sciences*, 111(7):2614–2619.

Harris, J. L. (1980). *A population model and its application to the study of honey bee colonies*. PhD thesis, University of Manitoba, unpublished thesis.

Harrison, R. G. (1980). Dispersal polymorphisms in insects. *Annual Review of Ecology and Systematics*, pages 95–118.

Hastings, A. (1977). Spatial heterogeneity and the stability of predator-prey systems. *Theoretical Population Biology*, 12(1):37–48.

Hastings, A. (1983). Can spatial variation alone lead to selection for dispersal? *Theoretical Population Biology*, 24(3):244–251.

Hayes Jr, J., Underwood, R. M., Pettis, J., et al. (2008). A survey of honey bee colony losses in the us, fall 2007 to spring 2008. *PloS one*, 3(12):e4071.

Hsu, S., Hubbell, S., and Waltman, P. (1977). A mathematical theory for single-nutrient competition in continuous cultures of micro-organisms. *SIAM Journal on Applied Mathematics*, 32(2):366–383.

Hsu, S.-B. (1978). On global stability of a predator-prey system. *Mathematical Biosciences*, 39(1):1–10.

Huang, Z. (2012). Varroa mite reproductive biology. *American Bee Culture http://www. extension. org/pages/65450/varroa-mite-reproductivebiology*.

Hutson, V. (1984). A theorem on average liapunov functions. *Monatshefte für Mathematik*, 98(4):267–275.

Ifantidis, M. D. (1988). Some aspects of the process of varroa jacobsoni mite entrance into honey bee (apis mellifera) brood cells. *Apidologie*, 19(4):387–396.

Jánosi, I. M. and Scheuring, I. (1997). On the evolution of density dependent dispersal in a spatially structured population model. *Journal of Theoretical Biology*, 187(3):397–408.

Jansen, V. A. (1995). Regulation of predator-prey systems through spatial interactions: a possible solution to the paradox of enrichment. *Oikos*, 74(345):384–390.

Jansen, V. A. (2001). The dynamics of two diffusively coupled predator–prey populations. *Theoretical Population Biology*, 59(2):119–131.

Kang, Y., Blanco, K., Davies, T., and Wang, Y. (2015). Disease dynamics of honeybees with varroa destructor as parasite and virus vector. *arXiv preprint arXiv:1505.03742*.

Kang, Y., Blanco, K., Davis, T., Wang, Y., and DeGrandi-Hoffman, G. (2016). Disease dynamics of honeybees with varroa destructor as parasite and virus vector. *Mathematical biosciences*, 275:71–92.

Kang, Y., Sasmal, S. K., and Messan, K. (2017). A two-patch prey-predator model with predator dispersal driven by the predation strength. *Mathematical Biosciences and Engineering*, 14(4):843–880.

Kareiva, P., Mullen, A., and Southwood, R. (1990). Population dynamics in spatially complex environments: theory and data [and discussion]. *Philosophical Transactions of the Royal Society of London. Series B: Biological Sciences*, 330(1257):175–190.

Khoury, D. S., Barron, A. B., and Myerscough, M. R. (2013). Modelling food and population dynamics in honey bee colonies. *PloS one*, 8(5):e59084.

Khoury, D. S., Myerscough, M. R., and Barron, A. B. (2011). A quantitative model of honey bee colony population dynamics. *PloS one*, 6(4):e18491.

Kiester, A. and Slatkin, M. (1974). A strategy of movement and resource utilization. *Theoretical population biology*, 6(1):1–20.

Klein, A.-M., Vaissiere, B. E., Cane, J. H., Steffan-Dewenter, I., Cunningham, S. A., Kremen, C., and Tscharntke, T. (2007). Importance of pollinators in changing landscapes for world crops. *Proceedings of the Royal Society of London B: Biological Sciences*, 274(1608):303–313.

Kraus, B. (1993). Preferences of varroa jacobsoni for honey bees (apis mellifera l.) of different ages. *Journal of Apicultural Research*, 32(2):57–64.

Kraus, B. and Page, R. E. (1995). Effect of varroa jacobsoni (mesostigmata: Varroidae) on feral apis mellifera (hymenoptera: Apidae) in california. *Environmental Entomology*, 24(6):1473–1480.

Kribs-Zaleta, C. M. and Mitchell, C. (2014). Modeling colony collapse disorder in honeybees as a contagion. *Mathematical biosciences and engineering: MBE*, 11(6):1275–1294.

Kruger, D. I. (2007). Coffee production effects on child labor and schooling in rural brazil. *Journal of Development Economics*, 82(2):448–463.

Kummel, M., Brown, D., and Bruder, A. (2013). How the aphids got their spots: predation drives self-organization of aphid colonies in a patchy habitat. *Oikos*, 122(6):896–906.

Le Conte, Y., Ellis, M., and Ritter, W. (2010). Varroa mites and honey bee health: can varroa explain part of the colony losses? *Apidologie*, 41(3):353–363.

Lengyel, I. and Epstein, I. R. (1991). Diffusion-induced instability in chemically reacting systems: Steady-state multiplicity, oscillation, and chaos. *Chaos: An Interdisciplinary Journal of Nonlinear Science*, 1(1):69–76.

Levin, S. A. (1974). Dispersion and population interactions. *American Naturalist*, pages 207–228.

Lihoreau, M., Deneubourg, J.-L., and Rivault, C. (2010). Collective foraging decision in a gregarious insect. *Behavioral Ecology and Sociobiology*, 64(10):1577–1587.

Liu, X. and Chen, L. (2003). Complex dynamics of holling type ii lotka–volterra predator–prey system with impulsive perturbations on the predator. *Chaos, Solitons & Fractals*, 16(2):311–320.

Liu, Y. (2010). The dynamical behavior of a two patch predator-prey model.

Marino, S., Hogue, I. B., Ray, C. J., and Kirschner, D. E. (2008). A methodology for performing global uncertainty and sensitivity analysis in systems biology. *Journal of theoretical biology*, 254(1):178–196.

Markin, G. P. (1970). Foraging behavior of the argentine ant in a california citrus grove. *Journal of Economic Entomology*, 63(3):740–744.

Martin, S. (1998). A population model for the ectoparasitic mite varroa jacobsoni in honey bee (apis mellifera) colonies. *Ecological Modelling*, 109(3):267–281.

Martin, S. J. (1994). Ontogenesis of the mite varroa jacobsoni oud. in worker brood of the honeybee apis mellifera l. under natural conditions. *Experimental & applied acarology*, 18(2):87–100.

Matthysen, E. (2005). Density-dependent dispersal in birds and mammals. *Ecography*, 28(3):403–416.

McGregor, S. E. et al. (1976). *Insect pollination of cultivated crop plants*, volume 496. Agricultural Research Service, US Department of Agriculture.

Messan, K., DeGrandi-Hoffman, G., Castillo-Chavez, C., and Kang, Y. (2017). Migration effects on population dynamics of the honeybee-mite interactions. *Mathematical Modelling of Natural Phenomena*, 12(2):84–115.

Messan, K. and Kang, Y. (2017). A two patch prey-predator model with multiple foraging strategies in predators. *DCDS-B*, 22(3):947–976.

Meyer, W. B. and Turner, B. L. (1992). Human population growth and global land-use/cover change. *Annual review of ecology and systematics*, 23(1):39–61.

Namba, T. (1980). Density-dependent dispersal and spatial distribution of a population. *Journal of theoretical biology*, 86(2):351–363.

Neuvonen, S. (1999). Random foraging by herbivores: complex patterns may be due to plant architecture. *Journal of Ecology*, 87(3):526–528.

Nguyen-Ngoc, D., Nguyen-Huu, T., and Auger, P. (2012). Effects of fast density dependent dispersal on pre-emptive competition dynamics. *Ecological Complexity*, 10:26–33.

Pascual, M. (1993). Diffusion-induced chaos in a spatial predator–prey system. *Proceedings of the Royal Society of London. Series B: Biological Sciences*, 251(1330):1–7.

Perry, C. J., Søvik, E., Myerscough, M. R., and Barron, A. B. (2015). Rapid behavioral maturation accelerates failure of stressed honey bee colonies. *Proceedings of the National Academy of Sciences*, 112(11):3427–3432.

Poggiale, J. (1998). From behavioural to population level: growth and competition. *Mathematical and computer modelling*, 27(4):41–49.

Ratti, V., Kevan, P. G., and Eberl, H. J. (2012). A mathematical model for population dynamics in honeybee colonies infested with varroa destructor and the acute bee paralysis virus. *Canadian Applied Mathematics Quarterly: accepted*.

Ratti, V., Kevan, P. G., and Eberl, H. J. (2015). A mathematical model of the honeybee–varroa destructor–acute bee paralysis virus system with seasonal effects. *Bulletin of mathematical biology*, 77(8):1493–1520.

Reeve, J. D. (1988). Environmental variability, migration, and persistence in host-parasitoid systems. *American Naturalist*, pages 810–836.

Rosenzweig, M. L. and MacArthur, R. H. (1963). Graphical representation and stability conditions of predator-prey interactions. *American Naturalist*, 97(895):209–223.

Sakofski, F., Koeniger, N., Fuchs, S., et al. (1990). Seasonality of honey bee colony invasion by varroa jacobsoni oud. *Apidologie*, 21(6):547–550.

Savino, J. F. and Stein, R. A. (1989). Behavioural interactions between fish predators and their prey: effects of plant density. *Animal behaviour*, 37:311–321.

Schmickl, T. and Crailsheim, K. (2004). Costs of environmental fluctuations and benefits of dynamic decentralized foraging decisions in honey bees. *Adaptive Behavior*, 12(3-4):263–277.

Schmickl, T. and Crailsheim, K. (2007). Hopomo: a model of honeybee intracolonial population dynamics and resource management. *Ecological modelling*, 204(1):219–245.

Schmid-Hempel, P. (1998). *Parasites in social insects*. Princeton University Press.

Silva, J. A., De Castro, M. L., and Justo, D. A. (2001). Stability in a metapopulation model with density-dependent dispersal. *Bulletin of mathematical biology*, 63(3):485–505.

Smith, H. (2010). *An introduction to delay differential equations with applications to the life sciences*, volume 57. Springer Science & Business Media.

Solé, R. V. and Bascompte, J. (2006). *Self-Organization in Complex Ecosystems.(MPB-42)*, volume 42. Princeton University Press.

Soro, A., Sundberg, S., and Rydin, H. (1999). Species diversity, niche metrics and species associations in harvested and undisturbed bogs. *Journal of Vegetation Science*, 10(4):549–560.

Southwick, E. E. and Southwick, L. (1992). Estimating the economic value of honey bees (hymenoptera: Apidae) as agricultural pollinators in the united states. *Journal of Economic Entomology*, 85(3):621–633.

Stamps, J. (1988). Conspecific attraction and aggregation in territorial species. *American Naturalist*, pages 329–347.

STEINER, J., DITTMANN, F., ROSENKRANZ, P., and ENGELS, W. (1994). The first gonocycle of the parasitic mite (varroa juobsoni) in relation to preimaginal development of its host, the honey bee (apis mellifra carnicar). *Invertebrate reproduction & development*, 25(3):175–183.

Sumpter, D. J. and Martin, S. J. (2004). The dynamics of virus epidemics in varroa-infested honey bee colonies. *Journal of Animal Ecology*, 73(1):51–63.

Taylor, F. (1977). Foraging behavior of ants: experiments with two species of myrmecine ants. *Behavioral Ecology and Sociobiology*, 2(2):147–167.

Thieme, H. R. (2003). *Mathematics in population biology*. Princeton University Press.

Traniello, J. F. (1989). Foraging strategies of ants. *Annual review of entomology*, 34(1):191–210.

Traniello, J. F., Fujita, M. S., and Bowen, R. V. (1984). Ant foraging behavior: ambient temperature influences prey selection. *Behavioral Ecology and Sociobiology*, 15(1):65–68.

Tsuruda, J. M. and Page Jr, R. E. (2009). The effects of young brood on the foraging behavior of two strains of honey bees (apis mellifera). *Behavioral ecology and sociobiology*, 64(2):161–167.

Visscher, P. K. and Seeley, T. D. (1982). Foraging strategy of honeybee colonies in a temperate deciduous forest. *Ecology*, 63(6):1790–1801.

Viswanathan, G. M., Afanasyev, V., Buldyrev, S., Murphy, E., Prince, P., Stanley, H. E., et al. (1996). Lévy flight search patterns of wandering albatrosses. *Nature*, 381(6581):413–415.

Waddington, K. D. and Holden, L. R. (1979). Optimal foraging: on flower selection by bees. *The American Naturalist*, 114(2):179–196.

Watanabe, M. E. et al. (1994). Pollination worries rise as honey-bees decline. *Science*, 265(5176):1170–1170.

Wells, H. and Wells, P. H. (1986). Optimal diet, minimal uncertainty and individual constancy in the foraging of honey bees, apis mellifera. *The Journal of Animal Ecology*, pages 881–891.

Wisz, M. S., Pottier, J., Kissling, W. D., Pellissier, L., Lenoir, J., Damgaard, C. F., Dormann, C. F., Forchhammer, M. C., Grytnes, J.-A., Guisan, A., et al. (2013). The role of biotic interactions in shaping distributions and realised assemblages of species: implications for species distribution modelling. *Biological Reviews*, 88(1):15–30.

Zimmerman, M. (1982). Optimal foraging: random movement by pollen collecting bumblebees. *Oecologia*, 53(3):394–398.

APPENDIX A

PROOFS

Proof of Theorem 1

Proof. Observed that $\frac{dx_i}{dt}\big|_{x_i=0} = 0$ and $\frac{dy_i}{dt}\big|_{y_i=0} = \rho_i s y_j \geq 0$ if $y_j \geq 0$ for $i = 1,2,\ j = 1,2,$ and $i \neq j$. The model (2.3) is positively invariant in $\mathbb{R}^4_+$ by theorem A.4 (p. 423) in Thieme (2003). It follows that the set $\{(x_1,y_1,x_2,y_2) \in \mathbb{R}^4_+ : x_i = 0\}$ is invariant for both $i = 1,2$ under the same theorem. The proof of boundedness is as follow

$$\frac{dx_i}{dt} = r_i x_i \left(1 - \frac{x_i}{K_i}\right) - \frac{a_i x_i y_i}{1+x_i} \leq r_i x_i \left(1 - \frac{x_i}{K_i}\right)$$

thus

$$\limsup_{t\to\infty} x_i(t) \leq K_i.$$

Now we define $L = \rho_2(x_1+y_1) + \rho_1(x_2+y_2)$, to get

$$\begin{aligned}
&\frac{dL}{dt} = \rho_2 \frac{d(x_1+y_1)}{dt} + \rho_1 \frac{d(x_2+y_2)}{dt} \\
&= \rho_2 x_1 \left(1 - \frac{x_1}{K_1}\right) + \rho_1 r x_2 \left(1 - \frac{x_2}{K_2}\right) \\
&- \rho_2 d_1 y_1 - \rho_1 d_2 y_2 + \rho_1\rho_2(1-s)\left(\frac{a_1 x_1 y_1 y_2}{1+x_1} - \frac{a_2 x_2 y_2 y_1}{1+x_2}\right) \\
&- \rho_1\rho_2(1-s)\left(\frac{a_1 x_1 y_1 y_2}{1+x_1} - \frac{a_2 x_2 y_2 y_1}{1+x_2}\right) + \rho_1\rho_2 s(y_1-y_2) - \rho_1\rho_2 s(y_1-y_2) \\
&= \rho_2 x_1 \left(1 - \frac{x_1}{K_1} + d_1\right) + \rho_1 x_2 \left(r - \frac{r x_2}{K_2} + d_2\right) - \rho_2 d_1(x_1+y_1) - \rho_1 d_2(x_2+y_2) \\
&\leq T - d_{\min}\left[\rho_2(x_1+y_1) + \rho_1(x_2+y_2)\right] = T - d_{\min} L
\end{aligned}$$

where $d_{\min} = \min\{d_1, d_2\}$ and

$$T = \max_{0\leq x_1\leq K_1} \left\{\rho_2 x_1 \left(1 - \frac{x_1}{K_1} + d_1\right)\right\} + \max_{0\leq x_2\leq K_2} \left\{\rho_1 x_2 \left(r - \frac{r x_2}{K_2} + d_2\right)\right\}.$$

consequently

$$\limsup_{t\to\infty} L(t) = \limsup_{t\to\infty} \rho_2(x_1(t)+y_1(t)) + \rho_1(x_2(t)+y_2(t)) \leq \frac{T}{d_{\min}}.$$

This shows that Model (2.3) is bounded in $\mathbb{R}^4_+$ which concludes the proof of theorem (1). □

Proof of Theorem 2

Proof. Item 1: Model (2.3) is positively invariant and bounded in $\mathbb{R}^4_+$ according to Theorem 1. From this, it follows that Model (2.3) is attracted to a compact set C in $\mathbb{R}^4_+$. Furthermore, if $x_j = 0,\ j = 1,$ or 2, then Model (2.3) is reduced to three species couple models (2.4).

Consider the fact that $\lim_{t\to\infty} y_i(t) = \lim_{t\to\infty} y_j(t) = 0$ when $x_i = 0$, we can conclude that $y_1 = y_2 = 0$ is an omega limit set of Model (2.4). Additionally

$$\frac{dx_i}{x_i dt}\Big|_{x_i=0} = r_i > 0$$

then by Theorem 2.5 of Hutson (1984) Hutson (1984), prey x_i persists.

Item 2: Define $V(y_i, y_j) = \rho_j y_i + \rho_i y_j$, then we have

$$\frac{dV}{dt} = \frac{a x_i y_i}{1+x_i}\rho_j - d_i y_i \rho_j - d_j y_j \rho_i = \left[\frac{a_i x_i}{1+x_i} - d_i\right] y_i \rho_j - d_j y_j \rho_i.$$

Notice that $\limsup_{t\to\infty} x_i(t) \le K_i$. Then if $\mu_i > K_i$ we have $\frac{a_i K_i}{1+K_i} - d_i < -\delta < 0$ and let $\delta^* = \min\{\delta, d_j\}$. This implies

$$\begin{aligned}\frac{dV}{dt} = \left[\frac{a_i x_i}{1+x_i} - d_i\right] y_i \rho_j - d_j y_j \rho_i &< -(\delta y_i \rho_j + d_j y_j \rho_i) \\ &< -\delta^*(y_i \rho_j + d_j y_j \rho_i) = -\delta^* V(y_i, y_j)\end{aligned}$$

Therefore both predators go extinct if $\mu_i > K_i$. Now Model (2.4) reduces to the following prey model since $\limsup_{t\to\infty} y_i(t) = \limsup_{t\to\infty} y_j(t) = 0$

$$\frac{dx_i}{dt} = r_i x_i \left(1 - \frac{x_i}{K_i}\right)$$

with prey x_i converging to K_i. Thus Model (2.4)is globally stable at $(K_i, 0, 0)$ when $\mu_i > K_i$.

Item 3: Now we focus on the persistence condition for predator y_i. Since x_i is persistent from Item 1 Theorem 2 then we can conclude that Model (2.4) is attracted to a compact set C_s subset of C that exclude E_{000}.Then according to Theorem 1 and 3, the omega limit set of Model (2.4) on the compact set C_s is $E_{K_i 00}$. Notice that the following inequalities,

$$\begin{aligned}\frac{dy_i}{dt} &= \frac{a_i x_i y_i}{1+x_i} - d_i y_i + \rho_i(1-s)\left(\frac{a_i x_i y_i}{1+x_i} y_j\right) + \rho_i s(y_j - y_i) \\ &\ge \frac{a_i x_i y_i}{1+x_i} - d_i y_i - \rho_i s y_i \quad \Rightarrow \\ \frac{dy_i}{y_i dt} &\ge \frac{a_i x_i}{1+x_i} - d_i - \rho_i s\end{aligned}$$

therefore, we have

$$\frac{dy_i}{y_i dt}\Big|_{E_{K_i 00}} \ge \frac{a_i K_i}{1+K_i} - (d_i + \rho_i s).$$

According to Theorem 2.5 of Hutson (1984) Hutson (1984), we can conclude that predator y_i is persistent if the following inequalities hold

$$\frac{a_i K_i}{1+K_i} - (d_i + \rho_i s) > 0 \Leftrightarrow \rho_i s < \frac{(a_i - d_i)(K_i - \mu_i)}{1+K_i}.$$

Now assume that $\rho_i s < \frac{(a_i-d_i)(K_i-\mu_i)}{1+K_i}$ holds, then we can conclude that predator y_i is persistent. This implies that when time large enough, there exists some $\varepsilon > 0$ such that

$$\frac{dy_i}{dt}\Big|_{y_i=0} = \rho_j s y_j > \rho_j s \varepsilon > 0.$$

Thus, we could conclude that predator in Patch j also persists due to the persistence of predator in Patch i. □

Proof of Proposition 1

Proof. The algebraic calculations imply that an interior equilibrium (x_i^*, y_i^*, y_j^*) of Model (2.4) satisfies the following equations:

$$\begin{aligned}
y_i^* &= \frac{r_i(K_i - x_i^*)(1+x_i^*)}{a_i K_i} \\
y_j^* &= \frac{r_i(K_i - x_i^*)[x_i^*(a_i-d_i)-d_i]\rho_j}{a_i K_i d_j \rho_i} \\
0 &= \underbrace{[(x_i^*)^3 - (\mu_i + K_i)(x_i^*)^2 - \alpha_i x_i^* + \beta_i]}_{f_i(x_i^*)}[x_i^* + 1]
\end{aligned}$$

where $\beta_i = \frac{[d_j\rho_i s + d_i(d_j+\rho_j s)]K_i}{r_i(a_i-d_i)(1-s)\rho_j}$ and

$$\alpha_i = \frac{[d_j s\rho_i + r_i d_i(1-s) - (a_i-d_i)(d_j+s\rho_j)]K_i}{r_i(a_i-d_i)(1-s)\rho_j} = \beta_i + \frac{[r_i d_i(1-s) - a_i(d_j+s\rho_j)]K_i}{r_i(a_i-d_i)(1-s)\rho_j}.$$

This implies that

$$0 < \mu_i = \frac{d_i}{a_i - d_i} < x_i^* < K_i \text{ and } f_i(x_i^*) = 0.$$

Therefore, if $a_i < d_i$ or $\mu_i > K_i$ or $f_i(x_i^*) = 0$ has no positive roots, then Model (2.4) has no interior equilibrium.

Now assume that $0 < \mu_i = \frac{d_i}{a_i-d_i} < K_i$, then we have $f_i(0) = \beta_i > 0$ and $\lim_{x_i \to -\infty} f_i(x_i) = -\infty$. This indicates that there exist $x_0 \in (-\infty, 0)$ such that $f_i(x_0) = 0$. Therefore, we can conclude that $f_i(x_i)$ has at least one negative root and at most two positive roots since $f_i(x_i)$ is a polynomial with degree 3. The derivative of $f_i(x_i)$ has the following form

$$f_i'(x_i) = 3x_i^2 - 2(\mu_i + K_i)x_i - \alpha_i = 0$$

which gives the following two critical points if $\Delta_i = (\mu_i + K_i)^2 + 3\alpha_i > 0$

$$x_i^{c_{+,-}} = \frac{(\mu_i + K_i) \pm \sqrt{(\mu_i+K_i)^2 + 3\alpha_i}}{3} = \frac{(\mu_i + K_i) \pm \sqrt{\Delta}}{3}.$$

Therefore if $\Delta_i \geq 0$, then $x_i^{c_+} = \frac{(\mu_i+K_i)+\sqrt{\Delta_i}}{3} > 0$ is the local minimum of $f_i(x_i)$ since $f_i''(x_i^{c_+}) = 2\sqrt{\Delta_i} \geq 0$ and $f_i''(x_i^{c_-}) = -2\sqrt{\Delta_i} \leq 0$. We note that $f_i(x_i)$ has two positive

roots if $f_i(x_i^{c+}) \leq 0$. It follows that $f_i(x_i)$ has two positive roots if the following equation is satisfied:

$$f\left(x_i^{c+}\right) = -\frac{1}{3}\left[\alpha_i(\mu_i+K_i)-3\beta_i\right] - \frac{1}{27}\left[(\mu_i+K_i)+3\alpha_i\right]^2\left[2(\mu_i+K_i)-\sqrt{\Delta_i}\right] - \frac{1}{3}\alpha_i\sqrt{\Delta_i} < 0.$$

Since

$$\alpha_i(\mu_i+K_i)-3\beta_i > 0 \quad \Rightarrow \quad \alpha_i > \frac{3\beta_i}{\mu_i+K_i}$$

and

$$2(\mu_i+K_i)-\sqrt{\Delta_i} = 2(\mu_i+K_i)-\sqrt{(\mu_i+K_i)^2+3\alpha_i} > 0 \quad \Rightarrow \quad \alpha_i < (\mu_i+K_i)^2$$

therefore we can conclude that $f_i(x_i)$ has two positive roots when $\frac{3\beta_i}{\mu_i+K_i} < \alpha_i < (\mu_i+K_i)^2$. Thus for $x^*_{i\ell}$ where $\ell = 1,2$ denote the two positive roots of the nullclines $f_i(x_i)$ and $i = 1,2$ represent the prey population in patch one and two, we have:

$$y^*_{i\ell} = \frac{(K_i - x^*_{i\ell})(1+x^*_{i\ell})}{a_i K_i}, \qquad y^*_{j\ell} = \frac{(K_i - x^*_{i\ell})[x^*_{i\ell}(a_i-d_i)-d_i]\rho_j}{a_i K_i d_j \rho_i}$$

if $\mu_i < x^*_{i\ell} < K_i, \ell = 1,2$.

From the arguments above we conclude that Model (2.4) can have up to two interior equilibria $E^{\ell}_{x_i,y_i,y_j} = (x^*_{i\ell}, y^*_{i\ell}, y^*_{j\ell})$ when $\frac{3\beta_i}{\mu_i+K_i} < \alpha_i < (\mu_i+K_i)^2$ and $\mu_i < x^*_{i\ell} < K_i, \ell = 1,2$.

On the other hand, if $\Delta_i = (\mu_i+K_i)^2 + 3\alpha_i < 0$ then $f_i(x_i)$ has no positive real roots and hence Model (2.4) has no interior equilibrium. □

Proof of Theorem 3

Proof. The local stability of the equilibrium $(x_1^*, y_1^*, x_2^*, y_2^*)$ of Model (2.3) is established by finding the eigenvalues λ_i, $i = 1,\ 2,\ 3,\ 4$ of the Jacobian matrix $J_{(x_1^*,y_1^*,x_2^*,y_2^*)}$ (A.16) evaluated at the equilibria.

$$J_{(x_1^*,y_1^*,x_2^*,y_2^*)} = \begin{bmatrix} \left(1-\frac{2x_1^*}{K_1}\right) - \frac{a_1 y_1^*}{(1+x_1^*)^2} & -\frac{a_1 x_1^*}{1+x_1^*} & 0 & 0 \\ \frac{a_1 y_1^*\left(1+y_2^*(\rho_1-s\rho_1)\right)}{(1+x_1^*)^2} & J^{22}_{(x_1^*,y_1^*,x_2^*,y_2^*)} & \frac{\rho_1 a_2(-1+s)y_1^* y_2^*}{(1+x_2^*)^2} & J^{24}_{(x_1^*,y_1^*,x_2^*,y_2^*)} \\ 0 & 0 & r\left(1-\frac{2x_2^*}{K_2}\right) - \frac{a_2 y_2^*}{(1+x_2^*)^2} & -\frac{a_2 x_2^*}{1+x_2^*} \\ \frac{\rho_2 a_1(-1+s)y_1^* y_2^*}{(1+x_2^*)^2} & J^{42}_{(x_1^*,y_1^*,x_2^*,y_2^*)} & \frac{a_2 y_2^*\left(1+y_1^*(\rho_2-s\rho_2)\right)}{(1+x_2^*)^2} & J^{44}_{(x_1^*,y_1^*,x_2^*,y_2^*)} \end{bmatrix} \tag{A.1}$$

where

$$J^{22}_{(x_1^*,y_1^*,x_2^*,y_2^*)} = \rho_1(1-s)\left(\frac{a_1 x_1^* y_2^*}{1+x_1^*} - \frac{a_2 x_2^* y_2^*}{1+x_2^*}\right) + \frac{a_1 x_1^*}{1+x_1^*} - d_1 - s\rho_1$$

$$J^{24}_{(x_1^*,y_1^*,x_2^*,y_2^*)} = s\rho_1 + \rho_1(1-s)\left(\frac{a_1 x_1^* y_1^*}{1+x_1^*} - \frac{a_2 x_2^* y_1^*}{1+x_2^*}\right)$$

$$J^{42}_{(x_1^*,y_1^*,x_2^*,y_2^*)} = s\rho_2 + \rho_2(1-s)\left(\frac{a_2 x_2^* y_2^*}{1+x_2^*} - \frac{a_1 x_1^* y_1^*}{1+x_1^*}\right)$$

$$J^{44}_{(x_1^*,y_1^*,x_2^*,y_2^*)} = \rho_2(1-s)\left(\frac{a_2 x_2^* y_1^*}{1+x_2^*} - \frac{a_1 x_1^* y_1^*}{1+x_1^*}\right) + \frac{a_2 x_2^*}{1+x_2^*} - d_2 - s\rho_2$$

By substituting the equilibria $E_{0000}, E_{K_1000}, E_{00K_20,}$ into the Jacobian matrix (A.16), it was found that these equilibria are saddle consider one of their eigenvalues is positive.

For the equilibrium $E_{K_10K_20}$ we obtain

$$\lambda_1 = -1\ (<0),\ \ \lambda_2 = -r\ (<0),$$

$$\lambda_3 + \lambda_4 = \frac{a_1K_1}{1+K_1} - d_1 + \frac{a_2K_2}{1+K_2} - d_2 - s\rho_1 - s\rho_2$$

and

$$\lambda_3\lambda_4 = \left[d_1 - \frac{a_1K_1}{1+K_1}\right]\left[1 - \frac{a_2K_2}{(s\rho_2+d_2)(1+K_2)}\right] + \frac{s\rho_1}{s\rho_2+d_2}\left[d_2 - \frac{a_2K_2}{1+K_2}\right]$$

Notice that the eigenvalue λ_3 and λ_4 being negative for $s \in (0,1)$ is equivalent to the case where the boundary equilibria $(K_i, 0)$ for the single patch is globally asymptotically stable. This is also equivalent to $\mu_i > K_i$ or $\frac{a_iK_i}{1+K_i} - d_i < 0$. We again observe that for $\frac{a_iK_i}{1+K_i} - d_i < 0$ the following holds

$$\lambda_3 + \lambda_4 = \frac{a_1K_1}{1+K_1} - d_1 + \frac{a_2K_2}{1+K_2} - d_2 - s\rho_1 - s\rho_2 < 0$$

$$\Rightarrow d_1 + d_2 + s\rho_1 + s\rho_2 > \frac{a_1K_1}{1+K_1} + \frac{a_2K_2}{1+K_2}$$

and

$$\lambda_3\lambda_4 = \left[d_1 - \frac{a_1K_1}{1+K_1}\right]\left[1 - \frac{a_2K_2}{(s\rho_2+d_2)(1+K_2)}\right] + \frac{s\rho_1}{s\rho_2+d_2}\left[d_2 - \frac{a_2K_2}{1+K_2}\right] > 0$$

which can be rewritten in the following form:

$$\sum_{i=1}^{2}\left[\frac{(a_i-d_i)(\mu_i-K_i)}{1+K_i} + s\rho_i\right] > 0$$

and

$$\left[\frac{(a_1-d_1)(\mu_1-K_1)}{1+K_1}\right]\left[s\rho_2 + \frac{(a_2-d_2)(\mu_2-K_2)}{1+K_2}\right] + s\rho_1\left[\frac{(a_2-d_2)(\mu_2-K_2)}{1+K_2}\right] > 0.$$

Based on the discussion above, we can conclude that the results on the local stability of four boundary equilibria of Theorem 3 holds.

Item 1: Let $p_i(x) = \frac{a_ix}{1+x}$ and $q_i(x) = \frac{r_i(K_i-x)(1+x)}{a_iK_i}$ then we have the following

$$\begin{aligned}
\frac{dx_i}{dt} &= r_ix_i\left(1 - \frac{x_i}{K_i}\right) - \frac{a_ix_iy_i}{(1+x_i)} = \frac{a_ix_i}{1+x_i}\left[\frac{r_i(K_i-x_i)(1+x_i)}{a_iK_i} - y_i\right] \\
&= p_i(x_i)\left[q_i(x_i) - y_i\right].
\end{aligned}$$

$$\begin{aligned}
\frac{dy_i}{dt} &= y_i\left[\frac{a_ix_i}{1+x_i} - d_i\right] + \rho_i(1-s)y_iy_j\left[\frac{a_ix_i}{1+x_i} - \frac{a_jx_j}{1+x_j}\right] + \rho_is\left[y_j - y_i\right] \\
&= y_i\left[p_i(x_i) - d_i\right] + \rho_i(1-s)y_iy_j\left[p_i(x_i) - p_j(x_j)\right] + \rho_is\left[y_j - y_i\right]
\end{aligned}$$

where both $i, j = 1,\ 2,$ with $i \neq j$. Now consider the following Lyapunov functions

$$V_1(x_1, y_1) = \rho_2 \int_{K_1}^{x_1} \frac{p_1(\xi) - p_1(K_1)}{p_1(\xi)} d\xi + \rho_2 y_1 \tag{A.2}$$

and

$$V_2(x_2, y_2) = \rho_1 \int_{K_2}^{x_2} \frac{p_2(\xi) - p_2(K_2)}{p_2(\xi)} d\xi + \rho_1 y_2 \tag{A.3}$$

Taking derivative of the functions (A.2) and (A.3) with respect to time t yield

$$\begin{aligned}
&\frac{d}{dt} V_1(x_1(t), y_1(t)) \\
&= \rho_2 \frac{p_1(x_1) - p_1(K_1)}{p_i(x_1)} \frac{dx_1}{dt} + \rho_2 \frac{dy_1}{dt} \\
&= \rho_2 \frac{1}{p_1(x_1)} [p_1(x_1) - p_1(K_1)]\, p_1(x_1)\, [q_1(x_1) - y_1] + \rho_2 y_1 [p_1(x_1) - d_1] \\
&+ \rho_1 \rho_2 (1-s) y_1 y_2 [p_1(x_1) - p_2(x_2)] + \rho_1 \rho_2 s [y_2 - y_1] \\
&= \rho_2 [p_1(x_1) - p_1(K_1)]\, q_1(x_1) + \rho_2 y_1 [p_1(K_1) - d_1] + \rho_1 \rho_2 (1-s) y_1 y_2 [p_1(x_1) - p_2(x_2)] \\
&+ \rho_1 \rho_2 s [y_2 - y_1]
\end{aligned} \tag{A.4}$$

and

$$\begin{aligned}
&\frac{d}{dt} V_2(x_2(t), y_2(t)) \\
&= \rho_1 \frac{p_2(x_2) - p_2(K_2)}{p_2(x_2)} \frac{dx_2}{dt} + \rho_1 \frac{dy_2}{dt} \\
&= \rho_1 \frac{1}{p_2(x_2)} [p_2(x_2) - p_2(K_2)]\, p_2(x_2)\, [q_2(x_2) - y_2] + \rho_1 y_2 [p_2(x_2) - d_2] \\
&+ \rho_1 \rho_2 (1-s) y_1 y_2 [p_2(x_2) - p_1(x_1)] + \rho_1 \rho_2 s [y_1 - y_2] \\
&= \rho_1 [p_2(x_2) - p_2(K_2)]\, q_2(x_2) + \rho_1 y_2 [p_2(K_2) - d_2] - \rho_1 \rho_2 (1-s) y_1 y_2 [p_1(x_1) - p_2(x_2)] \\
&- \rho_1 \rho_2 s [y_2 - y_1]
\end{aligned} \tag{A.5}$$

Also, we denote $V = V_1 + V_2$ and adding (A.4) and (A.5), we obtain

$$\begin{aligned}
\frac{d}{dt} V &= \frac{d}{dt} V_1(x_1(t), y_1(t)) + \frac{d}{dt} V_2(x_2(t), y_2(t)) \\
&= \rho_2 [p_1(x_1) - p_1(K_1)]\, [q_1(x_1) - y_1] + \rho_2 y_1 [p_1(x_1) - d_1] + \rho_1 [p_2(x_2) - p_2(K_2)]\, [q_2(x_2) - y_2] \\
&+ \rho_1 y_2 [p_2(x_2) - d_2] \\
&= \rho_2 [p_1(x_1) - p_1(K_1)]\, q_1(x_1) + \rho_2 y_1 [p_1(K_1) - d_1] + \rho_1 [p_2(x_2) - p_2(K_2)]\, q_2(x_2) \\
&+ \rho_1 y_2 [p_2(K_2) - d_2]\,.
\end{aligned}$$

We observe that the function $p_i(x_i)$ increases as x_i increases thus $p_i(x_i) - p_i(K_i) > 0$ if $x_i > K_i$ and $p_i(x_i) - p_i(K_i) < 0$ if $x_i < K_i$. Also, $q_i(x_i)$ is positive if $x_i < K_i$ and it is negative if $x_i > K_i$. This implies that the expressions $\rho_2 [p_1(x_1) - p_1(K_1)]\, q_1(x_1)$ and $\rho_1 [p_2(x_2) - p_2(K_2)]\, q_2(x_2)$ are both negative for all $x_i \geq 0$ since all the parameters are assumed to be positive. Also, Assume $\mu_i > K_i$. This implies that $\frac{d_i}{a_i - d_i} > K_i$ which is also equivalent to $\frac{a_i K_i}{1 + K_i} = p_i(K_i) < d_i$. Since $p_i(K_i) < d_i$ then $p_i(K_i) - d_i < 0$. The derivative $\frac{dV}{dt}$ is therefore negative which implies that both V_1 and V_2 are Lyapunov functions, and the boundary equilibrium $E_{K_1 0 K_2 0} = (K_1, 0, K_2, 0)$ is globally stable when $\mu_i > K_i$ by Theorem 3.2 in Hsu (1978).

Item 2: According to Theorem 1, we know that Model (2.3) is attracted to a compact set C in $\mathbb{R}^4_+$. Define $V_x = x_1 + x_2$, then we have

$$\frac{dV_x}{dt} = \frac{dx_1}{dt} + \frac{dx_2}{dt} = r_1 x_1 \left(1 - \frac{x_1}{K_1}\right) - \frac{a_1 x_1 y_1}{1+x_1} + r_2 x_2 \left(1 - \frac{x_2}{K_2}\right) - \frac{a_2 x_2 y_2}{1+x_2}.$$

Notice that if $x_i = x_j = 0$, then Model (2.3) converges to $(0,0,0,0)$, and

$$\frac{dV_x}{dt}\Big|_{x_1=x_2=0} = r_1 + r_2 > 0.$$

Therefore, according to Theorem 2.5 of Hutson (1984), we can conclude that prey population in two patches, i.e., $x_1 + x_2$, is persistent. Moreover, if $x_j = 0$, Model (2.3) is reduced to the subsystem (2.4) where prey x_i is persistent according to Theorem 2. Thus, we can conclude prey population in at least one patch is persistent.

Define $V_y = \rho_2 y_1 + \rho_1 y_2$, then we have

$$\frac{dV_y}{dt} = \rho_2 \frac{dy_1}{dt} + \rho_1 \frac{dy_2}{dt} = \rho_2 y_1 \left(\frac{a_1 x_1}{1+x_1} - d_1\right) + \rho_1 y_2 \left(\frac{a_2 x_2}{1+x_2} - d_2\right).$$

Notice that if $y_i = y_j = 0$, then Model (2.3) converges to $(K_1, 0, K_2, 0)$. Since we have $K_i > \mu_i$ for both $i = 1, 2$, then we have

$$\min_{i=1,2} \{\frac{a_i K_i}{1+K_i} - d_i\} = \delta > 0.$$

This implies that

$$\begin{aligned}\frac{dV_y}{dt}\Big|_{y_1=y_2=0} &= \rho_2 y_1 \left(\frac{a_1 K_1}{1+K_1} - d_1\right) + \rho_1 y_2 \left(\frac{a_2 K_2}{1+K_2} - d_2\right) \\ &\geq \delta(\rho_2 y_1 + \rho_1 y_2) = \delta V_y > 0.\end{aligned}$$

Therefore, according to Theorem 2.5 of Hutson (1984) and the proof of Proposition 1, we can conclude that predator population in each patch is persistent. □

Proof of Theorem 4

Proof. First we show the existence of the interior equilibrium $E = (\mu, \nu, \mu, \nu)$ in the symmetric case (i.e. $a_1 = a_2 = a, d_1 = d_2 = d, K_1 = K_2 = K, r = 1$). The interior equilibrium can be obtained by the positive intersection of the two nullclines $x_1 = F_1(x_2)$ and $x_2 = F_2(x_1)$ (2.11). Recall from the nullcines (2.11) that

$$x_i(x_j) = \frac{(\mu + K) \pm \sqrt{(\mu+K)^2 - 4\phi_i(x_j)}}{2}.$$

where $\phi_i(x_j) = \mu K + \frac{\rho_i}{\rho_j}(x_j - \mu)(x_j - K)$ which indicate that

$$x_i^+(\mu) = \frac{(\mu+K) + \sqrt{(\mu+K)^2 - 4\phi_i(\mu)}}{2} = K \text{ and } x_i^-(\mu) = \frac{(\mu+K) - \sqrt{(\mu+K)^2 - 4\phi_i(\mu)}}{2} = \mu$$

This implies that $x=\mu$ is a positive solution of the nullcline (2.11) when $a>d$ in the symmetric case. We can accordingly say that $E=(\mu,\nu,\mu,\nu)$ is an interior equilibrium of Model (2.3) when $a_1=a_2=a, d_1=d_2=d, K_1=K_2=K, r=1$.

The local stability of $E=(\mu,\nu,\mu,\nu)$ is obtained by the eigenvalues of the Jacobian matrix (A.16) evaluated at this equilibrium as follow:

$$\lambda_1\lambda_2=\frac{d(K-\mu)}{K(1+\mu)}>0 \text{ if } K>\mu \text{ and } \lambda_1\lambda_2=\frac{d(K-\mu)}{K(1+\mu)}<0 \text{ if } K<\mu$$

$$\lambda_1+\lambda_2=\frac{K-1-2\mu}{K(1+\mu)}<0 \text{ if } \mu>\frac{K-1}{2} \text{ and } \lambda_1+\lambda_2=\frac{d(K-\mu)}{K(1+\mu)}>0 \text{ if } \mu<\frac{K-1}{2}$$

$$\lambda_3\lambda_4=\frac{(\rho_1+\rho_2)[(1-s)(K-\mu)d\nu-((K-1)-2\mu)s\mu)]+d(K-\mu)}{K(1+\mu)}>0 \text{ for } K>\mu$$
$$\text{and } \mu>\frac{K-1}{2} \text{ when } s\in[0,1]$$

$$\lambda_3+\lambda_4=-\left[\frac{-\mu(K-1)+2\mu^2+Ks(\rho_1+\rho_2)(1+\mu)}{K(1+\mu)}\right]<0 \text{ for } \mu>\frac{K-1}{2} \text{ when } s\in[0,1]$$

Notice that the eigenvalues $\lambda_1,\ \lambda_2,\ \lambda_3,$ and λ_4 being negative correspond to the case where the unique interior equilibrium (μ,ν) of the single patch Model (2.2) is locally asymptoticaly stable. We can hence conclude that E has the same local stability as the interior equilibrium (μ,ν) for the single patch model (2.2). Consequently $\frac{K-1}{2}<\mu<K$ are sufficients conditions for $E=(\mu,\nu,\mu,\nu)$ to be locally asymptotically stable while unstable when $\mu<\frac{K-1}{2}$ for $s\in[0,1]$. □

Proof of Theorem 5

Proof. Observe that $\frac{dH_i}{dt}\big|_{H_i=0}=0$ and $\frac{dM_i}{dt}\big|_{M_i=0}=\rho_{ij}\frac{H_i}{a_i+H_i}M_j\geq 0$ if $M_j\geq 0$ for $i=1,2,\ j=1,2,$ and $i\neq j$, thus we can conclude that model (3.2) is positive invariant in $\mathbb{R}^4_+$ by Theorem A.4 (p.423) in Thieme (2003). We now proceed with the boundedness as follows:

$$\frac{dH_i}{dt}=\frac{r_iH_i^2}{K_i+H_i^2}-d_{h_i}H_i-\alpha_iH_iM_i\leq\frac{r_iH_i^2}{K_i+H_i^2}-d_{h_i}H_i$$

for $i=1,2$. This implies that $\limsup_{t\to\infty}H_i(t)\leq\frac{\left(\frac{r_i}{d_{h_i}}\right)+\sqrt{\left(\frac{r_i}{d_{h_i}}\right)^2-4K_i}}{2}=N^*_{h_i}$. Thus if $\frac{r_i}{2\sqrt{K_i}}<d_{h_i}$ or $H_i(0)<\frac{\left(\frac{r_i}{d_{h_i}}\right)-\sqrt{\left(\frac{r_i}{d_{h_i}}\right)^2-4K_i}}{2}=N^c_{h_i}$ then $\limsup_{t\to\infty}H_i(t)=0$. This proves Item 2 and 4 of the theorem.

Define $V=c_1H_1+M_1+c_2H_2+M_2$, then we have

$$\begin{aligned}\frac{dV}{dt} &= c_1\frac{dH_1}{dt}+\frac{dM_1}{dt}+c_2\frac{dH_2}{dt}+\frac{dM_2}{dt}\\ &= \frac{c_1r_1H_1^2}{K_1+H_1^2}-c_1d_{h_1}H_1-d_{m_1}M_1+\frac{c_2r_2H_2^2}{K_2+H_2^2}-c_2d_{h_2}H_2-d_{m_2}M_2\\ &\leq T-\min\{d_{h_1},d_{m_1},d_{h_2},d_{m_2}\}(c_1H_1+M_1+c_2H_2+M_2)=T-d_{\min}V\end{aligned}$$

where

$$T = \max_{N_{h_1}^c \le H_1 \le N_{h_1}^*} \left\{ \frac{c_1 r_1 H_1^2}{K_1 + H_1^2} \right\} + \max_{N_{h_2}^c \le H_2 \le N_{h_2}^*} \left\{ \frac{c_2 r_2 H_2^2}{K_2 + H_2^2} \right\}.$$

Therefore, we have

$$\limsup_{t\to\infty} V(t) = \limsup_{t\to\infty} (c_1 H_1(t) + M_1(t) + c_2 H_2(t) + M_2(t)) \le \frac{T}{d_{\min}}$$

which implies that Model (3.2) is bounded in $\mathbb{R}_+^4$.

E_{0000} always exist and is always locally stable, however we will return to the existence and local stability of E_{0000} when we prove Item 1 of Theorem **??**. In addition, if $\frac{r_i}{2\sqrt{K_i}} < d_{h_i},\ i = 1$ and 2, then the extinction equilibrium E_{0000} is the only locally stable equilibrium from the upper bound argument of the honeybee population presented above. we can conclude that E_{0000} is globally stable.

Recall that $\frac{dH_i}{dt}\big|_{H_i=0} = 0$ and $\frac{dM_i}{dt}\big|_{M_i=0} = \rho_{ij}\frac{H_i}{a_i+H_i}M_j \ge 0$ if $M_j \ge 0$ for $i = 1,2,\ j = 1,2,$ and $i \ne j$ thus the set $\{(H_1, M_1, H_2, M_2) \in \mathbb{R}_+^4 : H_i = 0\}$ is invariant for both $i = 1,2$. This indicates that if $H_i(0) = 0$, then $H_i(t) = 0$ for all $t > 0$. Thus, the population M_i converges to 0 since $\lim_{t\to\infty} M_j = \lim_{t\to\infty} M_i = 0$ when $H_i = 0$. This prove item 1 of the theorem.

Now the proof of Item 5 is as follow. Define $M = M_1 + M_2$ and from Model (3.2), we have

$$\begin{aligned}
\frac{dM}{dt} &= (c_1\alpha_1 H_1 - d_{m_1})M_1 + (c_2\alpha_2 H_2 - d_{m_2})M_2 \\
&= c_1\alpha_1\left(H_1 - \frac{d_{m_1}}{c_1\alpha_1}\right)M_1 + c_2\alpha_2\left(H_2 - \frac{d_{m_2}}{c_2\alpha_2}\right)M_2 \\
&\le \max_{\substack{N_{h_1}^c \le H_1 \le N_{h_1}^* \\ N_{h_2}^c \le H_2 \le N_{h_2}^*}} \left\{ c_1\alpha_1\left(H_1 - \frac{d_{m_1}}{c_1\alpha_1}\right), c_2\alpha_2\left(H_2 - \frac{d_{m_2}}{c_2\alpha_2}\right) \right\}(M_1 + M_2)
\end{aligned}$$

For $N_{h_i}^* < H_i^* = \frac{d_{m_i}}{c_i\alpha_i},\ i = 1$ and 2,

$$\frac{dM}{dt} \le \max_{\substack{N_{h_1}^c \le H_1 \le N_{h_1}^* \\ N_{h_2}^c \le H_2 \le N_{h_2}^*}} \left\{ c_1\alpha_1\left(H_1 - \frac{d_{m_1}}{c_1\alpha_1}\right), c_2\alpha_2\left(H_2 - \frac{d_{m_2}}{c_2\alpha_2}\right) \right\}(M_1 + M_2) \le 0 \Rightarrow \limsup_{t\to\infty} M(t) = 0.$$

Consequently the populations M_1 and M_2 go extinct when $N_{h_i}^* < H_i^* = \frac{d_{m_i}}{c_i\alpha_i},\ i = 1$ and 2. This concludes the proof of Theorem 5. □

Proof of Theorem 6

Proof. We note that Model (3.2) is reduced to Model (3.3) when $H_i = 0, i = 1$ or 2 which always have the extinction equilibrium E_{000}. From the results of Theorem (7), we know that Model (3.2) has the boundary equilibria $E_{N_{h_1}^c 0 N_{h_2}^c 0}$ and $E_{N_{h_1}^* 0 N_{h_2}^* 0}$ when $\frac{r_i}{2\sqrt{K_i}} \ge d_{h_i},\ i = 1,2$

thus when $H_i = 0,\ i = 1$ or 2, Model (3.3) has the boundary equilibria $E_{0N_{h_2}^c 0}$ and $E_{0N_{h_2}^* 0}$ for $i = 1$ or $E_{N_{h_1}^c 00}$ and $E_{N_{h_1}^* 00}$ for $i = 2$. Now we prove the existence of the interior equilibria of Model (3.3). Recall that Model (3.2) is reduced to the following when $H_i = 0$

$$\begin{aligned}
\frac{dM_i}{dt} &= -d_{m_i}M_i + \rho_{ji}\frac{H_j}{a_j+H_j}M_j \\
\frac{dH_j}{dt} &= \frac{r_j H_j^2}{K_j+H_j^2} - d_{h_j}H_j - \alpha_j H_j M_j \\
\frac{dM_j}{dt} &= c_j\alpha_j H_j M_j - d_{m_j}M_j - \rho_{ji}\frac{H_j}{a_j+H_j}M_j
\end{aligned}$$

for $i, j = 1,2,\ i \neq j$. Solving for M_i in $\frac{dM_i}{dt} = 0$ and M_j in $\frac{dH_j}{dt} = 0$ yields respectively

$$M_i = \frac{\rho_{ji}H_jM_j}{d_{m_i}(a_j+H_j)} \qquad \text{and} \qquad M_j = \frac{1}{\alpha_j}\left[\frac{r_jH_j}{H_j^2+K_j} - d_{h_j}\right]$$

Now we note that $H_i^* = \frac{d_{m_i}}{c_i\alpha_i},\ i = 1,2$ and solving for H_j in $\frac{dM_j}{dt} = 0$ yields the following unique positive solution

$$\hat{H}_j^* = \frac{\left(H_j^* - a_j + \frac{\rho_{ji}}{c_j\alpha_j}\right) + \sqrt{4a_jH_j^* + \left(H_j^* - a_j + \frac{\rho_{ji}}{c_j\alpha_j}\right)^2}}{2} > 0.$$

Also, $\limsup_{t\to\infty} H_j(t) \leq \frac{\left(\frac{r_j}{d_{h_j}}\right) + \sqrt{\left(\frac{r_j}{d_{h_j}}\right)^2 - 4K_j}}{2} = N_{h_j}^*$ and if $\frac{r_j}{2\sqrt{K_j}} < d_{h_j}$ or $H_j(0) < \frac{\left(\frac{r_j}{d_{h_j}}\right) - \sqrt{\left(\frac{r_j}{d_{h_j}}\right)^2 - 4K_j}}{2} = N_{h_i}^c$ then $\limsup_{t\to\infty} H_j(t) = 0$ as noted in Theorem 5. By the arguments above, Model (3.3) has the unique interior equilibrium $E_{\hat{M}_1^*\hat{H}_2^*\hat{M}_2^*}$ when $H_1 = 0$ or $E_{\hat{H}_1^*\hat{M}_1^*\hat{M}_2^*}$ when $H_2 = 0$ with

$$\hat{H}_j^* = \frac{\left(H_j^* - a_j + \frac{\rho_{ji}}{c_j\alpha_j}\right) + \sqrt{4a_jH_j^* + \left(H_j^* - a_j + \frac{\rho_{ji}}{c_j\alpha_j}\right)^2}}{2},\ \hat{M}_j^* = \frac{1}{\alpha_j}\left[\frac{r_j\hat{H}_j^*}{(\hat{H}_j^*)^2+K_j} - d_{h_j}\right],\ \text{and}\ \ \hat{M}_i^* = \frac{\rho_{ji}\hat{H}_j^*\hat{M}_j^*}{d_{m_i}(a_j+\hat{H}_j^*)}$$

for $i, j = 1,2,\ i \neq j$ under the condition $N_{h_j}^c < \hat{H}_j^* < N_{h_j}^*$.

We continue our proof with the local stability of the equilibria $E_{000},\ E_{0N_{h_j}^* 0}, E_{0N_{h_j}^c 0}$, and $E_{\hat{H}_1^*\hat{M}_1^*\hat{M}_2^*}$ which can be determined by the eigenvalues $\lambda_i,\ i = 1,2,3$ of the Jacobian matrix (A.6) evaluated at the equilibria

$$J_{(\hat{M}_i^*,\hat{H}_j^*,\hat{M}_j^*)} =$$

$$\begin{bmatrix} -d_{m_i} & \frac{a_j\hat{M}_j^*\rho_{ji}}{(a_j+\hat{H}_j^*)^2} & \frac{\hat{H}_j^*\rho_{ji}}{a_j+\hat{H}_j^*} \\ 0 & -d_{h_j} + \frac{2r_j\hat{H}_j^*K_j}{\left((\hat{H}_j^*)^2+K_j\right)^2} - \alpha_j\hat{M}_j^* & -\alpha_j\hat{H}_j^* \\ 0 & \hat{M}_j^*\left(c_j\alpha_j - \frac{a_j\rho_{ji}}{(a_j+\hat{H}_j^*)^2}\right) & -d_{m_j} + c_j\hat{H}_j\alpha_j - \frac{\hat{H}_j^*\rho_{ji}}{a_j+\hat{H}_j^*} \end{bmatrix} = \begin{bmatrix} -d_{m_i} & \frac{a_j\hat{M}_j^*\rho_{ji}}{(a_j+\hat{H}_j^*)^2} & c_j\alpha_j\hat{H}_j^* - d_{m_j} \\ 0 & -d_{h_j} + \frac{2r_j\hat{H}_j^*K_j}{\left((\hat{H}_j^*)^2+K_j\right)^2} - \alpha_j\hat{M}_j^* & -\alpha_j\hat{H}_j^* \\ 0 & \hat{M}_j^*\left(c_j\alpha_j - \frac{a_j\rho_{ji}}{(a_j+\hat{H}_j^*)^2}\right) & 0 \end{bmatrix} \tag{A.6}$$

since

$$\frac{dM_j}{dt} = 0 \Rightarrow -d_{m_j} + c_jH_j\alpha_j - \frac{H_j\rho_{ji}}{a_j+H_j} = 0 \text{ or } c_j\alpha_jH_j - d_{m_j} = \frac{H_j\rho_{ji}}{a_j+H_j}$$

1. After substitution of the equilibrium E_{000} into the Jacobian matrix (A.6), we obtain the eigenvalues:

$$\lambda_1 = -d_{h_j} < 0, \;\; \lambda_2 = -d_{m_i} < 0, \;\; \lambda_3 = -d_{m_j} < 0$$

thus we can conclude that E_{000} is always locally asymptotically stable.

2. The proof for the local stability of the boundary equilibria $E_{0N^c_{h_j}0}$ and $E_{0N^*_{h_j}0}$ are as follows. Recall that $\frac{r_j}{2\sqrt{K_j}} \geq d_{h_j}$ is the necessary condition for $E_{0N^*_{h_j}0}$ and $E_{0N^c_{h_j}0}$ to exist. Substitution of the equilibrium $E_{0N^*_{h_j}0}$ into the the Jacobian Matrix (A.6) yield the following eigenvalues :

$$\lambda_1 = -d_{h_i} < 0, \;\; \lambda_2 = \frac{r_j \hat{H}^*_j [K_j - (N^*_{h_j})^2]}{[K_j + (N^*_{h_j})^2]^2}, \;\; \lambda_3 = c_j \alpha_j (N^*_{h_j} - H^*_j) - \frac{\rho_{ij} N^*_{h_j}}{a_j + N^*_{h_j}}.$$

Then we have:

$$\lambda_2 = \frac{r_j \hat{H}^*_j [K_j - (N^*_{h_j})^2]}{[K_j + (N_{h_j})^2]^2} < 0 \quad \text{since} \quad N^*_{h_j} = \frac{\left(\frac{r_j}{d_{h_j}}\right) + \sqrt{\left(\frac{r_j}{d_{h_j}}\right)^2 - 4K_j}}{2} > \sqrt{K_j} \Leftrightarrow \frac{r_j}{2\sqrt{K_j}} > d_{h_j}$$

and

$$\lambda_3 = c_1 \alpha_1 (N^*_{h_1} - H^*_1) - \frac{\rho_{12} N^*_{h_1}}{a_1 + N^*_{h_1}} = N^*_{h_j} \left(1 - \frac{\rho_{ji}}{c_j \alpha_j (\alpha_j + N^*_{h_j})}\right) < \frac{d_{m_j}}{c_j \alpha_j} = H^*_j < 0$$

$$\Rightarrow \; H^*_j > N^*_{h_j} \text{ or } H^*_j < N^*_{h_j} \text{ and } \rho_{ij} > \frac{c_j \alpha_j (N^*_{h_j} - H^*_j)(a_j + N^*_{h_j})}{N^*_{h_j}}.$$

Thus $E_{0N^*_{h_j}0}$ is sink if one of the following conditions is satisfied:

(i) $H^*_j > N^*_{h_j}$ or (ii)$\rho_{ji} > \frac{c_j \alpha_j (N^*_{h_j} - H^*_j)(a_j + N^*_{h_j})}{N^*_{h_j}} > 0$, otherwise, $(0, N^*_{h_j}, 0)$ is a saddle.

Now substitution of the boundary equilibrium $E_{0N^c_{h_j}0}$ into the the Jacobian Matrix (A.6) gives the following eigenvalues :

$$\lambda_1 = -d_{h_i} < 0, \;\; \lambda_2 = \frac{r_j \hat{H}^*_j [K_j - (N^c_{h_j})^2]}{[K_j + (N^c_{h_j})^2]^2}, \;\; \lambda_3 = c_j \alpha_j (N^c_{h_j} - H^*_j) - \frac{\rho_{ij} N^c_{h_j}}{a_j + N^c_{h_j}}.$$

Note that $\lambda_2 > 0$ consider $N^c_{h_j} = \dfrac{\left(\frac{r_j}{d_{h_j}}\right) - \sqrt{\left(\frac{r_j}{d_{h_j}}\right)^2 - 4K_j}}{2} < \sqrt{K_j} \quad \Leftrightarrow \dfrac{r_j}{2\sqrt{K_j}} > d_{h_j}$

therefore $E_{0N^c_{h_j}0}$ is saddle.

3. A substitution of the interior equilibrium $E_{\hat{M}^*_i \hat{H}^*_j \hat{M}^*_j}$ into the Jacobian matrix (A.6) yield the following characteristic polynomial

$$\lambda^3 - \left[\sum_{k=1}^{3}\lambda_k\right]\lambda^2 + \left[\sum_{k,s=1,k\neq s}^{3}\lambda_k\lambda_s\right]\lambda - \prod_{k=1}^{3}\lambda_k$$

where the eigenvalues $\lambda_k(\hat{M}_i^*, \hat{H}_j^*, \hat{M}_j^*)$, $k = 1,2,3$ are the roots of the above characteristic equation. We then have:

$$\sum_{k=1}^{3}\lambda_k = -d_{m_i} + \frac{r_j\hat{H}_j^*[K_j - (\hat{H}_j^*)^2]}{[K_j + (\hat{H}_j^*)^2]^2} < 0 \quad \text{if} \quad \hat{H}_j^* > \sqrt{K_j}$$

$$\sum_{k,s=1,k\neq s}^{3}\lambda_k\lambda_s = -d_{m_i}\frac{r_j\hat{H}_j^*[K_j - (\hat{H}_j^*)^2]}{[K_j + (\hat{H}_j^*)^2]^2} + \alpha_j\hat{M}_j^*\hat{H}_j^*\left(c_j\alpha_j - \frac{a_j\rho_{ji}}{(a_j + \hat{H}_j^*)^2}\right) > 0 \quad \text{if} \quad \hat{H}_j^* > \sqrt{K_j}$$

$$\prod_{k=1}^{3}\lambda_k = -d_{m_i}\alpha_j\hat{M}_j^*\hat{H}_j^*\left(c_j\alpha_j - \frac{a_j\rho_{ji}}{(a_j + \hat{H}_j^*)^2}\right) < 0 \quad \text{if} \quad 0 < \rho_{ji} < \frac{c_j\alpha_j(a_j + \hat{H}_j^*)^2}{a_j}$$

consider

$$c_j\alpha_j - \frac{a_j\rho_{ji}}{(a_j + \hat{H}_j^*)^2} = \frac{c_j\alpha_j\left[\left(\hat{H}_j^*\right)^2 + a_jH_j^* + a_j\sqrt{4a_jH_j^* + \left(H_j^* - a_j + \frac{\rho_{ji}}{c_j\alpha_j}\right)^2}\right]}{(a_j + \hat{H}_j^*)^2} > 0.$$

Thus $E_{\hat{M}_i^*\hat{H}_j^*\hat{M}_j^*}$ is locally stable when $\hat{H}_j^* > \sqrt{K_j}$ and saddle otherwise.

This concludes the proof of Theorem (6).

□

Proof of Theorem 7

Proof. Observe that the single Colony Model (3.1) always has the extinction equilibrium $(0,0)$. Therefore Model (3.2) always has the extinction equilibrium E_{0000} as well. In addition the boundary $(N_{h_i}^c, 0)$ and $(N_{h_i}^*, 0)$ exists for Model (3.1) when $\frac{r_i}{2\sqrt{K_i}} \geq d_{h_i}$, $i = 1,2$ and these conditions guarantee the existence of the equilibria $E_{N_{h_1}^c 000}$, $E_{N_{h_1}^* 000}$, $E_{00N_{h_2}^c 0}$, $E_{00N_{h_2}^* 0}$, $E_{N_{h_1}^c 0N_{h_2}^c 0}$, $E_{N_{h_1}^* 0N_{h_2}^c 0}$, $E_{N_{h_1}^c 0N_{h_2}^* 0}$, $E_{N_{h_1}^* 0N_{h_2}^* 0}$. Now we look at the local stability of the boundary equilibria which can be determined by the eigenvalues λ_i, $i = 1,2,3,4$ of the Jacobian matrix (A.7) evaluated at the equilibrium

$$J_{(\bar{H}_1^*, \bar{M}_1^*, \bar{H}_2^*, \bar{M}_2^*)} =$$

$$\begin{bmatrix} -d_{\bar{H}_1^*} - \alpha_1\bar{M}_1^* + \frac{2r_1K_1\bar{H}_1^*}{\left[K_1 + (\bar{H}_1^*)^2\right]^2} & -\alpha_1\bar{H}_1^* & 0 & 0 \\ c_1\alpha_1\bar{M}_1^* - \frac{\rho_{12}a_1\bar{M}_1^*}{(a_1 + \bar{H}_1^*)^2} & -d_{\bar{M}_1^*} + c_1\alpha_1\bar{H}_1^* - \frac{\rho_{12}\bar{H}_1^*}{a_1 + \bar{H}_1^*} & \frac{\rho_{21}a_2\bar{M}_2^*}{(a_2 + \bar{H}_2^*)^2} & \frac{\rho_{21}\bar{H}_2^*}{a_2 + \bar{H}_2^*} \\ 0 & 0 & -d_{\bar{H}_2^*} - \alpha_2\bar{M}_2^* + \frac{2r_2K_2\bar{H}_2^*}{\left[K_2 + (\bar{H}_2^*)^2\right]^2} & -\alpha_2\bar{H}_2^* \\ \frac{\rho_{12}a_1\bar{M}_1^*}{(a_1 + \bar{H}_1^*)^2} & \frac{\rho_{12}\bar{H}_1^*}{a_1 + \bar{H}_1^*} & c_2\alpha_2\bar{M}_2^* - \frac{\rho_{21}a_2\bar{M}_2^*}{(a_2 + \bar{H}_2^*)^2} & -d_{\bar{M}_2^*} + c_2\alpha_2\bar{H}_2^* - \frac{\rho_{21}\bar{H}_2^*}{a_2 + \bar{H}_2^*} \end{bmatrix} \quad \text{(A.7)}$$

1. After substitution of the equilibrium E_{0000} into the Jacobian Matrix (A.7), we obtain the eigenvalues:

$$\lambda_1 = -d_{h_1} < 0,\ \ \lambda_2 = -d_{m_1} < 0,\ \ \lambda_3 = -d_{h_2} < 0,\ \ \lambda_4 = -d_{m_2} < 0$$

thus we can conclude that E_{0000} is always locally asymptotically stable.

2. Now we look at the stability of the boundary equilibria $E_{N^*_{h_1}000}$, $E_{N^c_{h_1}000}$, $E_{00N^*_{h_2}0}$, and $E_{00N^c_{h_2}0}$. Substitution of the equilibrium $E_{N^*_{h_1}000}$ into the the Jacobian Matrix (A.7) yields the following eigenvalues :

$$\lambda_1 = -d_{h_2} < 0,\ \ \lambda_2 = -d_{m_2} < 0,\ \ \lambda_3 = -\left(\frac{d^2_{h_1}}{r_1}\right)\sqrt{\left(\frac{r_i}{d_{h_i}}\right)^2 - 4K_i} < 0,\ \ \lambda_4 = c_1\alpha_1(N^*_{h_1} - H^*_1) - \frac{\rho_{12}N^*_{h_1}}{a_1 + N^*_{h_1}}$$

We note that

$$\lambda_4 = c_1\alpha_1(N^*_{h_1} - H^*_1) - \frac{\rho_{12}N^*_{h_1}}{a_1 + N^*_{h_1}} < 0 \Rightarrow H^*_1 > N^*_{h_1} \text{ or } H^*_1 < N^*_{h_1} \text{ and } \rho_{12} > \frac{c_1\alpha_1(N^*_{h_1} - H^*_1)(a_1 + N^*_{h_1})}{N^*_{h_1}}$$

Consequently the equilibrium $E_{N^*_{h_1}000}$ is locally asymptotically stable if

(i) $H^*_1 > N^*_{h_1}$ or

(ii) $H^*_1 < N^*_{h_1}$ and $\rho_{12} > \frac{c_1\alpha_1(N^*_{h_1} - H^*_1)(a_1 + N^*_{h_1})}{N^*_{h_1}}$

and a saddle otherwise. We continue with the local stability of $E_{N^c_{h_1}000}$. Substitution of the equilibrium $E_{N^c_{h_1}000}$ into the the Jacobian Matrix (A.7) yield the following eigenvalues :

$$\lambda_1 = -d_{h_2} < 0,\ \ \lambda_2 = -d_{m_2} < 0,\ \ \lambda_3 = \left(\frac{d^2_{h_1}}{r_1}\right)\sqrt{\left(\frac{r_1}{d_{h_1}}\right)^2 - 4K_1} > 0,\ \ \lambda_4 = c_1\alpha_1(N^c_{h_1} - H^*_1) - \frac{\rho_{12}N^c_{h_1}}{a_1 + N^c_{h_1}}$$

Thus $E_{N^c_{h_1}000}$ is always saddle. Similarly we can obtain the stability condition of the equilibria $E_{00N^*_{h_2}0}$ and $E_{00N^c_{h_2}0}$ therefore the proof is omitted.

3. We now provide the stability of the boundary equilibria $E_{N^*_{h_1}0N^*_{h_2}0}$, $E_{N^*_{h_1}0N^c_{h_2}0}$, $E_{N^c_{h_1}0N^*_{h_2}0}$, and $E_{N^c_{h_1}0N^c_{h_2}0}$ which are obtain by the eigenvalues of the Jacobian matrix (A.7) evaluated at the equilibria.

At first, the detail on the stability of $E_{N^*_{h_1}0N^*_{h_2}0}$ is given below through the eigenvalues of $J_{E_{N^*_{h_1}0N^*_{h_2}0}}$:

$$\lambda_1\lambda_2 = \left[-\left(\frac{d_{h_1}^2}{r_1}\right)\sqrt{\left(\frac{r_1}{d_{h_1}}\right)^2 - 4K_1}\right]\left[-\left(\frac{d_{h_2}^2}{r_2}\right)\sqrt{\left(\frac{r_2}{d_{h_2}}\right)^2 - 4K_2}\right] > 0$$

$$\lambda_1 + \lambda_2 = -\left[\left(\frac{d_{h_1}^2}{r_1}\right)\sqrt{\left(\frac{r_1}{d_{h_1}}\right)^2 - 4K_1} + \left(\frac{d_{h_2}^2}{r_2}\right)\sqrt{\left(\frac{r_2}{d_{h_2}}\right)^2 - 4K_2}\right] < 0$$

$$\lambda_3\lambda_4 = \frac{c_2\alpha_2(a_2+N_{h_2}^*)(H_2^*-N_{h_2}^*)[c_1\alpha_1(a_1+N_{h_1}^*)(H_1^*-N_{h_1}^*)+\rho_{12}N_{h_1}^*]+\rho_{21}c_1\alpha_1(a_1+N_{h_1}^*)(H_1^*-N_{h_1}^*)N_{h_2}^*}{(a_1+N_{h_1}^*)(a_2+N_{h_2}^*)}$$

$$\lambda_3+\lambda_4 = -\frac{(a_2+N_{h_2}^*)[(a_1+N_{h_1}^*)(c_1\alpha_1(H_1^*-N_{h_1}^*)+c_2\alpha_2(H_2^*-N_{h_2}^*))+\rho_{12}N_{h_1}^*]+\rho_{21}(a_1+N_{h_1}^*)N_{h_2}^*}{(a_1+N_{h_1}^*)(a_2+N_{h_2}^*)}$$

Observe that for $H_i^* > N_{h_i}^*$, $i = 1$ and 2, $\lambda_3\lambda_4 > 0$ and $\lambda_3+\lambda_4 < 0$. In addition,

$$\begin{aligned}\lambda_3\lambda_4 &= \frac{c_2\alpha_2(a_2+N_{h_2}^*)(H_2^*-N_{h_2}^*)[c_1\alpha_1(a_1+N_{h_1}^*)(H_1^*-N_{h_1}^*)+\rho_{12}N_{h_1}^*]+\rho_{21}c_1\alpha_1(a_1+N_{h_1}^*)(H_1^*-N_{h_1}^*)N_{h_2}^*}{(a_1+N_{h_1}^*)(a_2+N_{h_2}^*)}\\ &= \frac{\rho_{12}c_2\alpha_2N_{h_1}^*(H_2^*-N_{h_2}^*)}{a_1+N_{h_1}^*} + c_1\alpha_1c_2\alpha_2(H_1^*-N_{h_1}^*)(H_2^*-N_{h_2}^*) + \frac{\rho_{21}c_1\alpha_1N_{h_2}^*(H_1^*-N_{h_1}^*)}{a_2+N_{h_2}^*}\end{aligned}$$

and

$$\begin{aligned}\lambda_3+\lambda_4 &= -\frac{(a_2+N_{h_2}^*)[(a_1+N_{h_1}^*)(c_1\alpha_1(H_1^*-N_{h_1}^*)+c_2\alpha_2(H_2^*-N_{h_2}^*))+\rho_{12}N_{h_1}^*]+\rho_{21}(a_1+N_{h_1}^*)N_{h_2}^*}{(a_1+N_{h_1}^*)(a_2+N_{h_2}^*)}\\ &= -\frac{\rho_{12}N_{h_1}^*}{a_1+N_{h_1}^*} - \frac{\rho_{21}N_{h_2}^*}{a_2+N_{h_2}^*} - c_1\alpha_1(H_1^*-N_{h_1}^*) - c_2\alpha_2(H_2^*-N_{h_2}^*)\end{aligned}$$

If $H_1^* < N_{h_1}^*$ and $H_2 > N_{h_2}^*$ then from the equations above

$$\lambda_3\lambda_4 > 0 \quad\Rightarrow\quad \frac{\rho_{12}c_2\alpha_2N_{h_1}^*(H_2^*-N_{h_2}^*)}{a_1+N_{h_1}^*} > c_1\alpha_1c_2\alpha_2(N_{h_1}^*-H_1^*)(H_2^*-N_{h_2}^*) + \frac{\rho_{21}c_1\alpha_1N_{h_2}^*(N_{h_1}^*-H_1^*)}{a_2+N_{h_2}^*}$$

$$\lambda_3+\lambda_4 < 0 \quad\Rightarrow\quad \frac{\rho_{12}N_{h_1}^*}{a_1+N_{h_1}^*} + \frac{\rho_{21}N_{h_2}^*}{a_2+N_{h_2}^*} + c_2\alpha_2(H_2^*-N_{h_2}^*) > c_1\alpha_1(N_{h_1}^*-H_1^*)$$

Therefore $E_{N_{h_1}^*0N_{h_2}^*0}$ is locally asymptotically stable if one of the following two conditions is satisfied:

(i) $H_i^* > N_{h_i}^*$ for both $i = 1,2$

(ii) $H_i^* < N_{h_i}^*, H_j^* > N_{h_j}^*$ for $i,j = 1,2, i \neq j$ and

$$\frac{\rho_{ij}N_{h_i}^*}{a_i+N_{h_i}^*} + \frac{\rho_{ji}N_{h_j}^*}{a_j+N_{h_j}^*} + c_j\alpha_j(H_j^*-N_{h_j}^*) > c_i\alpha_i(N_{h_i}^*-H_i^*)$$

and

$$\frac{\rho_{ij}c_j\alpha_jN_{h_i}^*(H_j^*-N_{h_j}^*)}{a_i+N_{h_i}^*} > c_i\alpha_ic_j\alpha_j(N_{h_i}^*-H_i^*)(H_j^*-N_{h_j}^*) + \frac{\rho_{ji}c_i\alpha_iN_{h_j}^*(N_{h_i}^*-H_i^*)}{a_j+N_{h_j}^*}.$$

$E_{N^*_{h_1}0N^*_{h_2}0}$ is saddle when $H^*_i > N^*_{h_i}, i = 1$ and 2. We now proceed with the local stability of the boundary equilibrium $E_{N^c_{h_1}0N^c_{h_2}0}$. The following eigenvalues of $J_{E_{N^c_{h_1}0N^c_{h_2}0}}$ are obtain from the Jacobian matrix (A.16):

$$\lambda_1\lambda_2 = \left[\left(\frac{d^2_{h_1}}{r_1}\right)\sqrt{\left(\frac{r_i}{d_{h_i}}\right)^2 - 4K_i}\right]\left[\left(\frac{d^2_{h_2}}{r_2}\right)\sqrt{\left(\frac{r_2}{d_{h_2}}\right)^2 - 4K_2}\right] > 0$$

$$\lambda_1 + \lambda_2 = -\left[\left(\frac{d^2_{h_1}}{r_1}\right)\sqrt{\left(\frac{r_i}{d_{h_i}}\right)^2 - 4K_i} + \left(\frac{d^2_{h_2}}{r_2}\right)\sqrt{\left(\frac{r_2}{d_{h_2}}\right)^2 - 4K_2}\right] < 0$$

$$\lambda_3\lambda_4 = \frac{c_2\alpha_2(a_2+N^c_{h_2})(H^*_2 - N^c_{h_2})[c_1\alpha_1(a_1+N^c_{h_1})(H^*_1 - N^c_{h_1}) + \rho_{12}N^c_{h_1}] + \rho_{21}c_1\alpha_1(a_1+N^c_{h_1})(H^*_1 - N^c_{h_1})N^c_{h_2}}{(a_1+N^c_{h_1})(a_2+N^c_{h_2})}$$

$$\lambda_3 + \lambda_4 = -\frac{(a_2+N^c_{h_2})[(a_1+N^c_{h_1})(c_1\alpha_1(H^*_1 - N^c_{h_1}) + c_2\alpha_2(H^*_2 - N^c_{h_2})) + \rho_{12}N^c_{h_1}] + \rho_{21}(a_1+N^c_{h_1})N^c_{h_2}}{(a_1+N^c_{h_1})(a_2+N^c_{h_2})}$$

Again notice that $\lambda_3\lambda_4 > 0$ and $\lambda_3 + \lambda_4 < 0$ when $H^*_i > N^c_{h_i}$, $i = 1$ and 2. Therefore $E_{N^c_{h_1}0N^c_{h_2}0}$ is a saddle if $H^*_i > N^c_{h_i}$ and a source if $H^*_i < N^c_{h_i}$, $i = 1$ and 2. Similar argument follow for the stability of the equilibria $E_{N^*_{h_1}0N^c_{h_2}0}$ and $E_{N^c_{h_1}0N^*_{h_2}0}$ thus the proof is omitted.

Based on the discussions above, we can conclude that Theorem (7) holds.

□

Proof of Theorem 8

Proof. First we show the existence of the symmetric interior equilibrium $E = (H^*, M^*, H^*, M^*)$ of Model (3.7). We denote

$$H^* = \frac{d_m}{c\alpha} \quad \text{and} \quad M^* = \frac{1}{\alpha}\left[\frac{rH^*}{H^{*2}+K} - d_h\right]$$

And notice that

$$H_1 = \left[H^* + \frac{(H^*M_2 - H_2M_2)}{M_1}\right] = F_1(H_2) \quad \text{and} \quad H_2 = \left[H^* + \frac{(H^*M_1 - H_1M_1)}{M_2}\right] = F_2(H_1)$$

are nullclines of Model (3.7) and we have the following properties:

$$F_1(M^*) = F_2(M^*) = M^*$$

This conclude that $H = H^* = \frac{d_m}{c\alpha}$ is a positive solution of the nullclines $F_1(H_2)$ and $F_2(H_1)$. We can hence say that $E = (H^*, M^*, H^*, M^*)$ is an interior equilibrium of Model (3.7).

The local stability of $E = (H^*, M^*, H^*, M^*)$ is obtained by the eigenvalues of the Jacobian matrix (A.7) evaluated at this equilibrium as follow:

$$\lambda_1 + \lambda_2 = \frac{rH^*(K - H^{*2})}{(K + H^*)^2} < 0 \text{ if } H^* > \sqrt{K}$$

$$\lambda_1 \lambda_2 = c\alpha^2 H^* M^* > 0$$

$$\lambda_3 + \lambda_4 = \frac{H^*(K - H^{*2})}{(K + H^*)^2} - \frac{2H^*\rho}{H^* + a} < 0 \text{ if } H^* > \sqrt{K}$$

$$\lambda_3 \lambda_4 = 2H^* \left[\frac{a\alpha M^*}{(a + H^*)^2} - \frac{rH^*(H^* - K)}{[K + (H^*)^2](a + H^*)} \right] \rho + c\alpha^2 H^* M^*$$

First note that the eigenvalues λ_1 and λ_2 being negative is equivalent to the case where the unique interior equilibrium (H_1^*, M_1^*) is locally asymptotically stable for the single patch Model (3.1) under the condition $H^* > \sqrt{K}$. We now explore the sufficient condition for λ_3 and λ_4 being negative through the following two cases when $H^* > \sqrt{K}$:

1. $\lambda_3 + \lambda_4 < 0$ when $H^* > \sqrt{K}$ and if

$$M^* \leq \frac{rH^*(a + H^*)[(H^*)^2 - K]}{a\alpha[(H^*)^2 + K]^2}$$

then the first term in the right hand side of the second equality of $\lambda_3 \lambda_4$ is positive and therefore $\lambda_3 \lambda_4 > 0$. Since $\lambda_3 + \lambda_4 < 0$ and $\lambda_3 \lambda_4 > 0$ then both λ_3 and λ_4 are negative.

2. For

$$M^* > \frac{rH^*(a + H^*)[(H^*)^2 - K]}{a\alpha[(H^*)^2 + K]^2} \text{ and } \rho < \frac{c\alpha^2 M^*(a + H^*)^2[(H^*)^2 + K]^2}{2\left(a\alpha M^*[(H^*)^2 + K]^2 - rH^*(a + H^*)[(H^*)^2 - K]\right)}$$

$\lambda_3 \lambda_4 > 0$ then both λ_3 and λ_4 are negative since $\lambda_3 + \lambda_4 < 0$.

Summarizing the discussions above, we can conclude that the symmetric interior equilibrium $E = (H^*, M^*, H^*, M^*)$ of Model (3.7) is locally asymptotically stable if $H^* > \sqrt{K}$ and one of the following conditions holds:

(a) $M^* \leq \frac{rH^*(a+H^*)[(H^*)^2 - K]}{a\alpha[(H^*)^2 + K]^2}$

(b) $M^* > \frac{rH^*(a+H^*)[(H^*)^2 - K]}{a\alpha[(H^*)^2 + K]^2}$ and $\rho < \frac{c\alpha^2 M^*(a+H^*)^2[(H^*)^2 + K]^2}{2\left(a\alpha M^*[(H^*)^2 + K]^2 - rH^*(a+H^*)[(H^*)^2 - K]\right)}$

And $E = (H^*, M^*, H^*, M^*)$ is a saddle if $H^* < \sqrt{K}$.

Based on the discussion above, we can conclude that the statement of Theorem 8 holds. □

Proof of Theorem 9

Proof. 1. We will proceed by first showing the positivity of our system

Case 1 For $0 < t < \tau_b$, $\frac{dB}{dt}$ can be integrated to obtain:

$$B(t) = \int_0^t \left[\frac{rH(s)^2}{K+H(s)^2} e^{-\int_s^t \left(d_b + \frac{\alpha_b M(u)}{a+B(u)}\right)du} \right] ds - \int_0^t \left[B_0(s-\tau_b) e^{-\int_{s-t}^t \left(d_b + \frac{\alpha_b M(u)}{a+B(u)}\right)du} \right] ds + B(0) \tag{A.8}$$

with $B(0) = \int_{-\tau_b}^0 B_0(t)dt > 0$. We now show that $B(t)$ in Equation (A.8) is in fact the solution of $\frac{dB}{dt}$ in Model (4.2). The derivative of $B(t)$ with respect to t in (A.8) yields:

$$\begin{aligned}
\frac{dB}{dt} &= \frac{rH(t)^2}{K+H(t)^2} - B_0(t-\tau_b) e^{-\int_{t-\tau_b}^t \left(d_b + \frac{\alpha_b M(u)}{a+B(u)}\right)du} \\
&\quad - \left[\frac{\alpha_b M(t)}{a+B(t)} + d_b \right] \left[\int_0^t \left(\frac{rH(s)^2}{K+H(s)^2} e^{-\int_s^t \left(d_b + \frac{\alpha_b M(u)}{a+B(u)}\right)du} \right) ds - \int_0^t \left(B_0(s-\tau_b) e^{-\int_{s-\tau_b}^t \left(d_b + \frac{\alpha_b M(u)}{a+B(u)}\right)du} \right) ds \right] \\
&= \frac{rH(t)^2}{K+H(t)^2} - B_0(t-\tau_b) e^{-\int_{t-\tau_b}^t \left(d_b + \frac{\alpha_b M(u)}{a+B(u)}\right)du} - \left[\frac{\alpha_b M(t)}{a+B(t)} + d_b \right] B(t)
\end{aligned}$$

which is equal to $\frac{dB}{dt}$ in Model (4.2). It is clear that $B(t) > 0$ for all $t > 0$. In addition, we have the following regarding $H(t)$

Suppose $H(0) > 0$. We prove by contradiction that there is no $T > 0$ such that $H(T) = 0$. To this end, define

$$T := \inf\{t \in [0,\infty) | H(t) = 0\}.$$

And note that $\{t \in [0,C] | H(t) = 0\}$ is a closed set for any $C \in [0,\infty)$, $H(t)$ is a continuous function, so $H(T) = 0$ provided that $T < \infty$. Thus, if $T \leq \tau_b$, then $H(t) > 0$ for all $t \in [0,T)$ and $H(T) = 0$, so $H'(t) \leq 0$ for all $t \in [0,T)$. Then, from the third equation of Model(4.2)-(4.3), we have

$$\begin{aligned}
&M'(t) \geq -d_m M(t) \\
&\Longrightarrow M(t) \geq M(0) e^{-d_m t} > 0, \quad \text{for all} \quad t > 0
\end{aligned} \tag{A.9}$$

when $M(0) > 0$. And from the third equation of Model(4.2), we also have

$$\begin{aligned}
&M'(t) \leq (c\alpha_b - d_m) M(t) \\
&\Longrightarrow M(t) \leq M(0) e^{(c\alpha_b - d_m)\tau_b} \quad \text{for} \quad t \in (0, \tau_b]
\end{aligned} \tag{A.10}$$

when $c\alpha_b > d_m \quad \Rightarrow \quad \frac{c\alpha_b}{d_m}$ and $M(0) > 0$. Hence, Model (4.2) implies $H'(t) \geq -(\frac{\alpha_h}{a} M(0) e^{(c\alpha_b - d_m)\tau_b} + d_h) H(t)$ for all $0 < t \leq T \leq \tau_b$. Therefore, we obtain

$$H(T) \geq H(0) e^{-(\frac{\alpha_h}{a} M(0) e^{(c\alpha_b - d_m)\tau_b} + d_h)T} > 0, \tag{A.11}$$

it is a contradiction. As a positive constant $T \leq \tau_b$ arbitrariness, we obtain $H(t) > 0$ for all $0 < t \leq \tau_b$ if $H(0) > 0$.

Case 2: For $t > \tau_b$, $\frac{dB}{dt}$ can be integrated to yield:

$$B(t) = \int_{t-\tau_b}^{t} \left[\frac{rH(s)^2}{K+H(s)^2} e^{-\int_s^t \left(d_b + \frac{\alpha_b M(u)}{a+B(u)}\right) du} \right] ds + B(0) e^{-\int_0^t \left(d_b + \frac{\alpha_b M(u)}{a+B(u)}\right) du} \tag{A.12}$$

Again we show that $B(t)$ in Equation (A.12) is the solution of $\frac{dB}{dt}$ in Model (4.3). The derivative of $B(t)$ with respect to t in (A.12) yields:

$$\begin{aligned}
\frac{dB}{dt} &= \frac{rH(t)^2}{K+H(t)^2} - \frac{rH(t-\tau_b)^2}{K+H(t-\tau_b)^2} e^{-\int_{t-\tau_b}^t \left(d_b + \frac{\alpha_b M(u)}{a+B(u)}\right) du} \\
&\quad - \left[\frac{\alpha_b M(t)}{a+B(t)} + d_b \right] \left[\int_{t-\tau_b}^{t} \left(\frac{rH(s)^2}{K+H(s)^2} e^{-\int_s^t \left(d_b + \frac{\alpha_b M(u)}{a+B(u)}\right) du} \right) ds + B(0) e^{-\int_0^t \left(d_b + \frac{\alpha_b M(u)}{a+B(u)}\right) du} \right] \\
&= \frac{rH(t)^2}{K+H(t)^2} - \frac{rH(t-\tau_b)^2}{K+H(t-\tau_b)^2} e^{-\int_0^t \left(d_b + \frac{\alpha_b M(u)}{a+B(u)}\right) du} - \left[\frac{\alpha_b M(t)}{a+B(t)} + d_b \right] B(t)
\end{aligned}$$

which is equal to $\frac{dB}{dt}$ in Model (4.3). We then have

$$B(t) \geq B(0) e^{-\int_0^t \left(d_b + \frac{\alpha_b M(u)}{a+B(u)}\right) du} > 0$$

Now, from the third equation of Model(4.3), we have

$$\begin{aligned}
&M'(t) \leq (c\alpha_b - d_m) M(t) \\
&\Longrightarrow M(t) \leq M(\tau_b) e^{(c\alpha_b - d_m)(t-\tau_b)} \quad \text{for} \quad t > \tau_b
\end{aligned} \tag{A.13}$$

when $c\alpha_b > d_m \quad \Rightarrow \quad \frac{c\alpha_b}{d_m}$. Hence, for $T > \tau_b$, Model (4.3) implies $H'(t) \geq -(\frac{\alpha_h}{a} M(\tau_b) e^{(c\alpha_b - d_m)(t-\tau_b)} + d_h) H(t)$ for all $\tau_b < t \leq T$. Then, we obtain

$$H(T) \geq H(\tau_b) e^{\left[-\frac{\alpha_h M(\tau_b)}{a(c\alpha_b - d_m)} e^{(c\alpha_b - d_m)(T-\tau_b)} - d_h (T-\tau_b) \right]} > 0, \tag{A.14}$$

it is a contradiction. As a positive constant $T > \tau_b$ arbitrariness, we obtain $H(t) > 0$ for all $\tau_b < t < T$ if $H(0) > 0$.

This implies that our Model (4.2) and (4.3) are positively invariant in $\mathbb{R}^3_+$. We now proceed with the boundedness of our system in Item 2 below.

2. Define $W = cB + cH + M$, then we have

$$\begin{aligned}
\frac{dW}{dt} &= c\frac{dB}{dt} + c\frac{dH}{dt} + \frac{dM}{dt} \\
&= \frac{crH^2}{K+H^2} - \frac{c\alpha_h HM}{a+H} - cd_b B - cd_h H - d_m M \\
&\leq \frac{crH^2}{K+H^2} - cd_b B - cd_h H - d_m M \\
&\leq T - \min\{d_b, d_h, d_m\}(cB + cH + M) = T - d_{\min} W
\end{aligned}$$

where

$$T = \max_{0 \leq H \leq cr} \left\{ \frac{crH^2}{K+H^2} \right\}.$$

Therefore, we have

$$\limsup_{t\to\infty} W(t) = \limsup_{t\to\infty}(cB(t)+cH(t)+M(t)) \leq \frac{T}{d_{\min}}$$

which implies that Model (4.2) and (4.3) are bounded in $\mathbb{R}^3_+$.

□

Proof of Theorem 10

Proof. First, we establish the existence of the boundary equilibria. The boundary equilibria are determined by setting $\frac{dB}{dt} = \frac{dH}{dt} = \frac{dM}{dt} = 0$ in Model (4.3). Thus we obtain Equations (4.4) in section (4.4). Notice from equation (4.4c) that $M^* = 0$ or $B^* = \frac{a}{\frac{c\alpha_b}{d_m}-1}$. The equations (4.4) reduce to the following when $M^* = 0$:

$$\begin{aligned}
&\frac{rH^2}{K+H^2} - d_bB - \frac{rH^2}{K+H^2}e^{-d_b\tau_b} = 0\\
&\frac{rH^2}{K+H^2}e^{-d_b\tau_b} - d_hH = 0
\end{aligned}$$

which yields the three boundary equilibria:

$$E_{000} = (0,0,0), \quad E_{B_1^*H_1^*0} = (B_1^*, H_1^*, 0), \quad \text{and} \quad E_{B_2^*H_2^*0} = (B_2^*, H_2^*, 0)$$

with

$$B_1^* = \left[\frac{r(H_1^*)^2}{K+(H_1^*)^2}\right]\left[\frac{1-e^{-d_b\tau_b}}{d_b}\right], \quad H_1^* = \left(\frac{re^{-d_b\tau_b}}{2d_h}\right) + \sqrt{\left(\frac{re^{-d_b\tau_b}}{2d_h}\right)^2 - K} > 0 \quad \Rightarrow \quad d_h > \frac{re^{-d_b\tau_b}}{2\sqrt{K}}$$

$$B_2^* = \left[\frac{r(H_2^*)^2}{K+(H_2^*)^2}\right]\left[\frac{1-e^{-d_b\tau_b}}{d_b}\right], \quad H_2^* = \left(\frac{re^{-d_b\tau_b}}{2d_h}\right) - \sqrt{\left(\frac{re^{-d_b\tau_b}}{2d_h}\right)^2 - K} > 0 \quad \Rightarrow \quad d_h > \frac{re^{-d_b\tau_b}}{2\sqrt{K}}$$

We proceed with the stability of the boundary equilibria E_{000}, $E_{B_1^*H_1^*0}$, and $E_{B_2^*H_2^*0}$ by linearizing our system. To facilitate our analysis, we introduce the variable $P(t) = e^{-\int_{t-\tau_b}^{t}\left(d_b+\frac{\alpha_b M(s)}{a+B(s)}\right)ds}$ and Model (4.3) becomes:

$$\begin{aligned}
\frac{dB}{dt} &= \frac{rH^2}{K+H^2} - \alpha_b\frac{B}{a+B}M - d_bB - \frac{rPH(t-\tau_b)^2}{K+H(t-\tau_b)^2}\\
\frac{dH}{dt} &= \frac{rPH(t-\tau_b)^2}{K+H(t-\tau_b)^2} - \alpha_h\frac{H}{a+H}M - d_hH\\
\frac{dM}{dt} &= cM\alpha_b\frac{B}{a+B} - d_mM\\
\frac{dP}{dt} &= \frac{\alpha_bPM(t-\tau_b)}{a+B(t-\tau_b)} - \frac{\alpha_bPM}{a+B}
\end{aligned} \tag{A.15}$$

.

Let (B^*,H^*,M^*,P^*) be the equilibrium of the system (A.15) where $P^* = e^{-\left(d_b+\frac{\alpha_b M^*}{a+B^*}\right)\tau_b}$. The linearization matrix of Model (A.15) at the equilibrium (B^*,H^*,M^*,P^*) can be represented as follows:

$$D\left(\begin{bmatrix}\dot{B}(t)\\ \dot{H}(t)\\ \dot{M}(t)\\ \dot{P}(t)\end{bmatrix}\right)\Big|_{(B^*,H^*,M^*,P^*)} = \begin{bmatrix} \frac{-a\alpha_b M^*}{(a+B^*)^2}-d_b & \frac{2rKH^*}{(K+(H^*)^2)^2} & -\frac{\alpha_b B^*}{a+B^*} & -\frac{r(H^*)^2}{K+(H^*)^2}\\ 0 & \frac{-a\alpha_h M^*}{(a+H^*)^2}-d_h & -\frac{\alpha_h H^*}{a+H^*} & \frac{r(H^*)^2}{K+(H^*)^2}\\ \frac{ac\alpha_b M^*}{(a+B^*)^2} & 0 & \frac{c\alpha_b B^*}{a+B^*}-d_m & 0\\ \frac{\alpha_b P^* M^*}{(a+B^*)^2} & 0 & -\frac{\alpha_b P^*}{a+B^*} & 0 \end{bmatrix}\begin{bmatrix}B(t)\\ H(t)\\ M(t)\\ P(t)\end{bmatrix}$$
$$+\begin{bmatrix} 0 & -\frac{2rKP^*H^*}{(K+(H^*)^2)^2} & 0 & 0\\ 0 & \frac{2rKP^*H^*}{(K+(H^*)^2)^2} & 0 & 0\\ 0 & 0 & 0 & 0\\ -\frac{\alpha_b P^* M^*}{(a+B^*)^2} & 0 & \frac{\alpha_b P^*}{a+B^*} & 0 \end{bmatrix}\begin{bmatrix}B(t-\tau_b)\\ H(t-\tau_b)\\ M(t-\tau_b)\\ P(t-\tau_b)\end{bmatrix}. \tag{A.16}$$

1. Denote $P_0^* = e^{-d_b\tau_b}$. The extinction equilibrium E_{000} evaluated at the matrix (A.16) yields

$$D\left(\begin{bmatrix}\dot{B}(t)\\ \dot{H}(t)\\ \dot{M}(t)\\ \dot{P}(t)\end{bmatrix}\right)\Big|_{(0,0,0,P_0^*)} = \begin{bmatrix} -d_b & 0 & 0 & 0\\ 0 & -d_h & 0 & 0\\ 0 & 0 & -d_m & 0\\ 0 & 0 & -\frac{\alpha_b e^{-d_b\tau_b}}{a} & 0 \end{bmatrix}\begin{bmatrix}B(t)\\ H(t)\\ M(t)\\ P(t)\end{bmatrix}$$
$$+\begin{bmatrix} 0 & 0 & 0 & 0\\ 0 & 0 & 0 & 0\\ 0 & 0 & 0 & 0\\ 0 & 0 & \frac{\alpha_b e^{-d_b\tau_b}}{a} & 0 \end{bmatrix}\begin{bmatrix}B(t-\tau_b)\\ H(t-\tau_b)\\ M(t-\tau_b)\\ P(t-\tau_b)\end{bmatrix} \tag{A.17}$$

and from (A.17), we obtain the following characteristic equation:

$$\begin{aligned} h(\lambda) &= \det\left(\lambda\mathscr{I} - \begin{bmatrix} -d_b & 0 & 0 & 0\\ 0 & -d_h & 0 & 0\\ 0 & 0 & -d_m & 0\\ 0 & 0 & -\frac{\alpha_b e^{-d_b\tau_b}}{a} & 0 \end{bmatrix} - e^{-\lambda\tau_b}\begin{bmatrix} 0 & 0 & 0 & 0\\ 0 & 0 & 0 & 0\\ 0 & 0 & 0 & 0\\ 0 & 0 & \frac{\alpha_b e^{-d_b\tau_b}}{a} & 0 \end{bmatrix}\right)\\ &= \det\left(\begin{bmatrix} \lambda+d_b & 0 & 0 & 0\\ 0 & \lambda+d_h & 0 & 0\\ 0 & 0 & \lambda+d_m & 0\\ 0 & 0 & \frac{\alpha_b e^{-d_b\tau_b}}{a}\left(1-e^{\lambda\tau_b}\right) & \lambda \end{bmatrix}\right)\\ &= \lambda\left(\lambda+d_b\right)\left(\lambda+d_m\right)\left(\lambda+d_h\right). \end{aligned}$$

which yields the following eigenvalues:

$$\lambda_1 = -d_b < 0,\ \ \lambda_2 = -d_h < 0,\ \ \lambda_3 = -d_m < 0,\ \ \lambda_4 = 0.$$

Notice that $\lambda_4 = 0$, thus we will use Center Manifold Theory to find the stability condition at the equilibrium $E_{000P_0^*}$ for system (4.3). We first simplify the system

using Taylor series expansion up to the first order to obtain

$$\begin{aligned}\frac{dB}{dt} &= -d_b B\\ \frac{dH}{dt} &= -d_h H\\ \frac{dM}{dt} &= -d_m M\\ \frac{dP}{dt} &= 0\end{aligned} \tag{A.18}$$

. Our system is already in the desired form $(\dot{x} = Cx + F(x,y)\ ,\ \dot{y} = Py + G(x,y))$, where

$$x = \begin{bmatrix} H \\ B \end{bmatrix},\quad y = \begin{bmatrix} M \\ P \end{bmatrix},\quad C = \begin{bmatrix} -d_b & 0 \\ 0 & -d_h \end{bmatrix},\quad F(x,y) = G(x,y) = \begin{bmatrix} 0 \\ 0 \end{bmatrix}, \text{ and } P = -d_m.$$

Now we consider the following function

$$\begin{aligned} h(x) = h(B,H) &= a_1B^2 + a_2BH + a_3H^3 + \mathscr{O}(B^3,H^3)\\ Dh(x) &= [2a_1B + a_2H + \ldots, 2a_3H + a_2B]\\ Dh(x)[Cx + G(x,h(x))] &= [2a_1B + a_2H + \ldots, 2a_3H + a_2B]\begin{bmatrix} -d_bB \\ -d_hH \end{bmatrix}\\ &= -2a_1d_bB^2 - 2a_3d_hH^2 - a_2(d_b + d_h)BH\\ Ph(x) + G(x,h(x)) &= -d_m(a_1B^2 + a_2BH + a_3H^2) = -a_1d_mB^2 - a_2d_mBH - a_3d_mH^2 \end{aligned}$$

Setting $Dh(x)[Cx + G(x,h(x))] = Ph(x) + G(x,h(x))$ and collecting terms yield

$$\begin{aligned} B^2:&\quad 2a_1d_b - d_ma_1 = a_1(2d_b - d_m) = 0 \quad \Rightarrow \quad a_1 = 0\\ H^2:&\quad -2a_3d_h + d_ma_3 = a_3(-2d_h + d_m) = 0 \quad \Rightarrow \quad a_3 = 0\\ BH:&\quad -a_2(d_b + d_h) + a_2d_m = a_2(-d_b - d_h - d_m) = 0 \quad \Rightarrow \quad a_2 = 0 \end{aligned}$$

thus $h(x) = h(B,H) = 0 + \mathscr{O}(B^3,H^3)$ and the flow of the center manifold is given by

$$\begin{aligned}\frac{dB}{dt} &= -d_b B\\ \frac{dH}{dt} &= -d_h H\end{aligned} \tag{A.19}$$

Therefore, we can conclude that the Model (4.2) and (4.3) is always asymptotically stable at the extinction equilibrium $E_{000N_0^*}$ (or E_{000}).

2. We now look at the stability of the boundary equilibria $E_{B_1^*H_1^*0P_0^*}$ and $E_{B_2^*H_2^*0P_0^*}$. Substitution of $E_{B_1^*H_1^*0P_0^*}$ into the matrix (A.16) gives:

$$D\left(\begin{bmatrix}\dot{B}(t)\\ \dot{H}(t)\\ \dot{M}(t)\\ \dot{P}(t)\end{bmatrix}\right)\Big|_{(B_1^*,H_1^*,0,P_0^*)} = \begin{bmatrix} -d_b & \frac{2rKH_1^*}{(K+(H_1^*)^2)^2} & -\frac{\alpha_b B_1^*}{a+B_1^*} & -\frac{r(H_1^*)^2}{K+(H_1^*)^2} \\ 0 & -d_h & -\frac{\alpha_h H_1^*}{a+H_1^*} & \frac{r(H_1^*)^2}{K+(H_1^*)^2} \\ 0 & 0 & \frac{c\alpha_b B_1^*}{a+B_1^*}-d_m & 0 \\ 0 & 0 & -\frac{\alpha_b e^{-d_b\tau_b}}{a+B_1^*} & 0 \end{bmatrix}\begin{bmatrix} B(t)\\ H(t)\\ M(t)\\ P(t)\end{bmatrix}$$
$$+\begin{bmatrix} 0 & -\frac{2rKH_1^*}{(K+(H_1^*)^2)^2}e^{-d_b\tau_b} & 0 & 0 \\ 0 & \frac{2rKH_1^*}{(K+(H_1^*)^2)^2}e^{-d_b\tau_b} & 0 & 0 \\ 0 & 0 & 0 & 0 \\ 0 & 0 & \frac{\alpha_b e^{-d_b\tau_b}}{a+B_1^*} & 0 \end{bmatrix}\begin{bmatrix} B(t-\tau_b)\\ H(t-\tau_b)\\ M(t-\tau_b)\\ P(t-\tau_b)\end{bmatrix}.$$

We then obtain the following characteristic equation:

$$h(\lambda) = \det\left(\lambda\mathscr{I} - \begin{bmatrix} -d_b & \frac{2rKH_1^*}{(K+(H_1^*)^2)^2} & -\frac{\alpha_b B_1^*}{a+B_1^*} & -\frac{r(H_1^*)^2}{K+(H_1^*)^2} \\ 0 & -d_h & -\frac{\alpha_h H_1^*}{a+H_1^*} & \frac{r(H_1^*)^2}{K+(H_1^*)^2} \\ 0 & 0 & \frac{c\alpha_b B_1^*}{a+B_1^*}-d_m & 0 \\ 0 & 0 & -\frac{\alpha_b e^{-d_b\tau_b}}{a+B_1^*} & 0 \end{bmatrix}\right.$$
$$\left. - e^{-\lambda\tau_b}\begin{bmatrix} 0 & -\frac{2rKH_1^*}{(K+(H_1^*)^2)^2}e^{-d_b\tau_b} & 0 & 0 \\ 0 & \frac{2rKH_1^*}{(K+(H_1^*)^2)^2}e^{-d_b\tau_b} & 0 & 0 \\ 0 & 0 & 0 & 0 \\ 0 & 0 & \frac{\alpha_b e^{-d_b\tau_b}}{a+B_1^*} & 0 \end{bmatrix}\right)$$
$$= \det\left(\begin{bmatrix} \lambda+d_b & -\frac{2rKH_1^*}{(K+(H_1^*)^2)^2}\left(1-e^{-(\lambda+d_b)\tau_b}\right) & \frac{\alpha_b B_1^*}{a+B_1^*} & \frac{r(H_1^*)^2}{K+(H_1^*)^2} \\ 0 & \lambda+d_h-\frac{2rKH_1^*}{(K+(H_1^*)^2)^2}e^{-d_b\tau_b}e^{-\lambda\tau_b} & \frac{\alpha_h H_1^*}{a+H_1^*} & -\frac{r(H_1^*)^2}{K+(H_1^*)^2} \\ 0 & 0 & \lambda+d_m-\frac{c\alpha_b B_1^*}{a+B_1^*} & 0 \\ 0 & 0 & \frac{\alpha_b e^{-d_b\tau_b}}{a+B_1^*}\left(1-e^{\lambda\tau_b}\right) & \lambda \end{bmatrix}\right)$$
$$= \lambda(\lambda+d_b)\left(\lambda+d_m-\frac{c\alpha_b B_1^*}{a+B_1^*}\right)\left(\lambda+d_h-\frac{2rKH_1^*}{(K+(H_1^*)^2)^2}e^{-d_b\tau_b}e^{-\lambda\tau_b}\right).$$

Then we obtain the following eigenvalues:

(a) $\lambda_1 = 0 \quad$ and $\quad \lambda_2 = -d_b < 0.$

(b) $\lambda_3 = \frac{c\alpha_b B_1^*}{a+B_1^*} - d_m < 0$ if $d_m > \frac{c\alpha_b B_1^*}{a+B_1^*} \quad$ or $\quad \lambda_3 = \frac{c\alpha_b B_1^*}{a+B_1^*} - d_m < 0$ if $d_m < \frac{c\alpha_b B_1^*}{a+B_1^*}$.

(c) It remains to show the sign of λ_4 and notice that

$$\lambda_4 + d_h - \frac{2rKH_1^*}{(K+(H_1^*)^2)^2}e^{-d_b\tau_b}e^{-\lambda_3\tau_b}$$

is identical to the characteristic equation of a particular one-dimensional problem illustrated in Chapter 4 of Smith (2010) with

$$\hat{A} = d_h, \quad \hat{B}_1 = -\frac{2rKH_1^*}{(K+(H_1^*)^2)^2} e^{-d_b\tau_b} \quad \text{and} \quad \hat{A}+\hat{B}_1 = \frac{2d_h^2 e^{d_b\tau_b}\sqrt{\left(\frac{re^{-d_b\tau_b}}{2d_h}\right)^2 - K}}{r} > 0.$$

Thus by Theorem 4.6 (p. 53) in Smith (2010), $E_{B_1^*H_1^*0P_0^*}$ (or $E_{B_1^*H_1^*0}$) is always unstable.

We now look at the stability of $E_{B_2^*H_2^*0N_0^*}$ which follow similar arguments presented above and we arrive at the following eigenvalues after evaluation of $E_{B_2^*H_2^*0}$ into the matrix (A.16):

(a) $\lambda_1 = 0 \quad$ and $\quad \lambda_2 = -d_b < 0.$

(b) $\lambda_3 = \frac{c\alpha_b B_2^*}{a+B_2^*} - d_m < 0$ if $d_m > \frac{c\alpha_b B_2^*}{a+B_2^*} \quad$ or $\quad \lambda_2 = \frac{c\alpha_b B_2^*}{a+B_2^*} - d_m < 0$ if $d_m < \frac{c\alpha_b B_2^*}{a+B_2^*}$.

(c) As before, we look at λ_4 and notice that

$$\lambda_3 + d_h - \frac{2rKH_2^*}{(K+(H_2^*)^2)^2} e^{-d_b\tau_b} e^{-\lambda_3\tau_b}$$

which is again identical to the characteristic equation of a particular one-dimensional problem in Chapter 4 of Smith (2010) where

$$\hat{A} = d_h, \quad \hat{B}_2 = -\frac{2rKH_2^*}{(K+(H_2^*)^2)^2} e^{-d_b\tau_b} \quad \text{and} \quad \hat{A}+\hat{B}_2 = -\frac{2d_h^2 e^{d_b\tau_b}\sqrt{\left(\frac{re^{-d_b\tau_b}}{2d_h}\right)^2 - K}}{r} < 0.$$

It can easily be seen that using the procedure of the Center Manifold Theory as in the case of the stability of E_{000} described above, the stability of $E_{B_2^*H_2^*0P_0^*}$ can be shown using the eigenvalues λ_2, λ_3, and λ_4 consider the Taylor series expansion of our Model (4.3) reduces to the linear system (A.18). Therefore $E_{B_2^*H_2^*0P_0^*}$ (or $E_{B_2^*H_2^*0}$) is locally asymptotically stable when $d_m > \frac{c\alpha_b B_2^*}{a+B_2^*}$ and it is unstable when $d_m < \frac{c\alpha_b B_2^*}{a+B_2^*}$ by Theorem 4.6 (p. 53) in Smith (2010).

This concludes the proof of the proof of Theorem 10. □

APPENDIX B

FIGURES AND TABLES

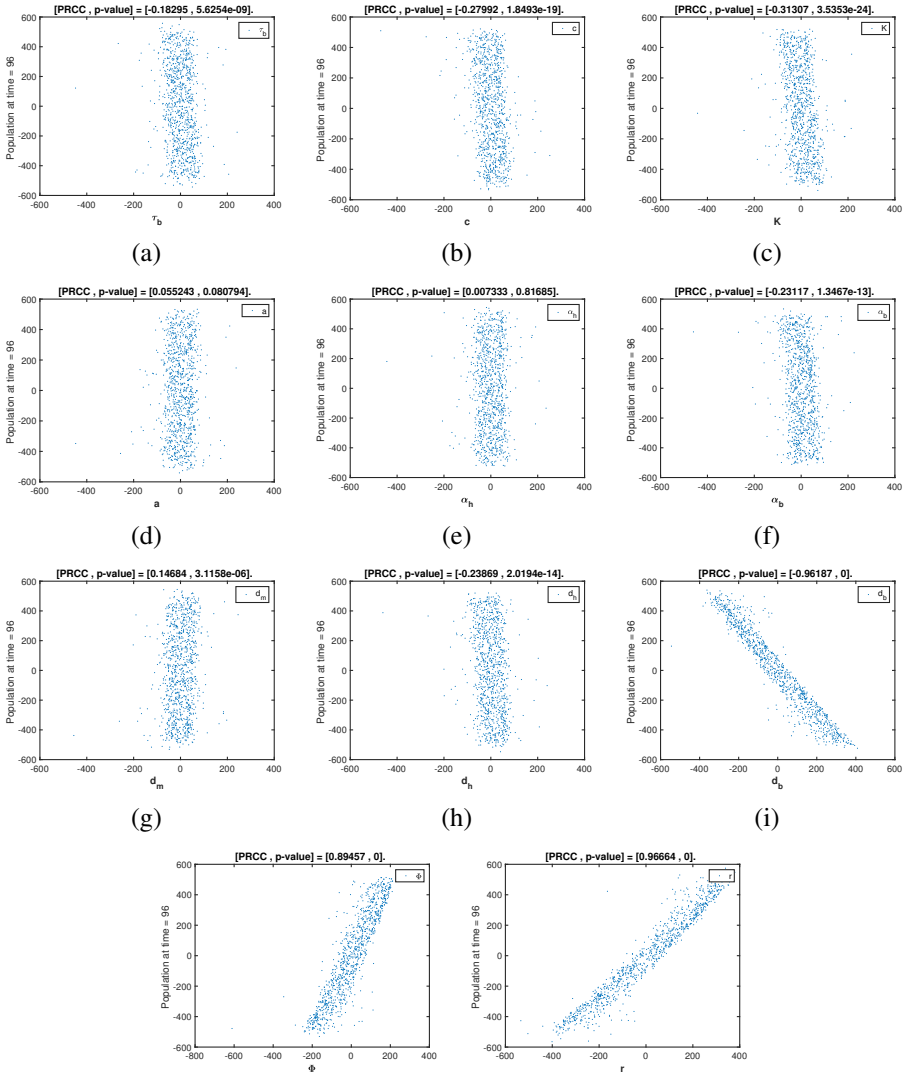

(a) (b) (c)

(d) (e) (f)

(g) (h) (i)

(j) (k)

Figure B.1: Scatter Plots of Parameters τ_b, c, K, a, α_h, α_b, d_m, d_h, d_b, Φ, r Which Were Calculated at Time 96 While Varying Each Parameter Simultaneously. Each Plot Has the PRCC Value with the Corresponding P-value as Title and We Used Sample Size of $N = 1000$. The x-axis Is the Residuals of the Linear Regression Between the Rank-transformed Values of the Parameter under Investigation Versus the Rank-transformed Values of All the Other Parameters. The y-axis Is the Residuals of the Linear Regression Between the Rank-transformed Values of the Output Versus the Rank-transformed Values of All the Parameter under Investigation.

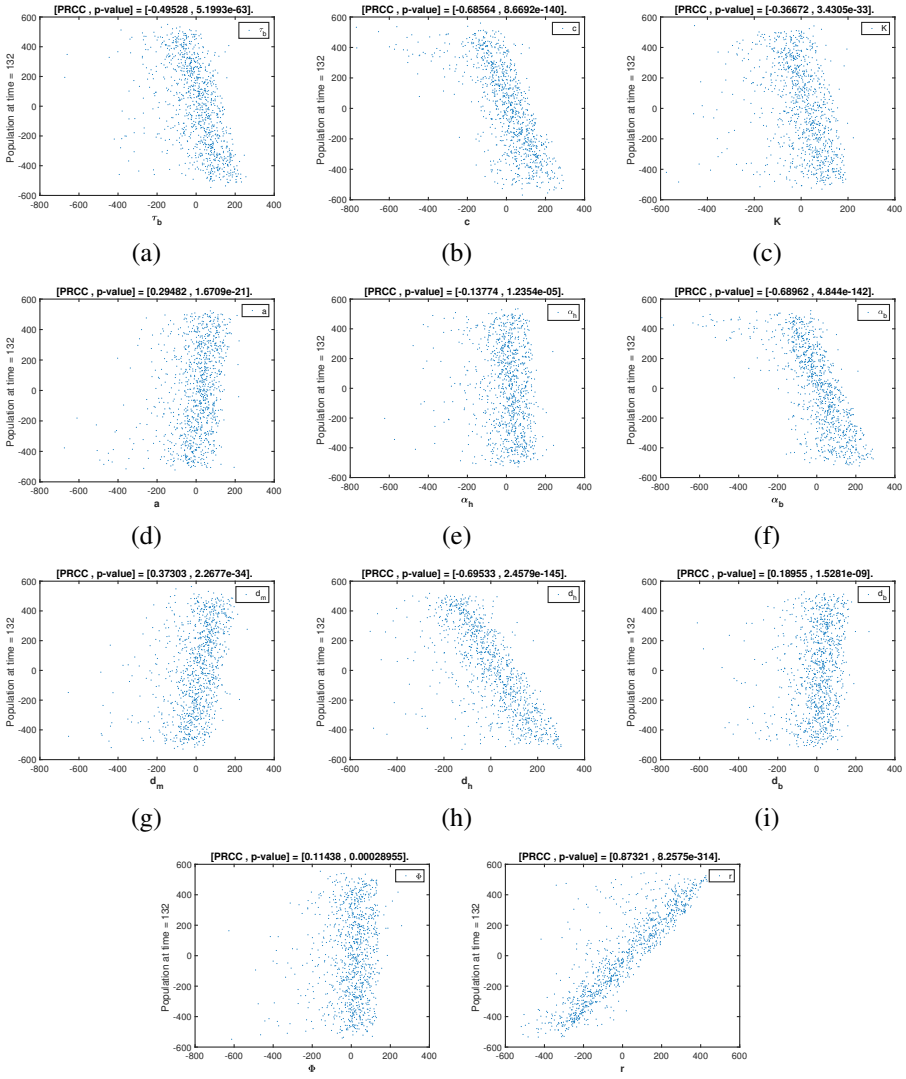

Figure B.2: PRCC Scatter Plots of Parameters τ_b, c, K, a, α_h, α_b, d_m, d_h, d_b, Φ, r Which Were Calculated at Time 132 While Varying Each Parameter Simultaneously. Each Plot Has the PRCC Value with the Corresponding P-value as Title and We Used Sample Size of $N = 1000$. The x-axis Is the Residuals of the Linear Regression Between the Rank-transformed Values of the Parameter under Investigation Versus the Rank-transformed Values of All the Other Parameters. The y-axis Is the Residuals of the Linear Regression Between the Rank-transformed Values of the Output Versus the Rank-transformed Values of All the Parameter under Investigation.

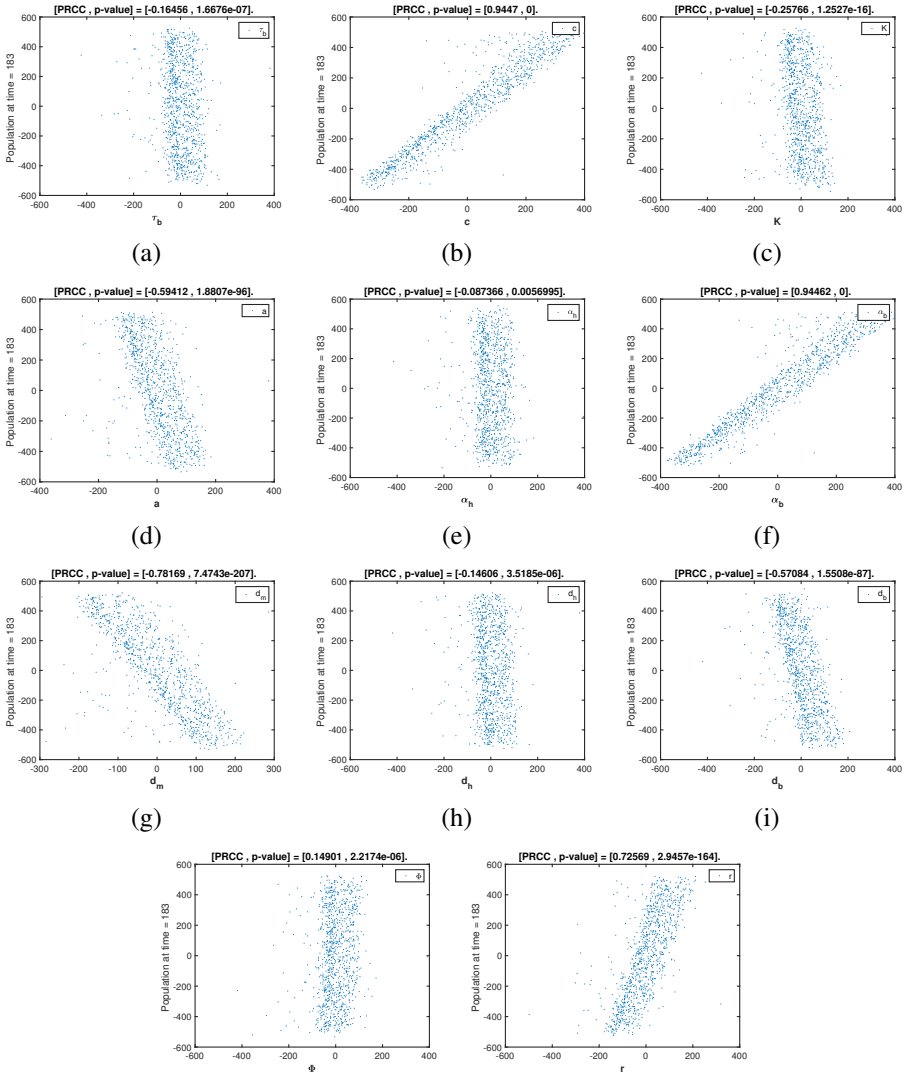

Figure B.3: PRCC Scatter Plots of Parameters τ_b, c, K, a, α_h, α_b, d_m, d_h, d_b, Φ, r Which Were Calculated at Time 183 While Varying Each Parameter Simultaneously. Each Plot Has the PRCC Value with the Corresponding P-value as Title and We Used Sample Size of $N = 1000$. The x-axis Is the Residuals of the Linear Regression Between the Rank-transformed Values of the Parameter under Investigation Versus the Rank-transformed Values of All the Other Parameters. The y-axis Is the Residuals of the Linear Regression Between the Rank-transformed Values of the Output Versus the Rank-transformed Values of All the Parameter under Investigation.

Parameters	PRCC		eFAST	
	sensitivity index	**p-value**	**first-order S_i**	**total-order S_{Ti}**
r	0.96664**	0	0.67936	0.68784
Φ	0.89457**	0	0.0068948	0.0082977
d_b	-0.96187**	0	0.3079	0.31461
d_h	-0.23869**	2.0194e-14	0.0080172	0.0095901
d_m	0.14684**	3.116e-06	3.7727e-05	0.00089457
α_b	-0.23117**	1.347e-13	0.00012458	0.0011038
α_h	0.007333	0.81685	1.2504e-05	0.00081607
a	0.055243	0.080794	3.3803e-05	0.001148
K	-0.31307**	3.535e-24	0.023235	0.024764
c	-0.27992**	1.849e-19	0.00014943	0.0010502
τ_b	-0.18295**	5.625e-09	0.0056511	0.006688

Table B.1: Comparison of PRCC and eFAST Values at Time 96 and * Implies Significance at 0.01 (i.e. $p < 0.01$) While ** Implies Significance at 0.0001 (i.e. $p < 0.001$).

Parameters	PRCC		eFAST	
	sensitivity index	**p-value**	**first-order S_i**	**total-order S_{Ti}**
r	0.8732**	8.2575e-314	0.37861	0.4092
Φ	0.1144**	2.8955e-04	0.00082837	0.0034278
d_b	0.1896**	1.5281e-09	0.0046109	0.010879
d_h	-0.6953**	2.4579e-145	0.12011	0.1243
d_m	0.3730 **	2.2677e-34	0.040672	0.10706
α_b	-0.6896**	4.844e-142	0.097734	0.1356
α_h	-0.1377**	1.2354e-05	0.0040036	0.010628
a	0.2948**	1.6709e-21	0.019395	0.043743
K	-0.3667**	3.4305e-33	0.020604	0.027903
c	-0.6856**	8.6692e-140	0.12116	0.21043
τ_b	-0.4953 **	5.1993e-63	0.01145	0.014629

Table B.2: Comparison of PRCC and eFAST Values at Time 132 and ** Implies Significance at 0.001 (i.e. $p < 0.001$).

Parameters	PRCC		eFAST	
	sensitivity index	**p-value**	**first-order S_i**	**total-order S_{Ti}**
r	0.7257 **	2.9457e-164	0.068869	0.11504
Φ	-0.1490**	2.2174e-06	0.004525	0.013015
d_b	-0.5708 **	1.5508e-87	0.030786	0.057749
d_h	-0.1461**	3.5185e-06	0.0021218	0.0058844
d_m	-0.7817 **	7.4743e-207	0.05834	0.10418
α_b	0.9446**	0	0.3487	0.010895
α_h	-0.08737*	5.6995e-03	0.0016142	0.041224
a	-0.5941**	1.8807e-96	0.016902	0.0093502
K	-0.2577**	1.2527e-16	0.0037531	0.41943
c	0.9447 **	0	0.27371	Yes
τ_b	-0.1646 **	1.6676e-07	0.0012931	0.0043944

Table B.3: Comparison of PRCC and eFAST Values at Time 183 and * Implies Significance at 0.01 (i.e. $p < 0.01$) While ** Implies Significance at 0.001 (i.e. $p < 0.001$).

Parameter	Description	Estimate/Units	Reference
r	maximum birth rate	0, 500, 1500 bees/day (depending on season)	see (Sumpter and Martin, 2004; Eberl et al., 2010)
d_b	average death rate of brood at the larvae and pupae stage	† 0.00602-0.036 (for unsealed brood) and 0.00303 (for sealed brood) day^{-1}	Fukuda and Sakagami (1968)
d_h	average death rate of adult honeybee	neglected (for hive bees) or 0.114-0.154 and 0.24-0.4 (for foragers) day^{-1}	(Khoury et al., 2011, 2013)
d_m	average death rate of phoretic mite	(0.016-0.45) or 0.002(winter), 0.006(summer) day^{-1}	(Branco et al., 2006; Martin, 1998)
c	conversion rate from honeybee consumption to mite reproduction	0-4.5	Huang (2012)
$\sqrt{K}$	colony size at which the birth rate is half maximal	$\leq$ 22007(fall, spring), and $\leq$ 37500(summer) bees/day (upper bound values)	Ratti et al. (2012)
α	parasitism rate	‡ (0.000556-0.00833) day^{-1}	Fries et al. (2006)
α_b	parasitism rate on brood	0.0447 day^{-1}	Estimated from data
α_h	parasitism rate on adult bee	0.8day^{-1}	Estimated from data
a	size of honeybee population at which rate of attachment is half maximal	8050 bees	Estimated from data
ρ	relative dispersal rate of honeybee	varied	assumption
τ_b	Development time from brood at the egg stage to adult bee	16 (queens), 21 (workers), 24 (drones) days	P. 83 in Graham (1992)

Table B.4: Standard parameters Values Used for Simulation of Honeybee and Mite Population of Model (3.2), (4.2), and (4.3) in Chapter 3 and 4 Respectively. Daily Mortality of ‡ is Calculated From the Winter Mortality Rate 0.05-0.75 in Fries et al. (2006) Divided by the 90 Winter Days. † is Calculated From the Daily Mortality $([1-\frac{330}{332}],[1-\frac{347}{360}])$ for Unsealed Brood and $(1-\frac{329}{330})$ for Sealed Brood.

APPENDIX C

STATEMENT OF AUTHORIZATION

The project "A two patch prey-predator model with multiple foraging strategies in predator: Applications to insects" (where I am the first author), which was recently published in the Journal of Discrete and Continuous Dynamical System - B (Messan and Kang (2017)) is elaborated in chapter 2 of the dissertation per request of the co-author Dr. Yun Kang.

The project "Migration effects on population dynamics of the honeybee-mite interactions" (where I am the first author), which was recently published in the Journal of Mathematical Modelling of Natural Phenomena (Messan et al. (2017)) is elaborated in chapter 3 of the dissertation per request of the co-authors Dr. Gloria DeGrandi-Hoffman, Dr. Carlos Castillo-Chavez, and Dr. Yun Kang.